UNIVERSITY OF CALGARY

Telomere Dynamics and Chemotherapy in Aging and Cancer

by

Brad Michael Unryn

A THESIS

SUBMITTED TO THE FACULTY OF GRADUATE STUDIES

IN PARTIAL FULFILMENT OF THE REQUIREMENTS FOR THE

DEGREE OF MASTER OF SCIENCE

DEPARTMENT OF BIOCHEMISTRY AND MOLECULAR BIOLOGY

CALGARY, ALBERTA

JUNE, 2005

UNIVERSITY OF CALGARY

FACULTY OF GRADUATE STUDIES

The undersigned certify that they have read, and recommend to the Faculty of Graduate Studies for acceptance, a thesis entitled "Telomere Dynamics and Chemotherapy in Aging and Cancer" submitted by Brad M. Unryn in partial fulfillment of the requirements for the degree of Master of Science.

Supervisor, Dr. K. Riabowol, Department of Biochemistry and Molecular Biology

---

Dr. Chris Mody, Department of Medical Science

Dr. Linda Cook, Department of Community Health Science

Dr. Frans van der Hoorn, Department of Biochemistry and Molecular Biology

---

External Examiner, Dr. Peter Lansdorp, Department of Medicine,
University of British Columbia

Date

ABSTRACT

Telomeres are structures located at eukaryotic chromosome ends which are critical to chromosome integrity and protection. As telomere length gradually shortens, so does the apparent residual replicative potential of the cell. A variety of disease states and disease treatment regimens increase telomere erosion both *in vivo* and *in vitro*, which may lead to the eventual compromise of immune function. This study examined the relationship between chemotherapeutic treatment and telomere length. The treatment of human fibroblasts with platinum agents resulted in accelerated shortening of telomeric DNA, *in vitro*. No significant telomere length difference was seen between head and neck cancer patients and individuals without cancer. A variety of factors, such as gender, pack years and paternal age, were correlated with differences in telomere length among individuals examined. In patients, an eight-week chemoradiotherapy treatment caused a dramatic loss in telomeres, equivalent to 22 years worth of attrition in normal individuals.

ACKNOWLEDGEMENTS

I would like to thank my graduate supervisor, Dr. Karl Riabowol, for granting me the opportunity to work in his laboratory on many aspects of telomere biology. I also would like to thank the members of my graduate committee, Dr. Linda Cook, Dr. Frans van der Hoorn and Dr. Chris Mody for their helpful comments and guidance. In addition, I thank Pamela Round for collecting data for the non-cancer group, and Leanne Kmet for help with the statistical analyses. I would like to thank Michael Russell for contributing to the western blot data seen in figure 6.

This work was supported by grants to Dr. Riabowol and Dr. Cook from the Canadian Institutes of Health Research.

TABLE OF CONTENTS

LIST OF TABLES

LIST OF FIGURES

LIST OF ABBREVIATIONS

A……... adenine
A-T…… Ataxia-telangiectasia
AIDS…….. acquired immune deficiency syndrome
ALL……acute lymphoblastic leukemia
ANOVA……analysis of variance
AP…….. apurinic or apyrimidinic site
Ara-C……. cytarabine
BER……base excision repair
β-Gal…….. β-Galactosidase
bp…….. base pairs
C…… cytosine
c-DDP……... cisplatin (cis-Platinum(II)-diammine dichloride)
$CD4^+$……. helper T lymphocyte
$CD8^+$……. cytotoxic T lymphocyte
cdk……. cyclin dependant kinase
CR……. complete response
CRT……... chemoradiotherapy
DNA…….. deoxyribonucleic acid
DS…….. Down syndrome
ECL……enhanced chemiluminescence
EDTA…… ethylenediaminetetraacetic acid
FACS……. fluorescence activated cell sorting
FBS…… fetal bovine serum
G…… guanine
G0…….. quiescence
G1…….. first gap phase
G2…….. second gap phase
GC……. germinal-centre cells
GG-NER…… global-genome nucleotide excision repair
Gy…….. Grays
H_2O_2…….. hydrogen peroxide
HeLa…….. human cervical carcinoma cell line
HNC…….. head and neck carcinoma
Hs68……... human foreskin fibroblast
hTER……..human telomerase RNA component
hTERT……... human telomerase catalytic component
HIV…… human immunodeficiency virus
HR……. homologous recombination
IC-50……. 50% inhibition of cell viability
IR……... ionizing radiation
Kb…….. kilobases

M…… mitotic
µg……... microgram
ml……... milliliter
µl…… microliter
mM…… millimolar
MMR…… mismatch repair
MPD…….. mean population doublings
mRNA…… messenger RNA
mTRF…… mean terminal restriction fragment
MTX…….. methotrexate (+/- amethopterin)
NER……nucleotide excision repair
NHEJ……. non-homologous end-joining
NHL……... non-Hodgkin's lymphoma
PBMC…… peripheral blood mononuclear cells
PBS…… phosphate buffered saline
PCNA…… proliferating cell nuclear antigen
PD……. population doubling
PI……... propidium iodide
PR…….. partial response
pRB…… retinoblastoma protein
RNA…….. ribonucleic acid
RT……. radiotherapy
S…… Synthesis phase
SA β-Gal……... senescence-associated β-Galactosidase
SIPS…….. stress-induced premature senescence
SV40……. simian virus 40
T…… thymine
TC-NER…… transcription-coupled nucleotide excision repair
t-DDP…… transplatin (trans-Platinum(II)-diammine dichloride)
TER……telomerase RNA component
TERT……. telomerase catalytic component
TRF…… terminal restriction fragment
TRF1…….. human telomeric repeat binding factor 1
TRF2…….. human telomeric repeat binding factor 2
Tx…….. treatment
UV……. ultraviolet radiation
WS…… Werner's syndrome
X-gal……. X-galactoside (5-Bromo-4-Chloro-3-indolyl-Beta-D-galactoside)
XP……. Xeroderma Pigmentosum
XPA…….. Xeroderma Pigmentosum A
yr…… year
5-FU…….. 5-fluorouracil

I. INTRODUCTION

The shortening of repetitive DNA structures at the ends of eukaryotic chromosomes, called telomeres, occurs due to the end-replication problem and the accumulation of oxidative damage in cells (Olovnikov 1973; von Zglinicki et al. 2000). Telomeres are critical to chromosome integrity and protection from degradation and end-to-end fusions. As lengths gradually shorten, so does the apparent residual replicative potential of the cell (Harley 1991). Attrition will continue in normal diploid human cells, until a critical point is reached and replicative senescence occurs (Harley et al. 1990). Unlike somatic cells, immortal cell lines and cancer cells escape the replication barrier through the expression of an enzyme called telomerase, which is able to synthesize the conserved TTAGGG telomeric repeats (Kim et al. 1994). The rate of telomere attrition *in vivo* is not constant throughout life. An accelerated telomere loss is seen in early childhood (Rufer et al. 1999). In adulthood, a declining rate of telomere loss is seen (Unryn et al. 2005). Various disease states (from accelerated aging and Down's syndrome to HIV infection) have a considerable effect on telomere length (and its associated replicative capacity), and erosion is seen at magnitudes up to 5-times higher than normal (Bestilny et al. 2000). Recent correlative evidence links shortened telomere length to increased probabilities of mortality from infectious or cardiovascular disease (Cawthon et al. 2003), a finding that reinforces the necessity to examine and expand our current knowledge of telomere maintenance and dysfunction.

II. BACKGROUND

A) Telomere structure and function

Eukaryotic chromosome ends are composed of repetitive sequences of DNA that "cap" the chromosome end and provide critical stability and protection from end-to-end fusions, degradation and recombination (Blackburn 1994). In the majority of organisms, telomeres consist of a G-rich sequence at the end of the 3' strand. In higher plants the telomeric repeat is AGGGTTT, while ciliated protozoa have a tract that consists of GGGGTT repeats. All vertebrates, including mammals, contain telomeric sequences that consist of the repetitive hexamer TTAGGG (Blackburn 1990). The amount of telomeric DNA is also seen to vary between organisms and species. In fungi and protozoa, the repetitive tracts are extremely short (20 – 600 basepairs), while in vertebrates and plants, the telomeres can be ten to a hundred kilobases (kb) in length. An abrupt end is not present at the extreme ends of telomeres in the majority of organisms, but rather a short single stranded G-rich extension is found on the 3' strand (reviewed in (Zakian 1995).

One of the primary functions of telomeres is to provide expendable DNA to the conventional DNA replication machinery (Wright et al. 2001). This DNA provides a solution to the end replication problem of linear chromosomes and the inability of machinery to replicate the very ends of linear DNA (Olovnikov 1971). Normal machinery is unable to fill the gap that remains between the final priming event and the chromosome end, thus leaving a small 3' overhang at one end of the chromosome. Each time replication occurs, the daughter strand generated will lack some DNA from the unreplicated lagging strand. The lengths of these extensions are again variable between

organisms. Electron microscopic examination of the telomeric overhangs in human fibroblasts revealed an average overhang length of 200 +/- 75 bases (Wright et al. 1997).

The telomeric ends are also associated with a number of telomere-associated and telomere-binding proteins, which have been identified in a large variety of species (Chong et al. 1995; Bilaud et al. 1997; Kim et al. 1999; Liu et al. 2004). The mammalian telomere loops back on itself, displaces one strand of the telomeric repeat, and associates with its complementary sequence. The displaced section of telomeric repeat is referred to as the displacement loop (d-loop), while the large telomere duplex loop is referred to as the t-loop or DNA lariat (Griffith et al. 1999). Although the size of the t-loop appears to vary and is correlated with telomere length itself in vertebrates, its function does not appear to be linked to size. The t-loop structure, which contains a large number of telomere-binding proteins, in effect, hides the short single stranded terminus, inhibits the ligation of chromosomes and also prevents the inappropriate activation of DNA damage repair and cell cycle checkpoint mechanisms (de Lange 2002). In human cells, the t-loop may also limit the access of the enzyme involved in telomere maintenance, telomerase, to the 3' end of the telomere (Kim Sh et al. 2002). The interaction of telomerase with proteins localized at the telomere may be essential for unfolding and telomere maintenance through telomerase activity.

To date in mammalian cells, at least six proteins have been shown to localize to telomeres (TRF1, TRF2, TIN2, RAP1, POT1 and PTOP) and these proteins appear to form a multi-subunit complex termed the telosome (Liu et al. 2004). Mutation, overexpression or alteration of any of those proteins has been shown to affect end-capping and/or telomere length itself. The telomere-repeat binding factor, TRF1 has a key

role in cell cycle control and in telomere length regulation while TRF2 is associated with t-loop formation and the maintenance of chromosome stability by preventing end-to-end fusion and degradation (Broccoli et al. 1997; van Steensel et al. 1998; Smogorzewska et al. 2000; Kim Sh et al. 2002). Evidence that telomere structure plays as significant a role as telomere length in terms of function continues to accumulate.

B) Telomerase function and regulation

The maintenance and replication of telomeres occurs through a specialized enzyme, telomerase. This ribonucleoprotein complex adds repetitive sequences directly to the G-rich single-stranded 3' telomeric overhang. The core portion of the enzyme is composed of a protein subunit with reverse transcriptase activity (telomerase reverse transcriptase; TERT) and an RNA molecule that contains a template of the telomere specific sequence (telomerase RNA; TER) (Feng et al. 1995). The TERT subunit contains regions which are highly conserved between organisms and other reverse transcriptases. The RNA subunit shows a common secondary structure (Chen et al. 2000) despite the fact that there is a large sequence divergence, even among closely related organisms (Romero et al. 1991).

Modification, overexpression or mutation of either of the core components *in vitro* is seen to affect both telomere and telomerase homeostasis (Blackburn 2005). Transfection of the gene encoding TERT into a variety of primary fibroblast cell lines not only resulted in telomerase activity and telomere maintenance, but cellular senescence was averted and division occurred indefinitely (Bodnar et al. 1998; Vaziri et al. 1998). When the RNA template is mutated, the corresponding mutated telomeric repeats might

cause cellular arrest or even result in telomere uncapping (Li et al. 2004). In cells that express high levels of telomerase activity, correspondingly high levels of the human TERT subunit (hTERT) are often found (Meyerson et al. 1997). *In vitro* reconstitution experiments provide evidence that the telomerase catalytic subunit is the limiting factor in most normal somatic cells (Weinrich et al. 1997; Beattie et al. 1998). The presence of human telomerase RNA (hTER) and hTERT alone was sufficient to cause cells to display telomerase activity.

Telomerase activity is found in the majority of human tumors and in immortal cancer cells (Kim et al. 1994). Enzyme activity is also found in fetal testes and ovaries, newborn and adult testes (Wright et al. 1996) and in developing embryonic tissues (Wright et al. 1996; Achi et al. 2000). Some stem or stem-like cells show a low level of telomerase activity in adults, but the enzyme activity present in basal keratinocytes and crypt cells (Harle-Bachor et al. 1996), as well as stimulated lymphocytes (Broccoli et al. 1995), is insufficient to maintain telomere length (Bodnar et al. 1996; Wright et al. 1996).

C) Cellular senescence

Normal human diploid fibroblasts are seen to undergo a limited number of population doublings *in vitro*, an event that is referred to as replicative senescence or the Hayflick limit (Hayflick 1965). This phenomenon occurs in most somatic cell populations that have the propensity to divide and regenerate, including lymphocytes, epithelial and endothelial cells, and results in a loss of replicative capacity, decreased efficiency of protein synthesis and degradation and decreased cell cycle enzyme activity (Chen et al. 1994). Senescent cells enter a state of cell cycle arrest (that is different from

G0 or quiescence) in which the cells remain viable and have some metabolic activity (yet they are unable to be stimulated by a variety of mitogens). Even though a number of artificial conditions can result in the induction of senescence in normal cells (such as stress-induced premature senescence), senescence may have evolved for tumor suppressive reasons to counteract rapid proliferation and suppress potential life-threatening cancer (Campisi et al. 2001).

One of the mechanisms proposed to play a key role in replicative senescence is telomere erosion. A gradual loss of telomeric DNA occurs with increasing age, both *in vitro* and *in vivo*, in the absence of telomerase. Links betweens replicative senescence and telomere length were first seen in fibroblast cells that expressed the catalytic subunit of telomerase (Bodnar et al. 1998; Vaziri et al. 1998). In cells with telomerase activity, division occurred indefinitely. Not only did these experiments reveal that telomerase in the cell could elongate telomeres, but if the telomerase activity was removed after elongation had occurred, lifespan was still extended.

In the absence of telomerase, telomere attrition occurs until a critical or threshold length is reached in one or more telomeres, which results in signaling to arrest growth and enter into a senescent state (Harley 1991). Telomere length at replicative senescence is seen to vary between cell types and clones. Recent findings suggest that end-associations between a group of chromosomes with short telomeres, not just a single short telomere inducing damage signals, could be the cause of growth arrest (Zou et al. 2004). The finite lifespan of mammalian cells can also be overcome through the introduction of certain viruses such as SV40 T-antigen, adenovirus and human papilloma virus (Shay et al. 1991). Proliferation continues in the cells that bypass senescence until

they reach an event called crisis. The majority of cells in crisis have critically short telomeres and the rate of cell death is equal to or exceeds the rate of cell growth. At this point, a mutation causing the activation of telomerase is one of the few mechanisms believed to enable cells to avoid crisis and continue to divide indefinitely.

A proliferation-independent condition referred to as stress-induced premature senescence (SIPS) can also be achieved through a variety of different stimuli (Toussaint et al. 2000). The treatment of cells with chemical agents such as H_2O_2 (von Zglinicki et al. 1995) or physical carcinogens such as ionizing radiation (Di Leonardo et al. 1994) results in rapid growth arrest and changes in cellular morphology and protein expression. Despite the phenotypic similarity to replicative senescence, cells that have undergone SIPS cannot be immortalized through hTERT expression and generally do not have shortened telomeres (Shay et al. 2005).

Many differences can be found between normal and senescent cells. Senescent fibroblasts have higher detectable oxidative DNA damage, which might suggest that damage plays a role in the onset of cell-cycle arrest (Chen et al. 1998). The increased levels could be attributed to less functional cellular defense mechanisms or mitochondria, which might cause an imbalance in the electron transport chain and a subsequent accumulation of hydrogen peroxide and reactive oxygen species (ROS) (Chen et al. 1995). Morphological changes seen in senescent cells, such as increased cell volume and increased cytoskeletal organization, could also increase the sensitivity of DNA to damage through chromatin relaxation.

The levels of many proteins also differ between low passage cells and senescent cells. The levels of the growth regulator protein $p21^{WAF1/CIP1/SDI1}$, which is an inhibitor of

cyclin A/E and cyclin-dependent kinase 2 (cdk2) complexes, increase in pre-senescent cells and then gradually decline during senescence (Noda et al. 1994). Activity of the tumor suppressor p53, also increases in high-passage cells even in the absence of increased mRNA and protein expression (Atadja et al. 1995). The protein $p16^{INK4a}$, an inhibitor of cyclin D and cdk4 and cdk6 complexes that is not normally expressed in adult tissues, is elevated and remains overexpressed throughout senescence (Hara et al. 1996; Wong et al. 1996). These increases result in the hypophosphorylation of the retinoblastoma tumor suppressor protein (pRB). RB hypophosphorylation inhibits activity of the E2F1 transcription factor (Chellappan et al. 1991) resulting in a subsequent lack of gene transcription critical for the G1-S transition to occur. This has the effect of blocking the cell cycle (reviewed in (Ohtani et al. 2004). Based upon these and other observations, it is generally thought that the p53 and p21 proteins play an essential role in initiating the senescence mechanism, while p16 may be involved in its maintenance.

One of the primary markers used to detect replicative senescence and SIPS is senescence-associated β-Galactosidase (SA β-Gal) activity. This activity is visualized in a single cell when X-galactoside (5-Bromo-4-Chloro-3-indolyl-Beta-D-galactoside or X-Gal) is cleaved and a local blue precipitate is formed. The majority of cells (senescent and young) will express a lysosomal β-Gal that is optimally active at pH 4. At a pH of 6, only senescent cells are stained (Dimri et al. 1995). The SA β-Gal activity is also related to the replicative lifespan of the culture, as seen by the inverse relationship between [^{3}H]thymidine incorporation and SA β-Gal staining. Exceptions to this relationship do exist. Various environmental stresses, such as H_2O_2, or even different cell types, such as adult melanocytes, show increased staining that is not related to the residual growth

potential of the cell (Severino et al. 2000). While the mechanism behind the differing SA β-gal activity in senescent cells still evades researchers, one proposed idea is that there is a difference in the abundance or localization of splicing components based on the observation that increased lysosomal β-Gal mRNA is seen in senescent cells (Dimri et al. 1995). Changes in mRNA expression and distribution would contribute to the appearance of activity at pH 6 in senescent cells (Severino et al. 2000).

D) Telomere length variation and attrition

Telomere length is seen as a potential index of replicative history for somatic cells and as a possible biomarker for cellular aging. In cultured fibroblasts, one population doubling (PD) results in a telomere length reduction of 50 to 100 basepairs (bp) (Harley et al. 1990). *In vivo*, it is not currently possible to directly measure the number of cell divisions that accumulate in the history of a somatic cell. The strong relationship between subject age and telomere length allows estimates derived from measurements of telomere length to be used as a cellular "mitotic clock" (Allsopp et al. 1995). The relationship was once believed to be linear and telomeres were believed to shorten by some relatively constant amount with each somatic cell division. The connection between telomere length and replicative aging appears to be much more complex. Not only is telomere length attrition variable at different stages of life, but external factors, such as DNA damage and other stresses, can alter telomere length in an organism and subsequently alter its perceived residual replicative capacity.

Evidence indicates that telomere shortening in peripheral blood mononuclear cells (PBMC) occurs at a rapid rate during the first few years of life (Frenck et al. 1998; Rufer

et al. 1999; Zeichner et al. 1999). This suggests that there is either a much higher rate of telomere loss early in life or that the rapid telomere loss observed reflects a correspondingly rapid rate of cellular turnover. It is likely that elevated shortening rates in children are a result of the striking changes that occur in the human immune system during the first few years of life (functional anatomical and lymphocyte changes) (Zeichner et al. 1999). It appears that the rate of loss from childhood to old age also is not constant in humans. The rate of telomere loss is greatest early in life and it continually decreases with increasing age (Unryn et al. 2005). This rate change mirrors decreasing cell turnover in the circulating portion of the immune system with age.

A large variation in telomere length is also seen within the population. The variation exists both between individuals and between tissues of the same individual. In human cells, average telomere length is seen to range from 5 to 15 kilobases (kb) between individuals (Cross et al. 1989). Strong correlations have been made between monozygotic and dizygotic twins and telomere length, revealing that variation was largely genetically determined (Slagboom et al. 1994; Rufer et al. 1999; Graakjaer et al. 2004). Not only was telomere length similar in twins at a young age, but similarities in length were maintained throughout life. This observation suggests that the total number of divisions and the rate of division in specific tissues are remarkably similar between related individuals. These results suggest that environmental and epigenetic effects on telomere length are relatively minimal during life, at least in lymphocytes (Graakjaer et al. 2004).

In the same individual, different tissues displayed different telomere lengths related to differences in the rate of attrition between organs (Friedrich et al. 2000; Takubo

et al. 2002). This tissue-specific difference was based on the predicted levels of cellular turnover. Shorter telomeres were found in tissues with a higher proliferation rate (lymphoid tissue, gastrointestinal epithelium), while longer telomeres generally came from tissues with a lower or near static rate of turnover (myocardium, cerebral cortex). Despite the differences in attrition rates between organs and tissues, subjects with long telomeres in one organ had long telomeres in the other three tissues analyzed. It is also of important interest that telomere length differences exist between closely related cells. In T-lymphocytes, telomeric DNA from naïve $CD4^+$ cells are approximately 1.4 kb longer and they are able to undergo more extensive clonal expansion *in vitro* than memory cells from the same donor (Weng et al. 1995; Rufer et al. 1999). In B cell subpopulations, the opposite trend appears. Naïve cells differentiate into germinal-centre (GC) cells that undergo extensive clonal expansion and eventually give rise to memory cells. In this case, the memory cells show a longer average telomere length than the naïve cells (Weng et al. 1997). This is attributed to the substantial telomerase activity present in GC cells that allows for telomere increase and maintenance in these cells. Despite all of the changes seen between subpopulations of cells and between tissues of the same individual, the variation between subjects is still larger and more significant (Takubo et al. 2002).

Inter-sex variability has been found in various animal studies. Telomere length in females of the wild western mouse, *Mus spretus*, were 0.5-1.0kb longer than males (Coviello-McLaughlin et al. 1997). Gender differences were seen in all tissues examined (liver, kidney, spleen and brain). The same variability is not as apparent in humans. In male and female newborns, no difference is observed (Okuda et al. 2002). One cross-sectional study of adults revealed that on average females had longer telomeres than

males (0.28kb increase) (Benetos et al. 2001). Other studies, including a large population study using telomere fluorescence measurements of granulocytes and T lymphocytes, found either marginal or no significant telomere length difference between sexes (Rufer et al. 1999; Unryn et al. 2005).

E) Telomeres and disease

The reduced replicative capacity of cells in many accelerated aging syndromes has made these disorders popular in the study of telomere shortening. In the rare genetic accelerated aging diseases Hutchinson-Gilford progeria and Werner's syndrome (WS), telomeres were found to be significantly shorter, and the rate of attrition was found to be twice that of age-matched controls (Allsopp et al. 1992; Schulz et al. 1996). The maximum population doubling (PD) levels of fibroblasts from WS patients were approximately half that of normal cells despite the fact that senescence was seen to occur at a longer average telomere length (7kb compared to 5-6kb in controls) (Schulz et al. 1996). This supports the idea that factors in addition to the average telomere length are implicated in the exit from the cell cycle.

The congenital disorder Ataxia-telangiectasia (A-T) also shows enhanced telomere erosion (Tchirkov et al. 2003). Individuals with A-T, an autosomal recessive disorder often referred to as the "chromosome breakage syndrome" due to its high frequency of chromosomal breaks and rearrangements, suffer from an increased incidence of cancer, sensitivity to ionizing radiation, immunodefiency and premature senescence (Lisker et al. 1970; Swift et al. 1991). Shortening of telomeres in this disease likely involves oxidative damage and DNA damage checkpoints, especially given the

extensive evidence accumulated regarding the role of the ATM protein, the product of the mutated gene in AT, in DNA repair. Hydrogen peroxide treatment causes DNA damage in the form of single-strand breaks. In normal fibroblast cells, treatment not only increased the rate of telomere loss, but resulted in prematurely senescent cells (von Zglinicki et al. 1995). In A-T cells, oxidative stress caused a much more pronounced increase in the rate of attrition and chromosomal instability, effects that were suppressed with the use of the anti-oxidant phenyl-butyl-nitrone (Tchirkov et al. 2003).

Individuals with Down syndrome (DS) (trisomy 21 by cytogenetic analysis) also showed an accelerated rate of telomere loss with donor age (Vaziri et al. 1993). These individuals exhibit many phenotypes including mental retardation, immune dysfunction, thymus abnormalities and premature T-cell aging. Not only were losses on the order of 130 bp per year seen in peripheral blood lymphocytes *in vivo* (three times that of control individuals), but similar losses were seen *in vitro* when DS lymphocytes were grown in culture.

Studies examining immune system turnover in subjects with human immunodeficiency virus (HIV) have revealed that infection results in a sustained high level of viral replication which is matched by a strong immune response characterized by the accelerated turnover of T lymphocytes (Ho et al. 1995; Wei et al. 1995). Upon examining mean telomere length in HIV patients, a 5-9 fold accelerated loss was seen (Bestilny et al. 2000). Differences in attrition rates were present between subpopulations of cells, with $CD8^+$ cells shortening at a rate three times that of $CD4^+$ cells. As the disease progressed, differences in length compared to uninfected individuals also increased. The accelerated aging of the immune system and possible exhaustion of the replicative

capacity of cells is further validated by the finding that disease progression is more rapid in elderly patients whose immune systems contain precursor cells that have a reduced ability to proliferate (Ferro et al. 1992; Operskalski et al. 1995).

Since the connection was made between telomeres and replicative capacity, there has been debate on whether or not telomeres do become short enough to become a limiting factor to longevity *in vivo*. In 2003, one study linked telomere shortening with mortality and age-related disease (Cawthon et al. 2003). Survival data was examined from 143 elderly individuals whose blood was drawn 15-20 years earlier. Individuals with shorter telomeres had a mortality rate nearly twice that of those with longer telomeres. Individuals whose telomere lengths lay in the bottom half of the telomere length distribution had a heart disease mortality rate three times higher than those with telomeres in the top half of the distribution. Individuals with shorter telomeres were eight times more likely to have infectious disease related mortality, a situation likely attributed to a reduction in the ability of immune cells to rapidly divide. The study revealed no significant elevated incidence of cancer and cerebrovascular disease related to telomere length. In all, the findings greatly support the beliefs that telomeres might play a role in human aging. Additional work is required to determine whether telomeres contribute directly to a rise in mortality rates or if they regulate the progression of a process of senescence that raises mortality (Cawthon et al. 2003).

The immune system responds to signals from a large range of systems in the body, including the nervous and endocrine system. One product of this is that environmental effects, such as acute or chronic stress, can also elicit responses from the immune system (Segerstrom et al. 2004). In the case of a chronic stressor, the

components of the immune system are affected in a potentially detrimental way and a global immunosupression is seen. A recent study that examined telomeres in mothers of chronically ill children (and mothers of healthy children) provides insight into stress and its relation to telomere length (Epel et al. 2004). An increase in the number of years spent as a caregiving mother (i.e. mother of a chronically ill child) was associated with shorter telomere length, lower telomerase activity, but higher oxidative stress. It is important to note that in control mothers, telomere length was shorter under circumstances where perceived stress was high. These findings give insight into how stress might be linked to and promote the onset of age-related disease (Epel et al. 2004). However, this study was only correlative and no causal link between stress-induced telomere erosion, decreased telomerase activity and age-related disease has been established to date.

F) DNA damage and repair

The majority of cells, throughout their life, are exposed to some form of DNA damage. This damage, whether it is simple base changes or complex deletions or translocations, can lead to mutations, aging, cancer or even death of a cell or organism. Genome instability occurs when DNA damage affects any of the following four pathways of DNA replication: DNA repair, DNA damage checkpoints, transcriptional response, and apoptosis (Sancar et al. 2004). Damage can be caused by a wide variety of environmental agents and also through replication, recombination and/or repair errors. DNA backbone damage includes both single and double strand breaks and is caused by oxidative damage, ionizing radiation (IR) or can be formed as an intermediate during the repair process. Single base damage includes reduced, oxidized or fragmented bases and is

caused by ultraviolet (UV) irradiation, reactive oxygen species or chemical and alkylating agents that form adducts. A DNA cross-link is damage that includes inter-strand, intra-strand and DNA-protein cross-links and is caused by agents such as cisplatin, mitomycin D and nitrogen mustard (Zwelling et al. 1979).

In eukaryotic and prokaryotic organisms, a variety of enzymes and other proteins monitor DNA for specific sequence and/or structural damage. These damage sensors enable the recruitment of additional proteins that can either directly repair the damaged DNA or that can excise the damaged segment. There are a variety of DNA repair mechanisms including base excision repair, mismatch repair, double-strand break repair, and nucleotide excision repair. The base excision repair system (BER) is involved in the removal of altered nucleotides that have little effect on DNA structure (Sancar et al. 2004). In BER, a problematic base (incorrect or damaged) is removed by DNA glycosylase and an apurinic or apyrimidinic site (AP) is formed. An AP endonuclease nicks the damaged strand upstream of the AP site and as the 3' side of the nick is extended using a DNA polymerase (or polymerase complex), the AP site is excised. To complete the repair process, a DNA ligase (or ligase complex) seals the newly synthesized strand to form double-stranded DNA (Fortini et al. 2003).

The mismatch repair mechanism (MMR) is involved with the correction of mismatched nucleotides and small loops in DNA. Some mismatches occur through replication errors while some occur through other mechanisms, such as deamination. Much of the research done on MMR involves the bacteria *Escherichia coli* (*E.coli*) (Modrich 1989). In *E.coli*, the protein MutS recognizes and binds to the mismatched nucleotide on the DNA. A second protein, MutL, then binds and stabilizes the complex,

which then activates MutH (a protein involved in nicking the DNA strand). Excision occurs using a Helicase II protein (responsible for unwinding the DNA) and a single-stranded exonuclease. After excision, the DNA is resynthesized and ligated. In humans, all of the essential proteins are conserved and the steps in MMR are similar (Marti et al. 2002). The monomeric *E.coli* proteins, such as MutS, are replaced by heterodimers of related eukaryotic proteins, such as hMSH2/3 or hMSH4/5. In addition a dynamic protein called proliferating cell nuclear antigen (PCNA) is involved in stabilizing the hMSH heterodimer at the DNA site and is an essential processivity factor required for DNA synthesis (Umar et al. 1996).

Double-strand break repair employs one of two different mechanisms: homologous recombination (HR) or non-homologous end-joining (NHEJ). These systems are responsible for repairing double-strand breaks caused by reactive oxygen species, various chemicals and ionizing radiation (the most cytotoxic form of damage). The mechanism of HR is not completely understood but considerable progress has been made in recent years to characterize this process. In brief, the Rad51-family proteins bind to the double-strand break and recruitment of a homologous double-stranded DNA occurs. Strand invasion occurs and a unique structure is formed between the two double-stranded sections (called a Holliday junction or intermediate). DNA synthesis extends the gaps on both sections of DNA and enzymes cleave the overlapping single-strand crossovers thus forming two complete double-strand duplexes. The repair process is completed through DNA ligation (Thompson et al. 2001).

In NHEJ, an abundant protein heterodimer (Ku 70/80) and DNA-binding protein binds the ends of the double-strand break. The Ku heterodimers then recruit a DNA-

dependant protein-kinase (DNA-PK), ligase and X-ray cross-complementing (XRCC) protein to the DNA ends. An end-processing process called synapsis, which brings the two ends together, prepares the DNA ends for ligation and again the repair process is finished by ligation, in this case by ligase IV and XRCC4 (Lieber et al. 2003).

Nucleotide excision repair (NER) is the major pathway involved in the removal of small DNA sections that contain bulky lesions. The NER mechanism consists of two separate pathways that converge into a common core (de Waard et al. 2003). Global-genome NER (GG-NER) is a sub-pathway that is involved with the repair of helix-distorting base damage for the entire genome (including fixing damage in non-expressed regions and on the non-transcribed strand of expressed sequences).

Transcription-coupled NER (TC-NER) is a fast repair system that specifically repairs transcription blocking lesions on the transcribed strand of active genes (Hanawalt 1996). In both sub-pathways, NER functions like a "cut and fill" mechanism. The damage is first recognized and a protein complex binds to the damaged site. In the next step excision and removal of the damaged area occurs. Finally, the single-strand gap is filled by a DNA polymerase followed by ligation.

Many of the proteins involved in NER were originally identified in genetic complementation studies of the human DNA repair disease, Xeroderma Pigmentosum (XP) (Tanaka et al. 1994). The majority of XP patients has extreme UV-sensitivity and suffers from pigmentation abnormalities in sun-exposed skin-areas (Cleaver et al. 1981). Some individuals show accelerated mental retardation and many die of neoplasia, likely due to their thousand-fold increased risk of developing skin cancer. Individuals with the

XP disorder have defects in one or both subpathways of NER as a result of mutations in one of several genes, including XPA through XPG (Boulikas 1996).

The majority of research on NER proteins comes from work in yeast (*Saccharomyces cerevisiae, S.cerevisiae*) and in humans. A number of proteins in both systems are necessary for dual incision activity including XPA, replication protein A (RPA), transcription factor IIH (TFIIH), XPC/HR23B, XPG, and XPF/excision repair cross complementing gene 1 (ERCC1) (Aboussekhra et al. 1995). Damage is recognized in the GG-NER pathway by the XPC/HR23B subunit. Binding to the damaged DNA causes an extended distortion of the helical DNA structure and results in the subsequent recruitment of the TFIIH complex. Additional proteins bind and stabilize the complex (including XPA, a protein involved both in stabilizing the open complex and in checking the DNA for damage). The XPC/HR23B subunit is released and the process proceeds to the double strand incision step (which is shared for both GG-NER and TC-NER). In this portion of NER, the XPG and XPF/ERCC1 subunits excise the lesion. After excision, the damage-containing oligonucleotide is displaced (along with the NER proteins) and gap-repair proteins, including PCNA and DNA polymerase, bind and fill the gap. The process is completed with ligation by DNA ligase I (Reardon et al. 2002).

In TC-NER, the initial recognition and processing steps are different (from GG-NER). The initiation of TC-NER is believed to occur through the stalling of RNA polymerase at damaged sites on transcribed strands. The stalled holoenzyme slightly unwinds the DNA helix and allows for binding of the TFIIH complex to the damaged region and the subsequent displacement of the polymerase (Winkler et al. 2001). After this is complete, the repair process proceeds in the same manner as GG-NER.

In most cell systems, repair systems do not work perfectly (despite the fact that most types of damage can be repaired) (Mitchell et al. 2003). Many forms of damage do not interfere with replication and transcription and therefore, do not prevent cellular division and proliferation. It is this type of damage that often leads to mutations and cancer development. Damage directly inhibiting transcription, when not repaired, will likely result in cell death or cellular senescence (both of which may contribute to premature aging in that cell) (Mitchell et al. 2003).

Links between decreasing DNA repair capacity with age led to studies on DNA damage and repair in telomeres. The unique sequence, structure and association with binding proteins makes telomeric repair different from repair elsewhere in the genome. The rate of telomeric repair of UV-induced damage was found to be much slower than the repair of transcribed genes, but slightly faster than an X-chromosome inactive region (Kruk et al. 1995). A declining rate of repair was also seen with increasing donor age. In a study that followed telomeric repair after treatment with hydrogen peroxide, the repair of repetitive non-transcribed sequences, called minisatellites, occurred at a rate much higher than damaged telomeric DNA (Petersen et al. 1998). While the majority of minisatellites were repaired within a 24 hour period, a significant amount of telomeric oxidative damage still remained unrepaired after nineteen days. This result suggests that BER might be deficient or inhibited in telomeric DNA regions.

A recent study examined the binding of telomere-maintenance proteins TRF1 and TRF2 after oxidative stress (Opresko et al. 2005). A DNA lesion called 8-dihydro-2'-deoxyguanine (8oxoG) that is produced by oxidative stress greatly disrupted the amount of bound TRF1 or TRF2. While TRF1 binding was unaffected in the presence of a single-

stranded nick, a nucleotide gap reduced binding threefold. The creation of an AP site (involved in BER) and the conversion of any of the guanine bases in the TTAGGG repeat also caused a large reduction in TRF1 and TRF2 binding, even when there was an absence in helical distortion. All of the studies mentioned highlight the critical nature of the repair of telomeric DNA damage and the loss of telomere-maintenance proteins.

G) Chemotherapeutics and treatment

Clinically, many solid tumors are being treated more frequently with concurrent radiotherapy (RT) and chemotherapy (compared to RT alone). This approach has led to more favorable treatment results and improved outcomes during the last decade or so (Bartelink et al. 2002). Clinical trials in head and neck, lung and cervical cancer have seen a lower recurrence rate and an improved survival, but the timing of chemotherapy appears critical to the outcome (Thomas 1999). The main principle behind chemoradiotherapy (CRT) is that the RT portion of treatment targets the primary tumor and the chemotherapy portion of treatment removes the metastases that might exist. In some cases, attempts to pre-treat the primary tumor with chemotherapeutics in order to reduce the volume or cell numbers were not successful, primarily due to rapid repopulation of cancer prior to RT (Tannock 1996).

Chemoradiotherapy is frequently studied in head and neck carcinoma (HNC), a cancer that accounts for 400,000 new diagnoses worldwide each year. Chemotherapy relies on kinetics in which the number of tumor cells killed by a drug is proportional to the dose that is used. Due to the fact that only a certain percentage of the total tumor cells are killed during each chemotherapy course, multiple doses are regularly administered.

The primary target of the radiation treatment is the DNA molecule. Despite the fact that a variety of DNA lesions can be formed through RT, double-strand breaks and the formation of chromosome abnormalities are responsible for the major cell killing. The use of various chemotherapeutics can also enhance the potentially lethal effects of radiation damage by weakening the DNA molecule and rendering it more susceptible to injury (Milas et al. 2003).

There are a wide variety of anti-cancer drugs that target a number of different mechanisms (Lewis et al. 1996). Many of these drugs act only in one phase of the cell cycle while others are non-specific. The most commonly used classes of agents include: antimetabolites, alkaloids and taxanes, antibiotics, hormones and alkylating agents. The antimetabolites, such as 5-fluorouracil (5-FU) or methotrexate (MTX), mimic essential cellular metabolites and interfere with the synthesis of DNA (S phase), resulting in cell death. Alkaloids and taxanes, such as vincristine or paclitaxel, are mitotic inhibitors. The majority of these drugs primarily act in the M phase of the cell cycle through interference with the mitotic spindle or replication machinery and cause cell death.

Anti-tumor antibiotics, such as doxorubicin, modify the function of DNA (through intercalating between base pairs, binding to DNA or generating oxygen free radicals) and interfere with ribonucleic acid (RNA) synthesis. This type of drug either causes immediate cell death or cell death when the cells attempt to divide. Hormones and hormone antagonists, such as tamoxifen, are a cell-cycle non-specific group of drugs that alter the cellular environment, cellular permeability, and decrease tumor proliferation. Alkylating agents, such as cisplatin or cyclophosphamide, exhibit their cytotoxicity through the transfer of their alkyl groups to DNA and other intracellular components.

These alkyl groups can cause incorrect base pairing, DNA breakage and cross-linking, which cause cell death either immediately or when the cells attempt to divide.

In the majority of chemo-RT cases, cisplatin, or *cis*-diammine-dichloro-platinum(II) (c-DDP) is used either alone or in a multidrug regimen. Cisplatin has a broad range of antitumor activity and was found to demonstrate the largest enhancement in cell killing after irradiation (Bartelink et al. 1986). It is normally administered intravenously and is modified by aquation to its active form under low chloride concentrations that are present within the cell. In active form, it is able to react with nucleophilic sites to form DNA adducts (Kartalou et al. 2001). The N7 position of guanine is the primary target for c-DDP and the principal adducts formed by cisplatin occur at adjacent deoxyguanines (GpG) and are 1,2-intrastrand cross-links. Cisplatin is also capable of producing other forms of cross-links including: 1,2-intrastrand (ApG), 1,3-intrastrand (GpNpG), and interstrand (non-adjacent).

Transplatin or *trans*-diamminedichloroplatinum(II) (*t*-DDP), is the *trans*-isomer of c-DDP and is clinically ineffective. The t-DDP molecule is stereochemically limited and is unable to form intrastrand cross-links between adjacent guanine residues. Transplatin is, however, capable of forming interstrand cross-links between 2 guanines or a guanine and a cytosine residue. The ability of a cell to repair interstrand cross-links more easily than intrastrand cross-links might help account for the lack of antitumor efficacy in t-DDP (Perez et al. 2000). Even though both isomers are cytotoxic, the *trans* isomer is less toxic by a factor of twenty, which also contributes to its lack of use as an anti-tumor agent.

The adducts formed by platinum agents result in the very efficient inhibition of DNA replication, RNA transcription, cell cycle arrest (at G2) or apoptosis, even at levels sixty-fold lower than saturation (Kartalou et al. 2001). Measurements of adduct profiles in patients that were treated with c-DDP has demonstrated that tumor response and a favorable outcome is correlated to an increased level of 1,2-intrastrand cross-links (Reed et al. 1986; Reed et al. 1987).

Telomeric repeats found in vertebrates are an excellent target for cisplatin. As long as two or more tandem guanines are present, c-DDP targeting to DNA occurs at its highest level (Burstyn et al. 2000). The telomeric six bp repeat, $TTAG_1G_2G_3$, contains two potential GG sites for every 12 nucleotides (or 16.7% of all dinucleotide pairs in telomere repeats). That value is ~2.6 fold higher than would be predicted to occur in random DNA. The repair of DNA-cisplatin adducts can proceed through two different repair pathways; nucleotide excision repair and mismatch repair (Kartalou et al. 2001).

The NER pathway is considered to be the main mechanism that is involved in DNA adduct removal. Bacteria and mammalian cells deficient in NER show increased c-DDP sensitivity, and in *E.coli* and human cells, the repair of plasmid DNA (damaged with c-DDP) was significantly decreased in deficient cells (Popoff et al. 1987; Hansson et al. 1989). The efficiency of repair also varies between the different type of cisplatin adducts (Zamble et al. 1996). The 1,3-d(GpNpG) adduct that constitutes 5-10% of c-DDP lesions is repaired twenty times more efficiently in an *in vitro* reconstitution system than the 1,2-d(GpG) or 1,2-d(ApG) adducts, which constitute 65% and 25% of c-DDP adducts, respectively. No repair of the interstrand cross-links generated by cisplatin was

detected (Zamble et al. 1996). This differing rate of repair is attributed to structural and helical unwinding differences in adduct-containing DNA.

Many cisplatin resistant cell lines are seen to acquire mutations in various mismatch repair genes (Kartalou et al. 2001). Recognition of the cisplatin (but not transplatin) adducts in MMR occurs through the MutS homologues (i.e. hMSH2). Since no correct base can be incorporated opposite the c-DDP adduct, strand breaks will accumulate and the mismatch repair proteins may trigger cell-cycle arrest or apoptosis (Nehme et al. 1997).

H) Chemotherapeutics and telomeres

There is limited research examining telomere length during or after chemotherapeutic treatment. The majority of the *in vitro* efforts have focused on platinum compounds and have been interested in exploring drug resistance and sensitivity in a variety of cancer cell lines. One multi-drug study utilized established colon carcinoma lines that were grown in c-DDP and 5-FU for 100 days to create cancer cells that were rapidly dividing and highly resistant to antitumor agents (Kuranaga et al. 2001). Throughout the study, cells were collected for telomere length, telomerase activity and proliferation assays. In drug-resistant cell lines, a steady elongation of telomeres and increased telomerase activity was seen during treatment. Since no experiments were performed using a single agent, the study represents the synergistic effect of the two drugs. The telomere lengthening that was seen did not correlate well with the telomerase activity in the cell. Telomerase levels peaked around 30-40 days into the study and then declined, while the telomere length increase was very consistent. The authors speculated

that cells with short telomeres were selected against by the chemotherapeutics, resulting in a sub-population with longer telomeres.

In many malignant tissues, mean telomere length is found to be lower than the normal control tissue. Two groups of cancer cell lines (13 esophageal and 11 ovarian) had significantly shorter telomeres than control lines (Asai et al. 1998; Kiyozuka et al. 2000). In all 24 lines, further telomere reduction and increased telomerase activity was seen after c-DDP treatment. However, in contrast to the colon carcinoma study, cells with short telomeres tended to be resistant to cisplatin (not selected against by the agent). Telomere reduction was also seen in a liver cancer cell line that has inherently short telomeres (Zhang et al. 2002). In that study, a dose-dependent decrease in telomerase activity and a dose-independent decrease in telomere length were seen following c-DDP treatment. The growth inhibition and cell cycle accumulation (at G2/M) found after treatment were not related to telomere length or telomerase activity.

A comprehensive telomere length and cisplatin study was performed by Ishibashi and Lippard in the late 1990's (Ishibashi et al. 1998). Human cervical carcinoma cells (HeLa) displayed significant shortening of telomeres after twenty-four hours of low dose cisplatin treatment (0.5μM), while no such loss was seen in cells treated with higher c-DDP doses (1-5μM). The high dose of cisplatin resulted in a cell cycle arrest and apoptosis prior to the first cellular division, while the low dose allowed the majority of HeLa cells to complete at least one round of division. At the 48 and 72 hour time points, there was substantial telomere loss at all concentrations. In the populations that survived until day ten (0.5μM, 1μM subsets), telomere length was seen to have returned to pre-treatment lengths.

The authors of that paper interpreted that extensive shortening that was seen after high dose drug treatment was due to the replication blockage and apoptosis caused by c-DDP adducts. It was also suggested that at low drug concentrations, the nucleotide excision repair system was able to repair adducts present throughout the genome, except at the telomeric ends, thus allowing cell cycle progression. The unrepaired telomeric ends were dramatically shorter after replication was completed, and these truncated ends likely signaled programmed cell death (as seen by the lack of short telomeres at 10 days). The *in vitro* telomere and chemotherapy studies that were carried out suggest that there is some cell specific variation in telomerase activity and telomere length after chemotherapeutic treatment. In general it is apparent that telomeres are an excellent target for cisplatin, and non-resistant cancer lines tend to show a decrease in telomere length after treatment.

The effect of chemotherapy on telomere length is not extensively studied *in vivo*. A few studies have shown that telomere length is reduced in malignant tissues compared to surrounding normal tissue, in a number of malignancies including thyroid, brain, liver and head and neck cancer (Ohashi et al. 1996; Hiraga et al. 1998; Kammori et al. 2000; Patel et al. 2002). In a study that contradicts that trend, increased telomere length was found in malignant meningiomas compared to benign tumors (Chen et al. 2000). In that study, analysis revealed that patients with the longest telomere lengths had a significantly worse two-year disease free survival. The authors suggested that a greater proliferative potential in cells with long telomeres could account for this variance.

The majority of telomere and chemotherapy studies involve the use of combination chemotherapy. In one such study, telomere length differences were

examined in breast cancer patients that received either a standard or high-dose regimen plus autologous stem cell transplantation (Schroder et al. 2001). Blood was collected prior to and approximately five weeks after chemotherapy. In leukocytes isolated from the 33 patients (17 standard and 16 high-dose), no significant change was seen in telomere length or telomerase activity. Telomere length was clearly affected in some individuals (shown by an increase or decrease of up to 2.2kb), but the results were not consistent. The re-infusion of stem cells was not correlated with any changes in telomere length.

A second combination chemotherapy study found different results after chemotherapy. A recent study performed in Korea examined the length of telomeric DNA in fifteen non-Hodgkin's lymphoma (NHL) patients and thirty-nine controls (Lee et al. 2003). Various combination chemotherapy and chemoradiotherapy regimens were used to treat the NHL (based on tumor classification). Telomere length reduction of approximately 500 basepairs was seen after chemotherapy in the five patients that had blood draws pre- and post-treatment. Telomere length in NHL patients was seen to be significantly shorter than the control individuals. The telomere length comparison between patients and controls utilized post-chemotherapy terminal restriction fragment (TRF) lengths (instead of pre-chemo differences). Due to the fact that a loss is seen from chemotherapy, the pre-chemo to control patient differences would be less significant and less drastic than was shown. The authors stated that shorter TRF lengths in lymphoma patients might be due to an increased turnover of the immune system and that this likely increases the risk of secondary malignant neoplasms (Lee et al. 2003).

Another lymphoma study also found a telomeric repeat reduction after treatment (Ricca et al. 2005). Thirty-seven patients with previously untreated lymphoma were administered a high-dose sequential chemotherapeutic regimen followed by autologous stem cell transplantation (first high dose used cyclophosphamide, and the second high dose used cytarabine (Ara-C)). Mobilized peripheral blood progenitor cells were collected prior to treatment, after the first and final chemotherapy cycle (1 month apart), and 48 months after treatment. A significant average loss of 1000 basepairs was seen between the two middle timepoints (after high-dose treatments). No difference was seen between the pre-treatment collection and the collection after the first high-dose cycle. A slight decrease was seen in telomere length after 4 years, however the difference did not achieve statistical significance. Combined, the results from this study show that a drastic telomere length shortening, equivalent to that observed over 20 years of life, occurs after high-dose chemotherapy and stem cell transplantation, and that this loss might be maintained years after treatment. Even though the dramatic loss is seen after the Ara-C administration, additional unpublished work has revealed that etoposide also causes a similar shortening pattern. The authors attribute the large telomeric reduction to increased proliferative stress of stem cells undergoing two consecutive treatments.

The most comprehensive work to date examining telomere length in mononuclear cells after combination chemotherapy was done in twenty-four pediatric acute lymphoblastic leukemia (ALL) and solid tumor patients (Engelhardt et al. 1998; Franco et al. 2003). A typical telomere loss of 1000 basepairs was seen in ALL cases (as measured in lymphocytes and granulocytes). The rates of attrition in lymphocytes and granulocytes were 480bp/year and 360bp/year, respectively. In solid tumor patients, a

much greater loss of telomeric DNA was seen after treatment. Mean telomere lengths in leukocytes before treatment, during maintenance and after therapy were 10.9kb, 10.1kb and 9.7kb, respectively. The rate of loss was also much higher in solid tumor patients (~1200bp/year). No difference was seen between the rates of telomere loss in bone marrow mononuclear cells as compared to peripheral blood mononuclear cells. Despite treatment, the telomere lengths of the pediatric ALL patients prior to receiving a standard regimen were comparable, or not statistically different, to those from normal subjects of that age. The subset of patients receiving high-dose therapy and that showed a dramatic telomeric reduction might be at a higher risk of developing secondary malignancies (Neglia et al. 2001).

III. OBJECTIVES

Despite the fact that telomeres and telomere regulation are thought to play a pivotal role in organismal aging, our understanding of telomere dynamics in normal cells during the lifespan and after chemotherapy is limited. As a result, the objectives of my thesis focused on the following:

1. Examining the effects of various doses of the alkylating agent cisplatin and its clinically inactive analog, transplatin, on telomere length in normal human primary cells and primary cells deficient in the nucleotide excision repair pathway.

2. Analysis of mean telomere length in peripheral blood mononuclear cells of head and neck cancer patients throughout cisplatin and radiation therapy treatment.

3. Analysis and comparison of age, gender and other factors related to telomere length variation in normal individuals without cancer. Data from these studies provided control baseline data for experiments using samples from head and neck cancer patients.

IV. MATERIALS AND METHODS

A) Cell Culture

The primary human foreskin fibroblast cells (Hs68 – ATCC# CKL-1635) used in these studies were grown in Dulbecco's modified Eagle's medium (DMEM) supplemented with 10% (vol/vol) fetal bovine serum (FBS) and 50μg/ml penicillin and streptomycin. The nucleotide excision repair-deficient human fibroblast cell line Xeroderma Pigmentosum A (XPA strain GM05292) was obtained from the Coriell Institute for Medical Research (Camden, NJ) at a mean population doubling level (MPD) of 8. The XPA fibroblasts were heterozygous for two mutations in the XPA gene. One allele carries a G-to-C transversion at the 3-prime acceptor site of intron 3, and the second allele carries a C-to-T substitution that creates a nonsense codon in exon 6. The cells were cultured in modified Eagle's medium (MEM) supplemented with 15% fetal bovine serum, 2x essential amino acids, nonessential amino acids and vitamins. Both the Hs68 and XPA cells were grown in 150mm tissue culture dishes in cell growth medium at 37°C (with 5% CO_2). All cells were seeded at a density between 1-5 x 10^3 cells per cm^2 and were subcultured regularly to ensure that they were in log phase, using trypsin/EDTA to make single cell suspensions.

B) Chemotherapeutic treatment *in vitro*

Cultures of exponentially growing cells (Hs68 and XPA) were treated with either cisplatin or transplatin for 8 weeks in a variety of regimens. Cisplatin (*cis*-diammine-dichloro-platinum(II)), transplatin (*trans*-diammine-dichloro-platinum(II)) and

methotrexate (+/- amethopterin) were obtained from Sigma Chemicals. The 0.5 mg/ml cisplatin, transplatin and methotrexate stock solutions were prepared by diluting 10 mg of drug in 20 ml of tissue culture media. All additional dilutions were made with tissue culture media in order to achieve concentrations ranging from 0.0001 to 100 μg/mL.

Six different regimens were used for the *in vitro* study. They include: one-time low-dose (L1T) treatment (single administration, left on cells for 5 days), two-time low-dose (L2T) treatment (administration at week 1 and 5, left on for 5 days in each case), low-dose continuous (LC) treatment (permanently in culture media), one-time high-dose (H1T) treatment (single administration, left on cells for 5 days), two-time high-dose (H2T) treatment (administration at week 1 and 5, left on for 5 days in each case), and high-dose continuous (HC) treatment (permanently in culture media). Hs68 cells were treated with low or high dose concentration of 1μM or 5μM, respectively, while XPA cells were given 0.2μM or 0.5μM of c-DDP. The t-DDP treatment regimens only included low (5 μM) or high dose (50 μM) continuous treatment for both Hs68 and XPA cells.

In all cells treated with either platinum agent or untreated fibroblasts, cells were subcultured at a ratio of 1:2 (under conditions where cell division was seen) or the media was changed (under conditions where cell growth was not occurring). At week 8, cells were harvested by trypsin/EDTA treatment.

Senescence-associated β-galactosidase staining, flow cytometry analysis and Western blot analysis were performed on separate populations of cells that had been treated continuously with various doses of cisplatin, transplatin or methotrexate (which was used as a control non-alkylating drug, in order to test apoptosis, cytotoxicity,

senescence-associated staining and the cell cycle). The β-gal staining, FACS analysis and cell harvesting for Western blot analysis was carried out at two weeks after initial treatment.

C) Cytotoxicity assay

Trypan blue exclusion was used to determine the number of viable cells present on each tissue culture plate for both strains. The method uses a dye (0.4% Trypan blue in 1x phosphate-buffered saline (PBS)) to stain the cytoplasm of non-viable cells blue (while viable cells remain clear) (Maniatis et al. 1982). At each desired collection point, a small aliquot of cells was collected following treatment with trypsin/EDTA. The cells were centrifuged and resuspended in 1ml of 1x PBS. Twenty microlitres of media containing cells were combined with 20 μl of trypan blue solution and mixed. After 5 minutes, the mixture was transferred to the hemacytometer via capillary action and the cells were counted using a light microscope. A single large square represents a volume of $0.1mm^3$ or 10^{-4} cm^3, which is equivalent to 10^{-4} ml. The total number of cells per ml was calculated by multiplying the average cell count per large square by the dilution factor and by 10^4. The % of viable cells is equal to the total viable cells (unstained) divided by the total cells x 100.

D) β-galactosidase assay

Cells to be stained for β-galactosidase activity, were subcultured in 10 cm tissue culture dishes 10-12 hrs prior to the start of the protocol. The cells were washed in 1x phosphate buffer saline (PBS pH 7.3), then fixed with 0.5% gluteraldehyde (made up in

PBS pH 7.3) for 5 minutes at room temperature. After removing the gluteraldehyde and washing the cells with a 1x PBS/1mM magnesium chloride solution, cells were stained overnight at 37°C (without CO_2) in a freshly made X-galactoside solution (1mg/ml X-gal solution, 0.0012M potassium ferricyanide, 0.0012M potassium ferrocyanide, 0.001M magnesium chloride and 1x PBS, pH 6.0). The next day, the cells were washed in 1x PBS, pH 7.3, and digitally photographed using AxioVision software and a Zeiss Axiovert 200 Inverted microscope.

E) Cell Cycle distribution and apoptosis assay

Cells were washed two times with ice-cold 1x PBS (pH 7.3), harvested with trypsin/EDTA and were used for cell cycle and apoptosis analyses using flow cytometry. After collection and centrifugation at 1000 x g for 5 minutes, the pelleted cells were washed in ice-cold 1x PBS containing 5mM EDTA (E-PBS). Following another round of centrifugation, the pellet was resuspended in 2 ml of E-PBS and transferred to a plastic FACS tube (Falcon 35/2054). The sample was centrifuged and the resulting pellet was resuspended in 0.5 ml E-PBS and 1.5 ml of 95% ethanol. At this point, the cells were stored at -20°C overnight. The next day, the cells were centrifuged, washed in E-PBS, re-centrifuged and the supernatant was aspirated. Cell pellets were resuspended in 1 ml of freshly prepared propidium iodide (PI) solution (2.5μg/ml PI, 1mg/ml RNAse A, 1x PBS, pH 7.3). The cells were incubated in the dark for up to 4 hours at room temperature prior to analysis using a Becton-Dickinson FACScan flow cytometer, at the University of Calgary Flow Cytometry Core Facility.

F) Western blotting

Whole cell protein extracts were used for all of the western blot analyses in these studies unless otherwise indicated. The cells to be harvested were washed twice in ice-cold PBS. Following the wash step, 200µl of 2x sodium dodecyl sulphate (SDS) loading buffer was added (to each 15 cm tissue culture plate) and the cells were gently scraped into 1.5 ml Eppendorf tubes. The resulting samples were then sonicated three times for 10 seconds (setting #4 on Mandel Scientific Sonicator, model XL2020). Prior to loading, the samples were boiled for one minute at 100°C. Equal quantities of protein (as determined by Coomassie staining and actin-specific western blotting) were loaded on 12.5% SDS polyacrylamide gels for electrophoresis. After electrophoresis, the proteins were transferred to a pure nitrocellulose blotting membrane (BioTrace NT from PALL) for 120 volt-hours (V h) and membranes were then blocked overnight in PBS containing 0.1% Tween and 10% skim milk at 4°C. The next day the membrane was incubated with one of the following rabbit polyclonal antibodies (anti-p21, anti-p16, anti-p53 or anti-actin, which were obtained from Santa Cruz Biotechnology) diluted to a final concentration of 0.2µg/ml in 3% skim milk/PBS-Tween for 2 hours at room temperature. The membrane was then washed three times for 10 minutes in PBS-Tween and incubated with a goat-anti-rabbit horseradish peroxidase (HRP) conjugated secondary antibody (Chemicon) at a concentration of 0.1-0.3 µg/ml for 1 hour at room temperature. Following further washes, the membrane was incubated with ECL (enhanced chemiluminescence) reagent and exposed to Kodak X-OMAT film.

G) Patient Selection and Treatment

Subjects for the non-treated study group were selected through random-digit dialing (within the Calgary, Alberta area), with participants agreeing to a short interview and a 10 ml blood sample donation. The interview was used to collect information on factors that may be related to peripheral blood mononuclear cell (PBMC) telomere length, such as a medical history, tobacco use, parental ages, and physical activity.

In 2001 and 2003, the *in vivo* telomere projects (non-cancer group and HNC group) were reviewed and approved by the Conjoint Health Research Ethics Board of the University of Calgary, Calgary, Alberta. The research conforms to the Tri-Council and ICH Guidelines and with the Helsinki Declaration. All of the patients enrolled in this study had locally advanced squamous cell carcinoma of the head and neck, and were to be treated at the Tom Baker Cancer Center in Calgary, Alberta. Patients were enrolled over a period of fourteen months (September 2003 until December 2004) and were deemed eligible to participate in the study if they had no past cancer or cancer treatment history. Two subsets of patients were enrolled in this study: one subset undergoing radiotherapy (RT) treatment (enlisted with the help of Dr. Harold Lau) and another subset undergoing chemoradiotherapy (CRT) (selected with the help of Dr. Desiree Hao). The treatment regimen for the radiotherapy subset entailed 35 fractions of 2 Grays (Gy) over 7 weeks for a total dose of 70 Gy. The treatment regimen for the chemoradiotherapy subset was 20 mg/m^2 of surface area of cisplatin on day 1, 2, 3, 4 (week 1) and day 1, 2, 3, 4 (week 5 – unless otherwise indicated), plus 35 fractions of 2 Gy over 7 weeks.

H) Lymphocyte and DNA preparation

Blood samples (10 ml per draw) were collected from patients at the Tom Baker Cancer Center at three different time points: before treatment, day 28 (prior to the second chemotherapy cycle) and at the completion of treatment. Following blood sample collection, peripheral blood mononuclear cells (PBMCs) were isolated from whole blood using a Ficoll-Hypaque gradient. Cells were then washed and resuspended in PBS. A cell count was performed using a hemocytometer prior to cell lysis. Half of the total cells isolated were stored at -80°C in FBS and dimethyl sulfoxide (DMSO), while the remaining cells were lysed with SDS lysis buffer and digested with 100 μg/ml of proteinase K for 4 hours at 50°C. Lysates were extracted once with phenol/chloroform/isoamyl alcohol (25:24:1), once with chloroform and nucleic acids were precipitated with the addition of 0.5 volumes of 7.5 M ammonium acetate and 1.5 volumes of 100% ethanol. Samples were rehydrated, digested with DNAse-free RNAse for one hour at 37°C and subjected to an additional round of proteinase K digestion and subsequent precipitation.

I) Terminal Restriction Fragment analysis

Following genomic DNA isolation, five μg/sample of DNA was digested overnight at 37°C with restriction endonucleases for which there are no recognition sites within the telomeric DNA repeats (HinfI: G/ANTC and RsaI: GT/AC). The following day, a small aliquot ($1/10^{th}$ volume) was loaded and separated on a 1% agarose gel (prepared with 0.5x Tris-Borate (TBE) buffer) containing 0.5μg/ml of ethidium bromide

for 150 volt hours (Vh). A photograph was taken of the gel, and the visual quantification of each DNA digested helped ensure equal loading in the final agarose gel.

The 0.6% agarose gels used for separating digested DNA measured 20 by 25 centimeters, and contained a total of 19 wells (each of which could hold a maximum of 50 μl). The outside two wells were set aside for molecular weight markers (2 μl loaded per well), while the 15 inside wells were allocated for digested DNA samples. After the samples were loaded, gels were run for 700 Vh (12 hours at 60 V). Gels were washed with gentle shaking in denaturation solution (0.5M sodium hydroxide, 1.5M sodium chloride) and neutralization solution (1M Tris pH 8.0, 1.5M sodium chloride) for 45 minutes each. After removal of excess fluid, gels were placed on Whatman paper, covered with Saran wrap and placed on a gel drier for two hours (one hour at room temperature followed by one hour at 60°C). Dried gels were then washed in denaturation and neutralization solutions for 10 minutes each. Gels were rolled and placed in hybridization bottles with 25 ml of 5x standard saline citrate (SSC) containing 40 x 10^6 counts per minute (cpm) of [γ-^{32}P] end-labeled telomere probe ($(CCCTAA)_3$). The bottle was placed in a rotating hybridization oven for 18 hours at 37°C. After hybridization the gel was washed three times in 2x SSC at 48°C. The gel was then dried for 30 minutes at 60°C on Whatman paper and exposed to Kodak BioMax MR film for 1-7 days.

J) Labeling of the telomere probe and molecular weight marker

A single stranded oligodeoxynucleotide probe $(CCCTAA)_3$ was synthesized and diluted to a final concentration of 100 ng/μl. Five μl of synthetic probe was combined

with 5 μl of 10x kinase buffer (10mM Tris-HCl, 10mM $MgCl_2$, 50mM NaCl, 1mM dithiothreitol), 10 μl of [γ-^{32}P]-ATP (3000 Ci/mmol), 1 μl of T4 polynucleotide kinase (10 units) obtained from USB and 29 μl of distilled water (dH_2O). The reagents were mixed and incubated at 37°C for one hour. DNA loading buffer (10 μl) was added to the sample that was then electrophoresed through a 15% non-denaturing polyacrylamide gel for 400-600 V h. The gel was removed, covered with Saran wrap, and exposed to Kodak XAR film for 30 seconds. To elute the labeled oligonucleotides, the band was cut from the gel and placed in 1.5 ml of Tris-EDTA (TE) pH 7.6 at 4°C overnight. The following day, one μl of eluted probe was counted by liquid scintillation on a Beckman LS5000CE (typical results were 20,000 to 50,000 cpm per μl).

To prepare the molecular weight marker used in the TRF assay, two μl of HindIII-digested lambda DNA (1 mg/ml), 1 μl of dNTP mix (dATP, dGTP, dTTP), 1 μl of Klenow enzyme (5 units) obtained from Gibco BRL, 5 μl of [α-^{32}P] dCTP (3000 Ci/mmol), and 11 μl of dH_2O were mixed and incubated at 37°C. After one hour, the reaction was terminated through the addition of one μl of ethylenedinitrilo-tetra acetic acid (EDTA). All of the radioisotopes used in this study (γ-^{32}P-ATP and α-^{32}P d-CTP) were obtained from Amersham Biosciences.

K) Telomere length and statistical analysis

Autoradiograms were photographed and analyzed using Image J freeware (available at http://rsb.info.nih.gov/ij). In brief, rectangular selections were made around the lanes to be analyzed and two-dimensional optical density distributions were

generated. The analysis software incorporated into Image J allowed for the precise measurement of the weighted center of mass of each plot profile. Mean terminal restriction fragment length (mTRF) was determined by comparing the numerical values generated from each plot profile to the profiles of known molecular weight standards (labeled HindIII-cut lambda DNA). Consistent low molecular weight bands that were visible in all samples after hybridization (which likely represent subtelomeric DNA containing repeats or interstitial telomeric sequence) were also used as gel migration landmarks. To ensure mTRF length measurements were accurate, each sample was digested, separated and analyzed in triplicate and the raw mTRF data from the multiple runs were compiled to generate a final mTRF value. To eliminate any additional inter-assay variability, all of the collection time points from each patient were run on the same gel.

Data analyses were performed using the STATA statistical package (StataCorp, version 8.0). Relationships between telomere length, age and gender were assessed by single and multiple linear regression analysis. Repeated measures analysis was used to assess the between-subject and within-subject effects.

V. RESULTS

Part 1: Telomere length variation in human primary cells treated with chemotherapeutic agents.

Numerous phenotypic changes and alterations in the length of chromosome ends (telomeres) are seen in human cells following various types of stress, such as DNA damage by classic agents such as UV light and oxidative damage (Ben-Porath et al. 2005). The effects that are seen *in vitro* vary between cell types and type of damage, and do not necessarily duplicate conditions seen within an organism *in vivo* (Gershon et al. 2001). Despite this problematic situation, *in vitro* studies allow us to increase our current understanding of cell behavior in a semi-controlled environment. While many conditions and interactions that are present *in vivo* will be absent, cell culture provides a simple route to examining several parameters that might influence telomere length and culture changes in the human organism. The use of primary human fibroblast cells, such as Hs68 foreskin fibroblasts, rather than an immortalized cell line that might have alterations in various repair pathways or telomere maintenance proteins is important to minimize artefactual outside effects. Xeroderma Pigmentosum complementation group A fibroblast cells, which are used in this study, represent a relatively normal strain that is deficient in both global genome and transcription coupled nucleotide excision repair, a DNA repair pathway believed to play a role in adduct removal in the cell (Reardon et al. 1993). Their particular molecular defect is in the XPA endonuclease that functions in the initial stages of NER.

A) Viability differences in cells based on the chemotherapeutic drug concentration.

To examine the effect of chemotherapeutic agents on human fibroblast cells *in vitro*, the cytotoxicity of various anti-cancer agents was assessed using trypan blue exclusion (Maniatis et al. 1982). The percentage of cell viability is determined by dividing the number of viable cells (represented by a clear cytoplasm) by the total number of cells (viable and non-viable or blue staining cells) measured using a haemocytometer. Actively dividing cells were treated with the alkylating agents cisplatin or transplatin, or the antimetabolite methotrexate, an inhibitor of nucleotide metabolism, for 72hrs. After the incubation, 3 independent samples were counted for each anti-cancer drug used. As expected, a decrease in cell viability was seen as the concentrations of chemotherapeutic agent were increased (Figure 1, both panels). Both normal foreskin fibroblasts and XPA fibroblasts were susceptible to cellular death at lower concentrations of cisplatin and methotrexate than of transplatin (Figure 1A and Figure 1B, respectively).

As seen in Figure 1A, the concentration at which 50% inhibition of cell viability is induced (as compared to controls) or IC_{50} for Hs68 cells treated with cisplatin, methotrexate and transplatin were 2.5 μM, 12 μM and 75 μM, respectively. In XPA cells that are deficient in both arms of nucleotide excision repair, the IC_{50} for all three agents was lower than normal fibroblasts (cisplatin – 0.2 μM, methotrexate – 9 μM, transplatin – 30 μM) (Figure 1B). The most significant increase in drug sensitivity in deficient fibroblasts was seen using c-DDP (over a ten fold difference), while no significant change in sensitivity between the two fibroblast strains was seen after treatment with the antimetabolite, methotrexate. These data demonstrate the differences in drug sensitivity

Figure 1. Cytotoxic effect of chemotherapeutic drugs on Hs68 and XPA cells. **Panel A).** The effect on cell viability in Hs68 cells was evaluated following treatment with cisplatin (c-DDP – circles), transplatin (t-DDP – squares) or methotrexate (MTX – triangles) for 72 hours. Cells were seeded at a density of 1-5 x 10^3 cells/cm^2 in 100mm plates and incubated at 37°C overnight prior to treatment. After 3 days of treatment at a certain drug concentration (0, 0.1, 0.2, 0.5, 1, 2, 5, 10, 20, 40 or 100μM), viability was determined by trypan blue exclusion. The values displayed represent the mean +/- the standard deviation (SD) for three separate experiments. The dotted line represents the IC_{50}. **Panel B).** The cell viability of XPA cells was determined after 3 days of treatment with (c-DDP – circles), transplatin (t-DDP – squares), or methotrexate (MTX – triangles). As in Panel A), viability was determined by trypan blue exclusion and the values represent mean +/- SD for three separate experiments. The dotted line represents the IC_{50}.

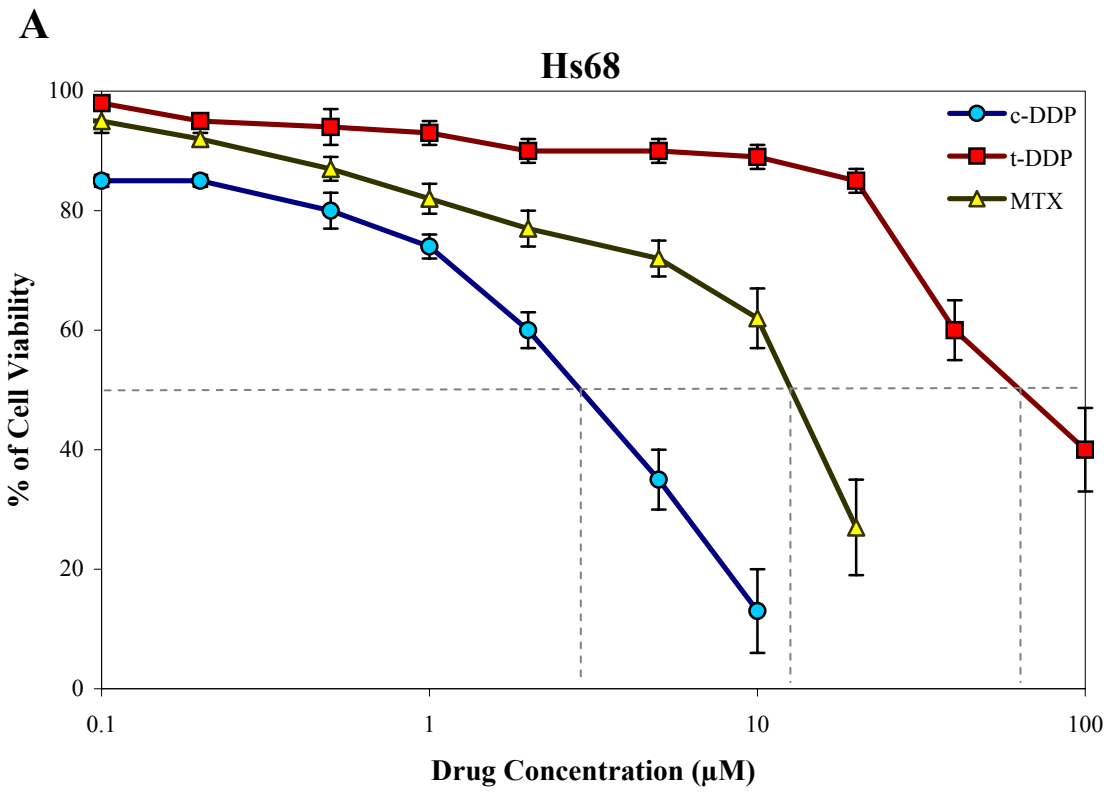
A
Hs68
100
80
60
40
20
0
% of Cell Viability
0.1
1
10
100
Drug Concentration (μM)
c-DDP
t-DDP
MTX

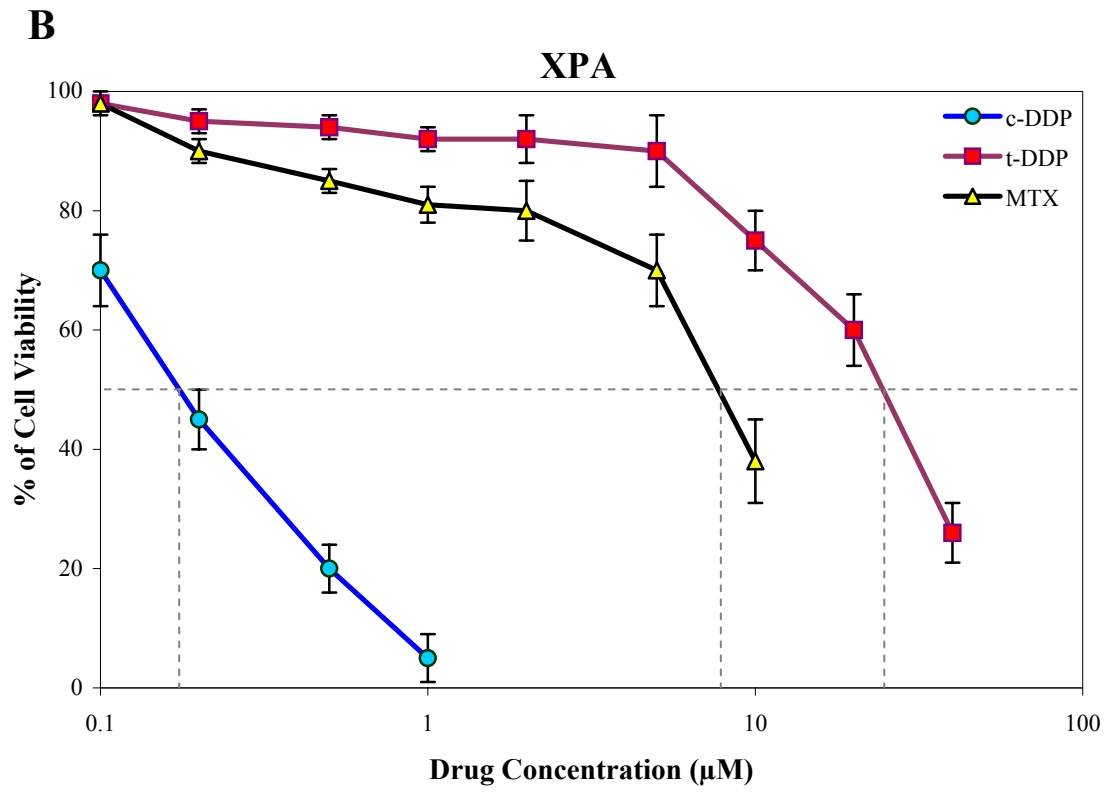
B
XPA
100
80
60
40
20
0
% of Cell Viability
0.1
1
10
100
Drug Concentration (μM)
c-DDP
t-DDP
MTX

between the two strains and the lack of substantial cytotoxicity in the cisplatin-analog transplatin, at similar drug concentrations.

B) Drug-induced cell cycle progression and cell patterns in normal and NER-deficient fibroblasts.

To evaluate whether the treatment of normal (Hs68) and NER-deficient (XPA) fibroblasts with various chemotherapeutics resulted in the alteration of cell cycle progression and distribution, the cell cycle patterns of both strains were examined for DNA content using propidium iodide (PI) staining and flow cytometry. An increase in sub-G1 population is associated with cells undergoing apoptosis. The sub-G1 population is associated with sub-diploid DNA content as a result of endonuclease activation and DNA diffusion (Nicoletti et al. 1991). Figure 2 shows histograms of DNA content for Hs68 cells. The left and right histograms of Panel A represent untreated cells at a confluence level of 80 and 95%, respectively.

The subset that had less contact inhibition had more cells in S-phase and G2 (8-10% each respectively, compared to 3-4%). When actively dividing Hs68 cells were continuously treated with 1 μM c-DDP for 24, 48 or 72 hours, a time-dependent accumulation of cells in the G2/M phase was seen. A small population of apoptotic cells was also evident by 72 hours of treatment. Panels C), D) and E), represent histograms of DNA content from Hs68 cells that were cultured in a low or high dose of cisplatin, transplatin or methotrexate for 2 weeks. A long-term low dose cisplatin treatment (Figure 2C –left panel) resulted in a G2/M phase accumulation similar to that seen after 72 hours (both had 33% of cells in G2). The high-dose c-DDP treatment of Hs68s (Figure 2C – right

Figure 2. Cell cycle progression in Hs68 cells treated with chemotherapeutic agents. Panel A). DNA content of Hs68 cells, which is represented by fluorescence intensity (FL2-area), was determined by flow cytometry before the addition of chemotherapeutic conditions. Analysis was done on cells that were approximately 80% confluent (left panel) and 95% confluent (right panel). DNA content at G0/G1 and G2/M are indicated by the left and right triangles on the X axis, respectively. Cells between these peaks are in S phase. **Panel B).** Histograms of DNA content in Hs68 cells after treatment with 1 μM of cisplatin (c-DDP) for 24, 48 and 72 hours, respectively. Cells treated continuously (without a change in medium) and collected at the indicated times. **Panel C-E).** Histograms of Hs68 cells after treatment with varying doses of chemotherapeutic agents (cisplatin – c-DDP, transplatin – t-DDP, methotrexate – MTX) for 2 weeks. The left and right panels represent a low and high dose of treatment, respectively.

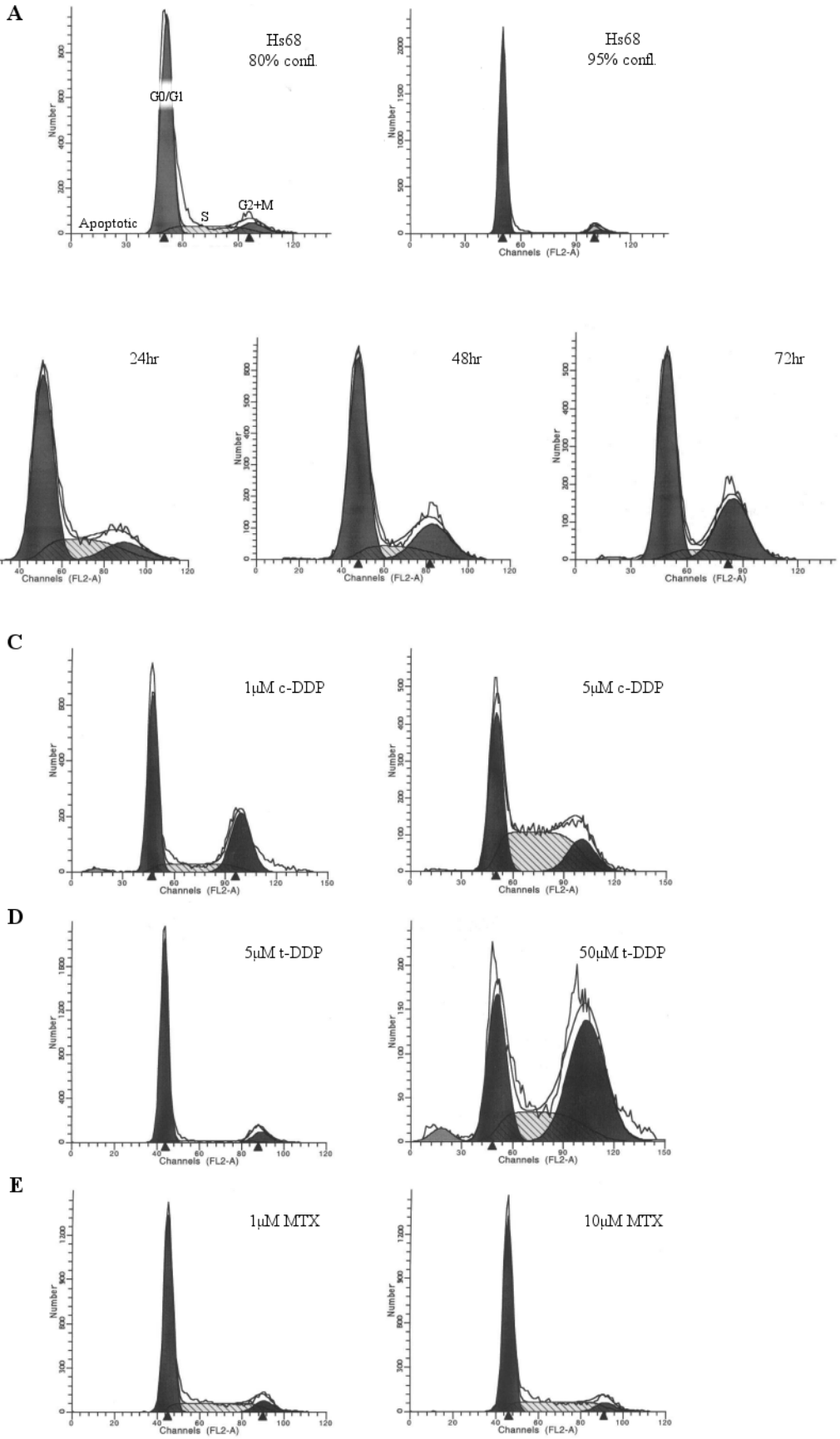
A
Hs68
80% confl.
G0/G1
S
G2+M
Apoptotic
Hs68
95% confl.
Number
Channels (FL2-A)
B
24hr
48hr
72hr
C
1μM c-DDP
5μM c-DDP
D
5μM t-DDP
50μM t-DDP
E
1μM MTX
10μM MTX

Figure 3. Flow cytometry analysis of XPA cells treated with chemotherapeutic agents. Panel A). DNA content of XPA cells, which is represented by fluorescence intensity (FL2-area), was determined by flow cytometry before the addition of chemotherapeutic conditions. Analysis was done on cells that were approximately 95% confluent. DNA content at G0/G1 and G2/M are indicated by the left and right triangles on the X axis, respectively. The cells between these peaks are in S phase. **Panel B).** Cell cycle progression in XPA cells after treatment with 0.5 μM of cisplatin (c-DDP) for 24, 48 and 72 hours, respectively. Cells treated continuously (without a change in medium) and collected at the indicated times. **Panel C-E).** Histograms of XPA cells after treatment with varying doses of chemotherapeutic agents (cisplatin – c-DDP, transplatin – t-DDP, methotrexate – MTX) for 2 weeks. The left and right panels represent a low and high dose of treatment, respectively.

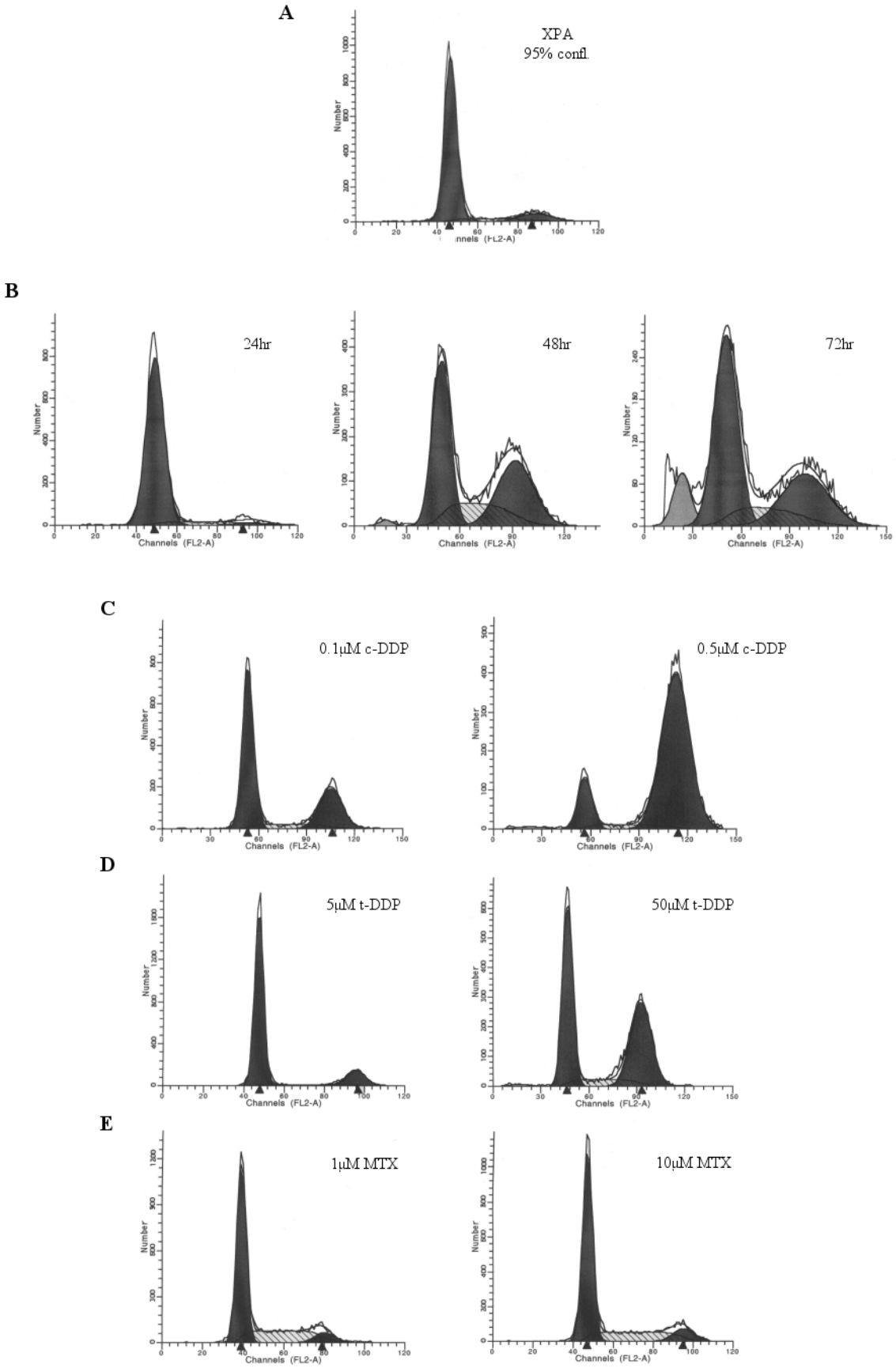
A
XPA
95% confl.
Number
B
24hr
48hr
72hr
Channels (FL2-A)
C
0.1μM c-DDP
0.5μM c-DDP
D
5μM t-DDP
50μM t-DDP
E
1μM MTX
10μM MTX

panel) gave a different cell cycle distribution (47% of cells in S-phase, 15% of cells in G2). Over the 2 week period of high-dose treatment, large proportions of cells had undergone apoptosis and were removed during routine media changes and subculturing (as seen through a very low cell density by visual inspection). The lack of substantial sub-G1 content could be due to variable drug susceptibility within a cell population. Cells that were more susceptible or less resistant, died within a few days of treatment, while some remaining cells that were less susceptible to high-dose treatment remained after 2 weeks of treatment. As evidenced by the histograms in Figure 2D, t-DDP caused a dose-dependent accumulation of cells in the G2/M phase. While continuous low t-DDP treatment of Hs68 cells (left panel) did not seem to affect cells (as compared to untreated), the high-dose t-DDP treatment caused a dramatic buildup of cells in G2 (48% in G2, 29% in G1, 20% in S). A small population of apoptotic cells was also evident. No difference in DNA content was seen between high and low dose MTX-treated Hs68 cells (Figure 2E). Both concentrations revealed an increase in S-phase cells. These results suggest that normal human fibroblast cells are arrested by cisplatin in the S and G2/M phases of the cell cycle and by transplatin at the G2/M phase of the cell cycle, while methotrexate caused a modest S-phase accumulation.

The cell cycle distribution of XPA cells after cisplatin, transplatin and methotrexate treatment is seen in Figure 3. The untreated cells (Panel A), were analyzed at a confluence level of approximately 95%. Contact inhibition is evident by the fluorescent-activated cell sorting (FACS) results (G1 – 91%, G2 - 6.5%, S – 2.5%). The second group of histograms (Panel B) represent DNA content of XPA cells after treatment with 0.5 μM cisplatin for 24, 48 or 72 hours. A substantial G2/M accumulation

is seen after 48 hours (G1 – 44%, G2 – 35%, S – 20%). By the 72 hour time point, an increase in sub-G1 (apoptotic) cells is seen, along with continued G2/M buildup. The long-term (2 week) treatment of NER-deficient cells as seen in Figure 3C, resulted in a dose-dependent G2/M arrest (low c-DDP G2 – 30.5%, high c-DDP G2 – 81.5%). A dramatic decrease in cell viability after 5-7 days prevented the FACS analysis of XPA fibroblasts at higher c-DDP concentrations.

Transplatin treatment of cells also resulted in a dose-dependent G2/M accumulation (Figure 3D). As in Hs68 cells, a low and high concentration of the antimetabolite, MTX, in XPA cells caused equal changes in the cell cycle (Figure 3E). Both doses displayed S-phase arrest (1μM – 28% S-phase, 10μM – 25% S-phase). In addition to results from flow cytometry, the cell cycle kinetics in XPA cells also appears exaggerated compared to normal foreskin fibroblasts following c-DDP treatment. Hs68 cells reached confluence faster and were subcultured more frequently than XPA cells (at low concentrations). Together, it is evident from these data that c-DDP dependent cell cycle effects are amplified in XPA cells versus Hs68 cells, despite the fact that both strains show cell cycle accumulation at similar stages of the cell cycle. Both cells behave in a similar manner after treatment with the same dose of transplatin or methotrexate suggesting that the effects being seen are not related to the XPA pathway.

C) Morphological changes and senescence-associated β-Galactosidase expression in fibroblasts after platinum treatment.

As young, healthy fibroblasts age *in vitro* and replicative senescence approaches, a gradual increase in cell size, cell flattening and increased heterogeneity is seen

(Cristofalo et al. 1969). As progression towards senescence proceeds, nucleus size, microfilaments in the cytoplasm and lysosomal bodies also increase (Cristofalo et al. 1993). A proliferation-independent senescence-like condition, in which growth arrest, protein expression changes and morphological changes occur, is seen in cells exposed to a variety of different stimuli and stresses (Drayton et al. 2002). To determine whether stress-induced premature senescence (SIPS) (Toussaint et al. 2000) occurs in young fibroblasts after anti-tumor treatment, Hs68 and XPA strains were continuously treated with cisplatin, transplatin or methotrexate for 2 weeks and SA-β-Gal activity and morphology were examined.

Young, healthy Hs68 cells (Figure 4A) show no SA-β-Gal staining, a relatively small cell size and homogeneity of cell sizes. SA-β-Galactosidase activity, which is normally seen in senescent cells, was present in young Hs68 cells (MPD 33) that were treated with low or high concentrations of c-DDP (Figure 4B). On average, half of cells at low concentrations and nearly all cells at high concentrations, displayed SA-β-Gal expression, but the staining intensity was much lower at 1μM c-DDP than 5μM c-DDP. The cisplatin-analog, transplatin, did not yield as much activity or intense staining as cisplatin (Figure 4C). Low-dose t-DDP treatment induced SA-β-Gal staining in one quarter of cells, while the high dose 50 μM treatment, resulted in activity in nearly all cells. The staining intensity at high concentrations of t-DDP was less intense than c-DDP treated cells, despite similar acquisition of senescent cell morphology. No increased SA-β-Gal staining was seen in MTX treated Hs68 cells compared to controls (Figure 4D). The Xeroderma Pigmentosum fibroblast strain that was used had a very low number of mean

Figure 4. Induction of β-galactosidase activity in normal fibroblasts following chemotherapeutic treatment. Panel A). Untreated early passage Hs68 cells (MPD = 33) were subcultured and treated with a freshly made X-galactoside solution (pH 6) overnight at 37°C (without CO_2). The following day, the cells were photographed with an inverted microscope. Cells that are positive for senescence-associated β-Gal (SA-β-Gal) activity are seen to stain blue. All panels are shown at equal magnification. **Panel B).** Hs68 cells that have been treated with low or high concentrations of cisplatin (c-DDP). Cells were cultured in c-DDP for 2 weeks prior to treatment with X-Gal solution. **Panel C).** β-galactosidase activity seen in Hs68 cells after treatment with low or high doses of transplatin (t-DDP) for 2 weeks. **Panel D).** Expression of β-gal in Hs68 human fibroblasts following methotrexate (MTX) treatment at low and high concentrations for 2 weeks.

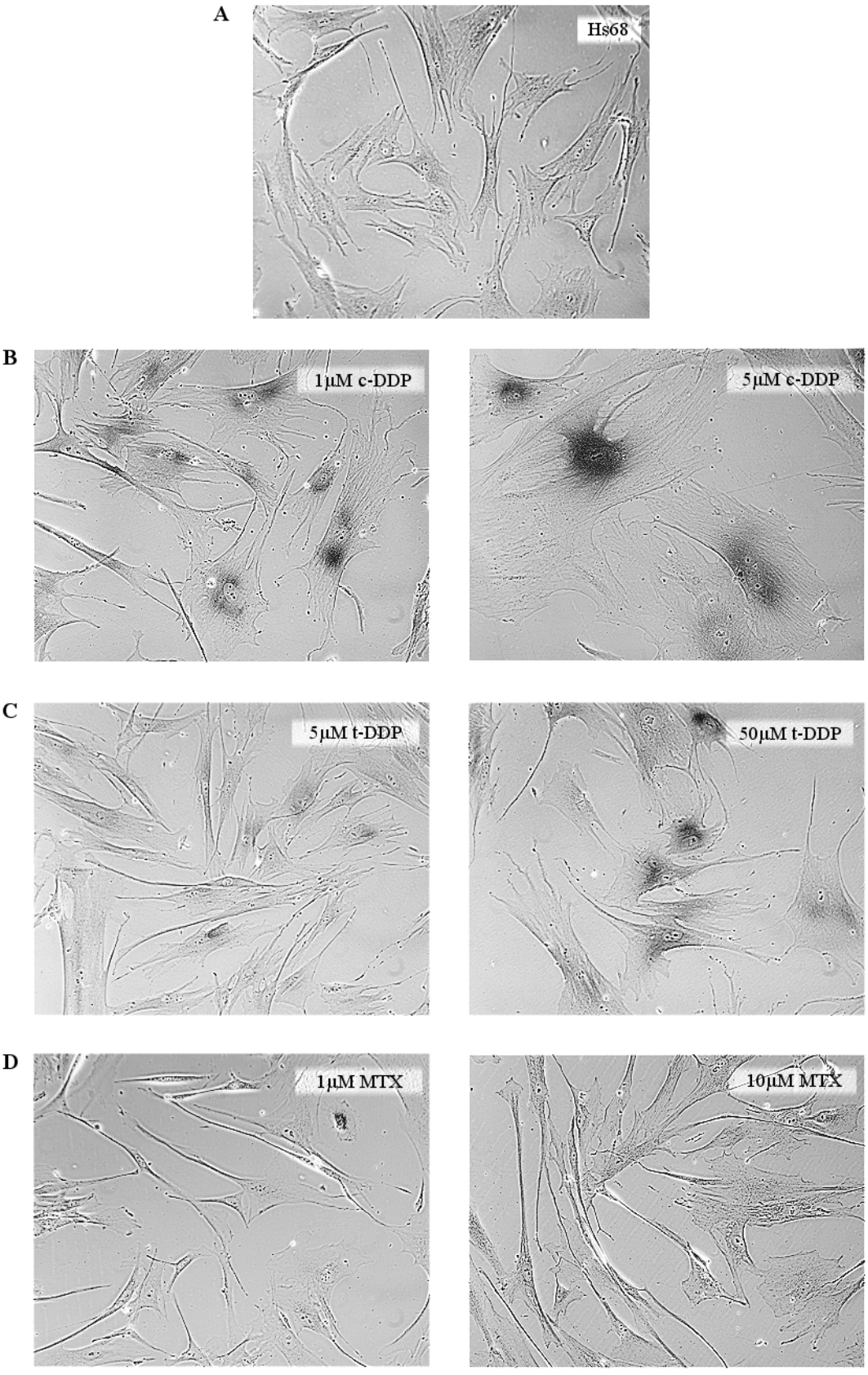
A
Hs68
B
1μM c-DDP
5μM c-DDP
C
5μM t-DDP
50μM t-DDP
D
1μM MTX
10μM MTX

Figure 5. Senescence-associated β-galactosidase activity in Xeroderma Pigmentosum A fibroblasts after chemotherapeutic drug treatment. Panel A). Untreated early passage XPA cells (MPD = 11) were subcultured and treated with a freshly made X-galactoside solution (pH 6) overnight at 37°C (without CO_2). The following day, the cells were photographed with an inverted microscope. Cells that are positive for senescence-associated β-Gal (SA-β-Gal) activity are seen to stain blue. All panels are shown at an equal magnification. **Panel B).** XPA cells that have been treated with low or high concentrations of cisplatin (0.1 μM or 0.5 μM c-DDP, respectively). Cells were cultured in c-DDP for 2 weeks prior to treatment with X-Gal solution. **Panel C).** β-galactosidase expression seen in XPA cells after treatment with low or high doses of transplatin (t-DDP) for 2 weeks. **Panel D).** Expression of SA β-Gal in XPA human fibroblasts following methotrexate (MTX) treatment at low and high concentrations for 2 weeks.

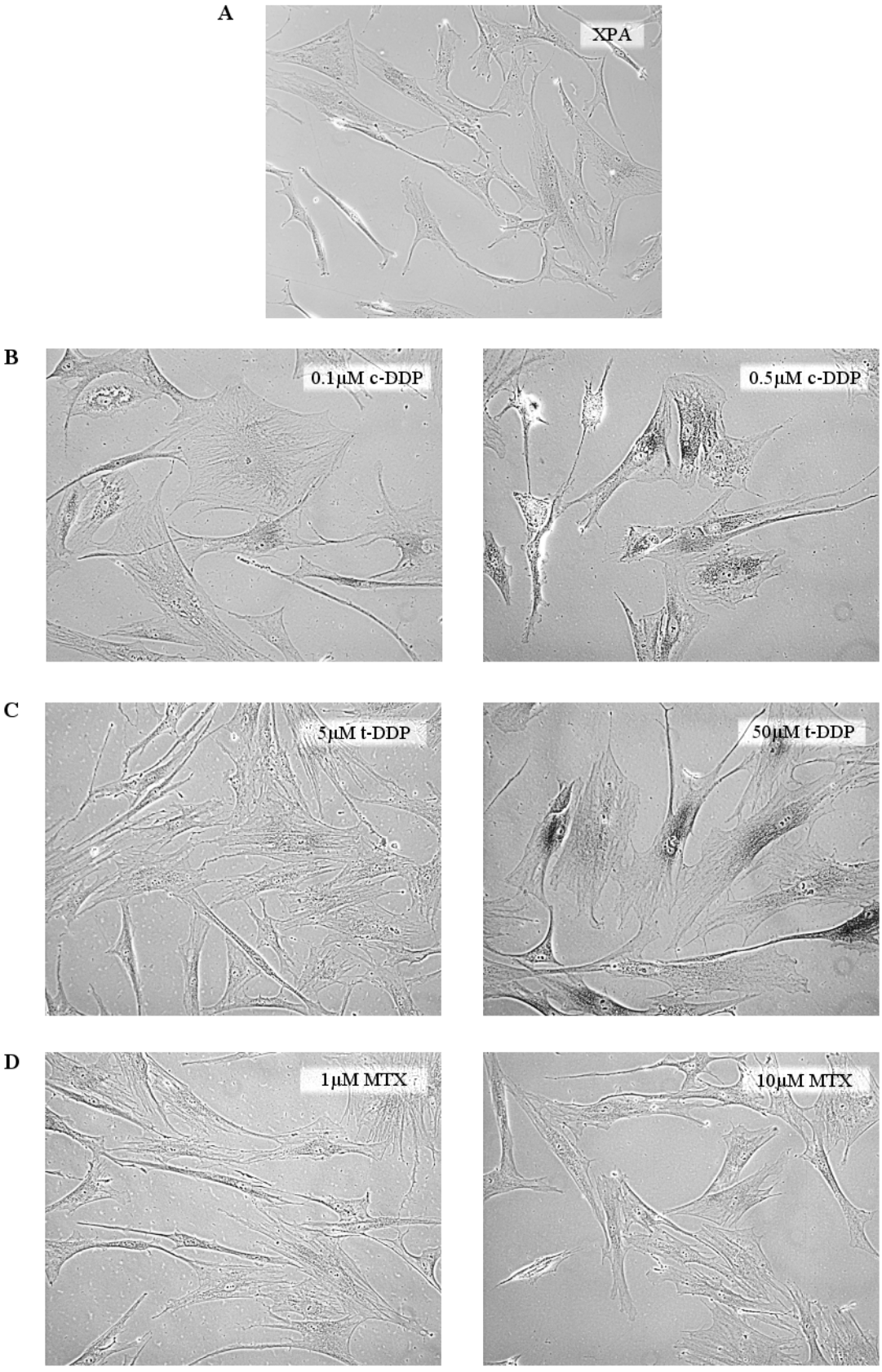
A
XPA
B
0.1μM c-DDP
0.5μM c-DDP
C
5μM t-DDP
50μM t-DDP
D
1μM MTX
10μM MTX

population doublings (MPD 11). In an untreated state, cells were similar to Hs68 fibroblasts in cell size, homogeneity, and in their absence of SA-β-Gal activity (Figure 5A). As the cells were cultured in cisplatin (Panel B), transplatin (Panel C) or methotrexate (Panel D), morphology changes were seen in many cells (even at the low doses used). Heterogeneity of cell size occurred within a few days of treatment, and the long term cultivation of cells over 2 weeks only increased the number of morphologically distinct cells. The low-dose c-DDP treatment of XPA cells resulted in lower SA-β-Gal activity compared to Hs68 cells (40% stained), but much more pronounced cell flattening and increase in cell size (Figure 5B –left panel). Many of the cells in the 0.5μM c-DDP (high-dose) treatment category displayed both elevated SA-β-Gal activity and characteristics of apoptosis such as cell shrinkage (Figure 5B – right panel). In contrast, very few apoptotic or pre-apoptotic cells were seen in XPA fibroblasts treated with a high-dose of t-DDP, even though over ninety percent of cells had visible and intense SA-β-Gal activity (Figure 5C). Both concentrations of MTX showed little, if any senescence-associated β-Gal staining (Figure 5D).

These data reveal that despite significant changes in morphology (which in some single cells exceeded the changes seen at high concentrations), none of the XPA cells at low c-DDP, t-DDP or MTX concentrations showed significant SA-β-Gal staining. From these data, senescence-associated β-Galactosidase staining after anti-cancer treatment appears to be independent of stress-induced morphology changes in this nucleotide excision repair deficient strain of human fibroblasts. This suggests that the XPA gene may be involved in the initiation or propagation of the signal that results in cells

acquiring SA-β-Gal activity, or that cells are so sensitive to these damaging agents that they undergo apoptosis (and are lost from the plate) before they begin to accumulate SA-β-Gal activity.

D) Expression of senescence-associated proteins after chemotherapeutic treatment

Numerous studies have linked the tumor suppressors, p53 and pRb, to the activation and induction of senescence, both replicative and stress-induced (Ben-Porath et al. 2005). The general proposal is that p53 activates its transcriptional targets, which in turn cause the inhibition of cell cycle progression through blocking the activity of various cyclin dependent kinases (de Magalhaes 2004). To clarify cell cycle, morphological and senescence-associated β-Gal changes seen in fibroblasts after alkylating agent treatment, three key players in the proposed senescence "program" were examined. The level of the tumor suppressor protein p53 and two of its transcriptional targets, $p16^{INK4A}$ and $p21^{WAF1/CIP1/SDI1}$, were studied after treatment in Hs68 and XPA fibroblast strains. Untreated Hs68 and XPA cells showed a low level of p21 (Figure 6A). In normal fibroblast cells there was no detectable basal p16, while XPA fibroblasts showed a low level of expression. Following treatment with low levels of c-DDP, t-DDP or MTX, Hs68 cells showed a modest increase in p16. Methotrexate treatment of cells at a concentration of 10μM caused a slight increase in p21 and a noticeable change in p16 (Panel A). Low or High concentrations of MTX had no effect on p53 status (Panel B). Both high c-DDP (5μM) and t-DDP (50μM) caused a dramatic increase in p16 and p21 levels (comparable or higher than those seen in newly senescent Hs68 cells). These effects were not seen in XP cells (right side of Panel A). While p16 levels were elevated under all treatment

Figure 6. Effect of chemotherapeutic agents on the expression of senescence-associated proteins. Panel A). Western blot analysis of growth regulator proteins, $p16^{INK4a}$ and $p21^{WAF1/CIP1/SDI}$ in Hs68 and XPA fibroblast cells after 2 week treatment with cisplatin (c-DDP), transplatin (t-DDP) or methotrexate (MTX). Low and high treatment with MTX represents 1 μM and 10 μM of drug, respectively. The low and high doses of t-DDP in both cell strains were 5 μM and 50 μM, respectively. Normal Hs68 fibroblasts were treated with concentrations of 1 μM c-DDP and 5 μM c-DDP, while XPA fibroblasts were incubated with 0.2 μM and 0.5 μM c-DDP (low and high doses, respectively). Hs68 whole cell lysate from cells at ~72 MPD was used as a control for senescent cells. **Panel B).** Analysis of p53 protein and β-actin (control) proteins in Hs68 foreskin fibroblasts following treatment with low or high MTX (1 μM, 10 μM), low or high c-DDP (1 μM, 5 μM), or low or high t-DDP (5 μM, 50 μM) for 14 days. The first lane (Hs68) represents an untreated control sample.

A

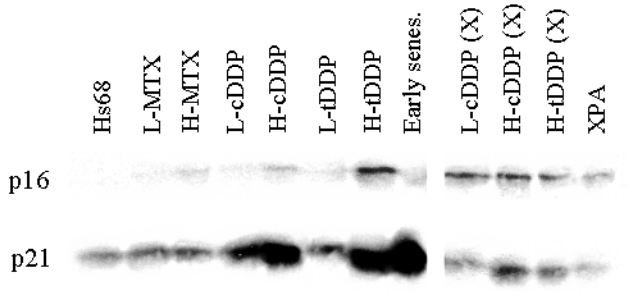
Hs68
L-MTX
H-MTX
L-cDDP
H-cDDP
L-tDDP
H-tDDP
Early senes.
L-cDDP (X)
H-cDDP (X)
H-tDDP (X)
XPA
p16
p21

B

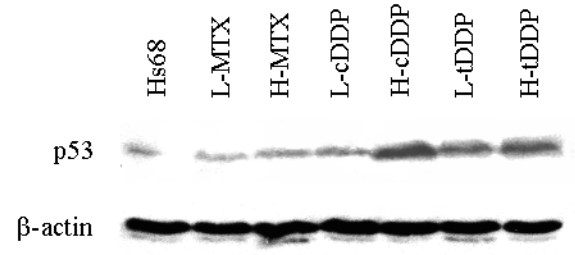
Hs68
L-MTX
H-MTX
L-cDDP
H-cDDP
L-tDDP
H-tDDP
p53
β-actin

conditions, a significant increase in p21 was only seen after c-DDP treatment at 0.5μM (high-dose). In normal fibroblasts, the only treatments that resulted in a significant p53 increase versus untreated cells were high- dose c-DDP and t-DDP (much higher in cisplatin) (Panel B). From these data it is evident that a high dose of either alkylating agent in Hs68s causes a significant increase in proteins that are involved in senescence and the inhibition of cell cycle progression, namely p16, p21, and p53. A low dose of any of the three agents did not affect the levels of the 3 proteins to a significant extent. In XPA cells, the level of p16 increased after any form or dose of platinum treatment , while p21 increases were only seen following high-dose treatment.

E) Telomere length changes in fibroblasts due to platinum treatment.

The attrition of telomeres in somatic cells throughout the replicative aging of a cell can be used as a biomarker for replicative cell history and biological cell age (Allsopp et al. 1995). While the age-related telomere loss appears relatively constant under unchanging cell culture conditions, the introduction of DNA damage, such as that due to oxidative damage, can dramatically alter the rate of loss that is seen (von Zglinicki et al. 1995). Regardless of the fact that a decrease in telomere length is seen after short-term cisplatin treatment in cancer cell lines, no study to date has examined the telomere length variation in primary cells after treatment. To determine if changes in telomere length occur after platinum treatment, a study was undertaken to compare mean terminal restriction fragment (mTRF) lengths in normal and NER-deficient fibroblasts following a variety of treatment regimens. The treatment design was meant to mimic the cisplatin

regimen given to head and neck cancer patients *in vivo* (see section IV), and was also design to address the effects of continuous platinum treatment.

In brief, 6 regimens were used for this *in vitro* study. They include: one-time low-dose (L1T) treatment (c-DDP single administration, left on cells for 5 days), two-time low-dose (L2T) treatment (c-DDP administration at week 1 and 5, left on for 5 days in each case), low-dose continuous (LC) treatment (c-DDP permanently in culture media), one-time high-dose (H1T) treatment (c-DDP single administration, left on cells for 5 days), two-time high-dose (H2T) treatment (c-DDP administration at week 1 and 5, left on for 5 days in each case), and high-dose continuous (HC) treatment (c-DDP permanently in culture media). Hs68 cells were treated with low or high doses of 1μM or 5μM, while XPA cells were given 0.2μM or 0.5μM of c-DDP. These doses were based upon initial studies determining the IC_{50} of each agent on the two cell strains. The t-DDP treatment regimens only included low (5 μM) or high dose (50 μM) continuous treatment for both Hs68 and XPA cells.

In all cells treated with either platinum agent (including controls), cells were harvested at week 8, genomic DNA was isolated and TRF analysis was performed. Figure 7 shows a Southern blot analysis containing telomere length distributions from a subset of the samples collected. A mean TRF loss is seen in the majority of treatment regimens. Figure 8 summarizes the treatments and their resulting mTRF lengths as compared to untreated controls. The top panel (A) represents the c-DDP treatment of Hs68 and XPA cells, while the bottom panel (B) represents continuous transplatin treatment in both strains. The most dramatic reductions in telomere length were seen in long-term and high-dose c-DDP treatment regimens. Unfortunately, extensive cell death and low cell viability after high-

Figure 7. Telomere length in Hs68 and XPA fibroblasts after long-term treatment with anti-cancer drugs. Autoradiogram showing telomere terminal restriction fragment (TRF) length distributions following the treatment of Hs68 (H) and XPA (X) cells with cisplatin (c-DDP) or transplatin (t-DDP). Genomic DNA isolated from both cell strains, after a eight week treatment period, was digested with RsaI and HinfI restriction enzymes and samples were electrophoresed in a random order on the gels to ensure that analyses were performed blind. M represents radiolabelled Hind-III digested lambda DNA (molecular weight marker).A variety of treatment regimens were performed on both cell strains. In Hs68 cells, c-DDP L represents a one-time treatment of 1 μM, L2 represents a two-time treatment of 1 μM (4 weeks apart) and Lcont represents a continuous treatment of 1 μM cisplatin. High dose one-time (cDDP H) and two-time (cDDP H2) treatments of Hs68 cells represent a concentration of 5 μM cisplatin. The high dose treatment of XPA cells (X cDDP H) represents a one-time treatment with 0.5 μM cisplatin. The continuous treatment of Hs68 and XPA cells with transplatin at low (tDDP Lcont) and high (tDDP Hcont) concentrations represent a final dosage of 5 and 50 μM, respectively.

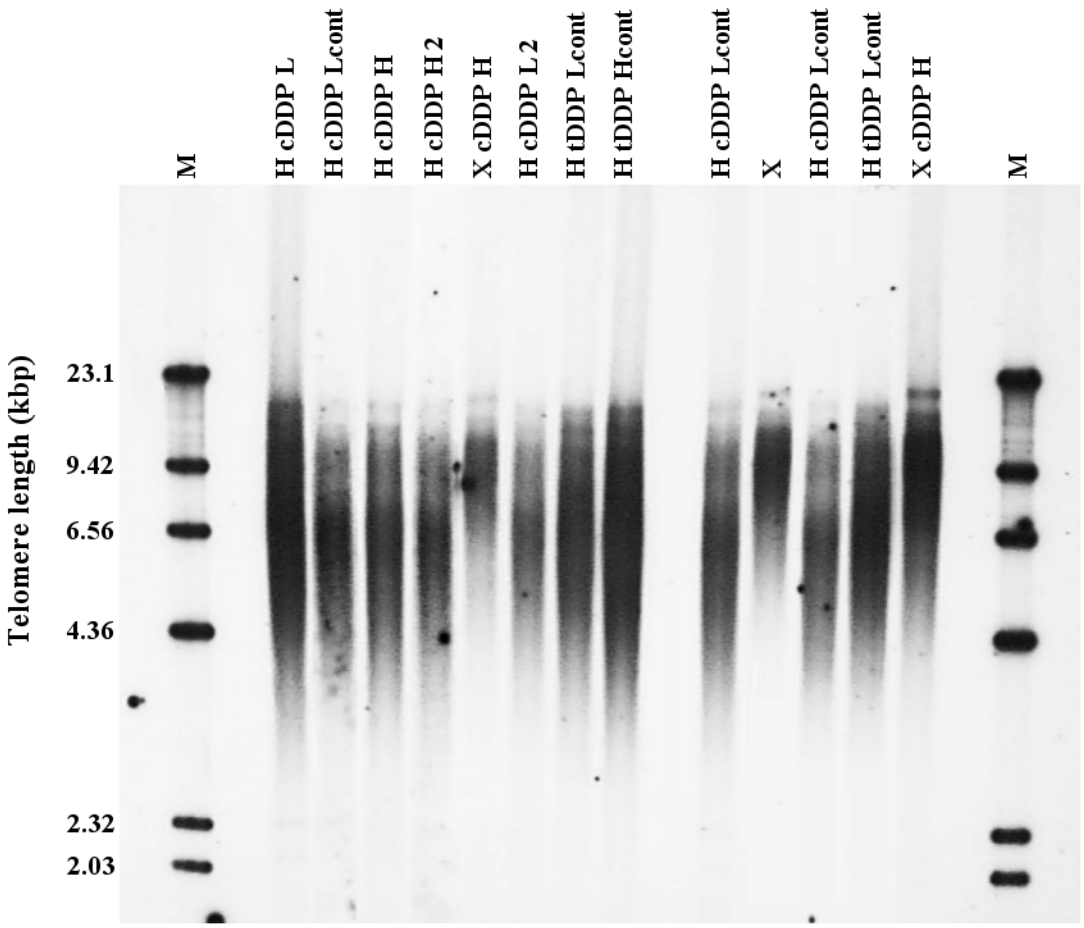
M
H cDDP L
H cDDP Lcont
H cDDP H
H cDDP H2
X cDDP H
H cDDP L2
H tDDP Lcont
H tDDP Hcont
H cDDP Lcont
X
H cDDP Lcont
H tDDP Lcont
X cDDP H
M
Telomere length (kbp)
23.1
9.42
6.56
4.36
2.32
2.03

Figure 8. Loss of telomere length following long-term treatment with chemotherapeutic drugs in Hs68 and XPA cells. Panel A). Mean telomere length changes (mTRF Δ) after a eight week cisplatin treatment period in Hs68 and XPA cells. Error bars represent standard deviation from three independent experiments. Cisplatin concentrations used were 1 μM (Hs68 Low), 5 μM (Hs68 High), 0.2 μM (XPA Low) and 0.5 μM (XPA High). **Panel B).** Changes in mTRF following continuous transplatin treatment in Hs68 and XPA fibroblasts. Transplatin concentrations used were 5 μM (Hs68 Low and XPA Low) and 50 μM (Hs68 High and XPA High). Standard deviation from three separate experiments was used to generate the error bars seen.

A

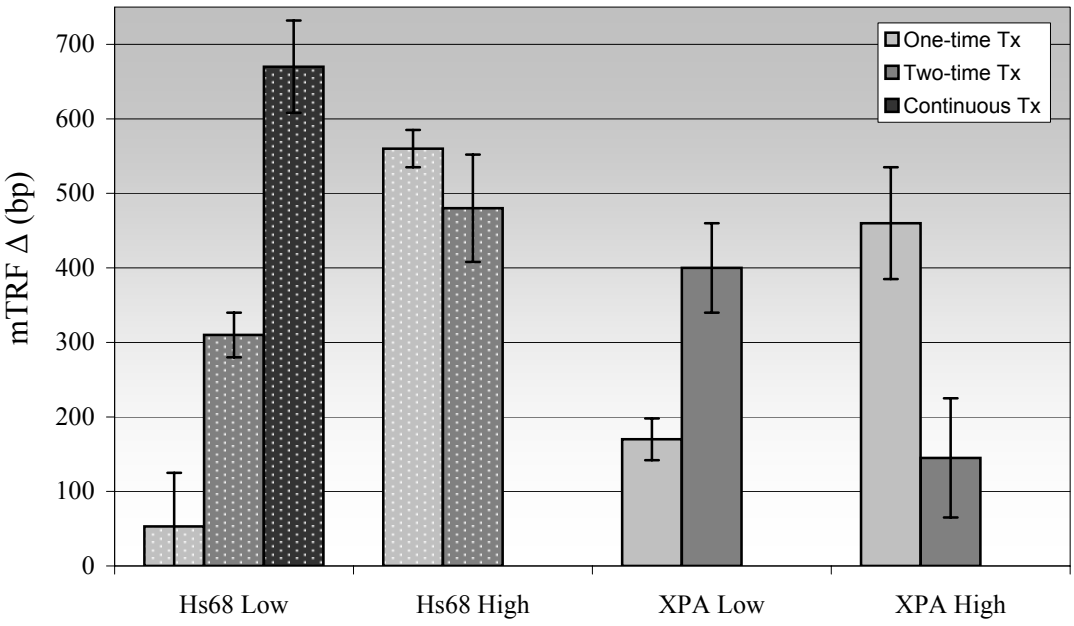
One-time Tx
Two-time Tx
Continuous Tx
mTRF Δ (bp)
0
100
200
300
400
500
600
700
Hs68 Low
Hs68 High
XPA Low
XPA High

B

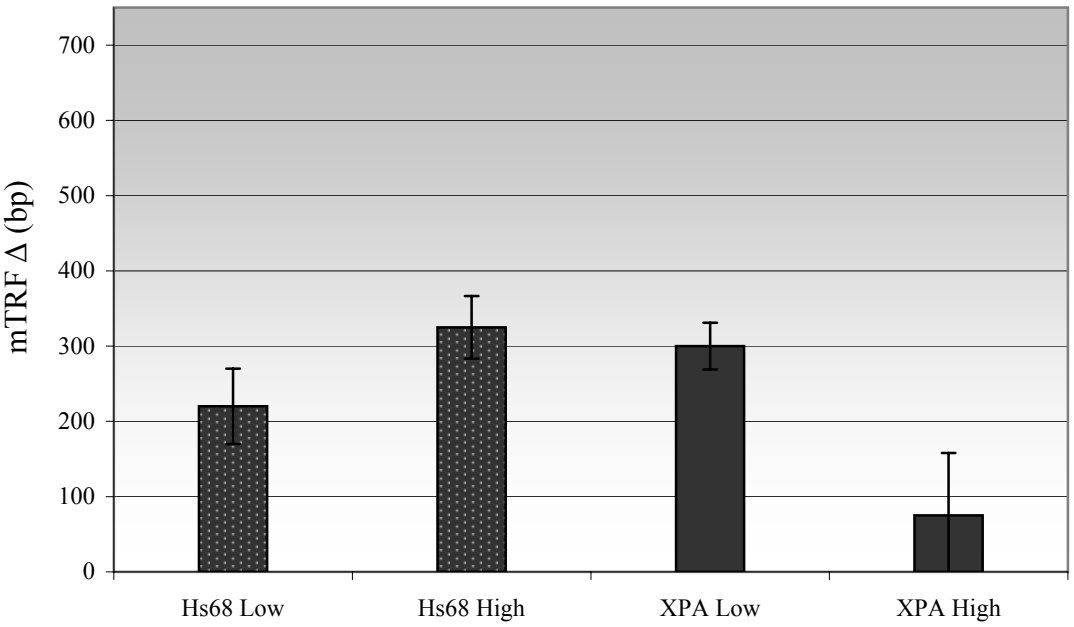
mTRF Δ (bp)
0
100
200
300
400
500
600
700
Hs68 Low
Hs68 High
XPA Low
XPA High

dose continuous treatment prevented Hs68 and XPA cells in that regimen from reaching the ten-week time-point (therefore no mTRF data is available at most continuous treatment conditions).

Repeated-measures analysis was used to compare control (untreated) samples to each treatment regimen. In c-DDP treated Hs68 cells, a significant difference was found in all the treatment regimens except the low dose single treatment. Low dose one-time, two-time and continuous treatment resulted in an average telomere loss of 53bp, 310bp and 670bp, respectively (p values at $\alpha = 0.05$: L1T – 0.292, L2T – 0.017, LC - <0.0001). High dose one-time and two-time treatment resulted in average losses of 560bp and 480bp, respectively (p values: H1T - <0.0001, H2T – 0.034). In XPA cells, significance was only seen in the two-treatment low dose (400bp loss, $p = 0.002$) and the one-treatment high dose regimens (460bp loss, $p = 0.036$). In addition, a one-way analysis of variance (ANOVA) was used to evaluate whether there were significant differences between the various groups. It was found that there was a significant difference between the Hs68 and XPA low cisplatin groups ($p < 0.001$), and that there were significant differences within the low c-DDP groups of each cell strain (Hs68 – $p < 0.0001$; XPA – $p = 0.009$). Other differences between groups that may have been present were not found to be significant. In transplatin treated fibroblasts, there was also a significant difference in all of the regimens, except for one. Low and high dose t-DDP treatment resulted in an average telomere loss of 220bp and 325bp, respectively, in Hs68 cells, while low and high doses of t-DDP resulted in losses of 300bp and 75bp, respectively, in XPA cells (p values: Hs68 LC – 0.016, Hs68 HC – 0.008, XPA LC – 0.001, XPA HC – 0.981). The high dose continuous treatment of XPA cells with t-DDP caused no significant change in

mTRF. Together these results suggest that platinum agents do cause significant telomere attrition in primary cells *in vitro*, and that there also appear to be differences to this general rule at certain doses in cells that are deficient in nucleotide excision repair.

Part 2: Telomere length variation in humans and chemotherapy

Chemotherapeutic agents cause cycles of injury and repair that may be involved in telomere shortening. The concept that telomeres represent cellular "clocks" for predicting proliferative potential (Vaziri et al. 1994), reinforces the importance of examining situations in which drastic rapid shortening might occur. If a significant telomere loss was substantiated *in vivo*, and the loss was indeed permanent, patient immune function may be compromised through a decreased residual replicative potential. To determine if telomere length is altered in individuals with cancer and if the treatment of those patients with chemotherapy causes a rapid and permanent reduction in telomeric DNA, the mTRF lengths of two subject groups were examined. The first group was limited to randomly recruited individuals without cancer (to comprise the control set), while the second group contained head and neck cancer patients.

A) Age and gender difference in the rate of telomere length loss

The age-related shortening of telomeres in somatic cells constitutes a rate of loss reported to be between 15 and 55 bp per year in adults (Hastie et al. 1990; Vaziri et al. 1993); (Slagboom et al. 1994; Mondello et al. 1999) (Rufer et al. 1999; Bestilny et al. 2000; von Zglinicki et al. 2000; Cawthon et al. 2003). The linear regression of mTRF data versus individual age for our control set of 125 individuals without cancer generated

a mean telomere length decrease of 22 bp for each increasing year of age ($p<0.0001$) (Figure 9A). When the individual age range was further broken down into smaller pieces, differences were seen between young and old control subjects. Individuals between the ages of 30 and 49 showed a mean TRF loss of 51.3 bp yr^{-1}, while subjects whose age was between 50 and 80 years showed an average telomere loss equal to 19.8 bp yr^{-1}. Upon further examination of the median ages of subjects from the eight studies listed above (Table 1), it was evident that a different average telomere loss occurred depending upon subject age (Figure 9B). From the control data set, it was also apparent that gender differences may also play a role in telomere loss. The slope generated from the linear regression of telomere length versus age was significantly different between males and females (Figure 9C), despite the fact that no overall mean TRF difference could be seen between the two groups (Males - 7020 bp, Females - 7090 bp). Males lost telomeric DNA at a rate twice that of females, a finding which is in agreement with a recent publication (Nawrot et al. 2004). Further analysis of the control set revealed a difference in the telomere length of offspring as a function of paternal age (Figure 10). Offspring had 22 more base pairs for each year that their father was older (after adjusting for subject age) ($p = 0.01$). This novel finding, published in a recent edition of the journal Aging Cell, might explain the variability of telomere length seen in the human population (Unryn et al. 2005). Although many of the findings in the control group were significant and novel, the major focus of the data set was to provide a control for the head and neck cancer patient group.

Figure 9. Differential rate of telomere length loss in healthy controls at different ages. Panel A). Plot generated from the linear regression of mean TRF from 125 control individuals versus age. Each open circle represents a subject sample, and the solid line represent the linear regression trendline. A loss of 22 base pairs per year of subject age is seen ($p < 0.0001$). **Panel B).** The line shown was generated from values in this study. The circles show the various rates of telomere blood loss in a variety of studies listed in Table 1, all of which have p values <0.01. **Panel C)** A difference in the rate of mTRF loss between males (open boxes) and females (closed circles) is seen by the differing trendlines in the left and right panels. Male mTRF and female mTRF were each regressed versus donor age (left and right panels). A loss of 31 and 14 base pairs per year is seen in males and females, respectively.

A

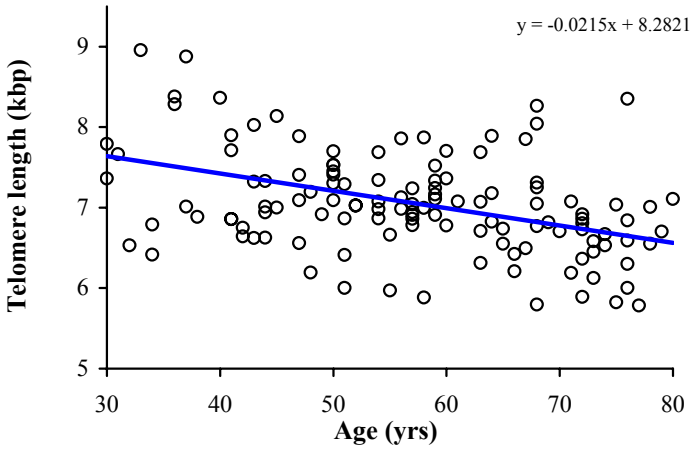
y = -0.0215x + 8.2821
Telomere length (kbp)
9
8
7
6
5
30
40
50
60
70
80
Age (yrs)

B

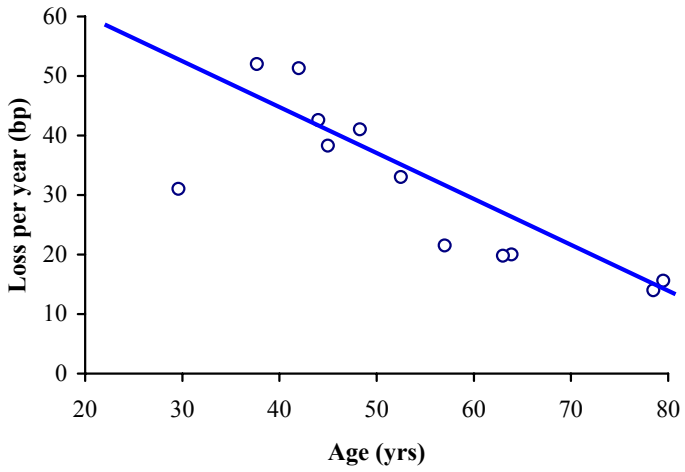
Loss per year (bp)
60
50
40
30
20
10
0
20
30
40
50
60
70
80
Age (yrs)

C

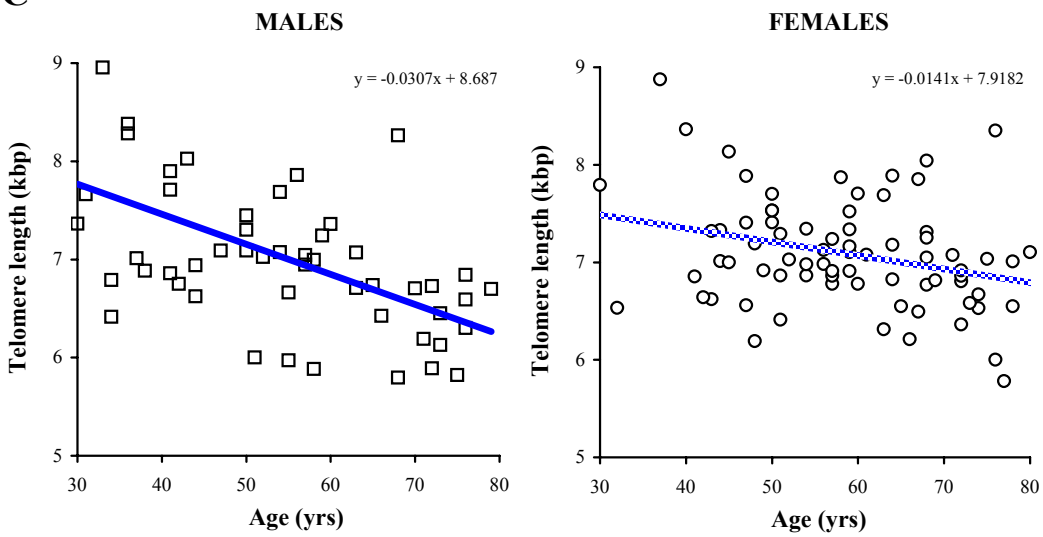
MALES
FEMALES
y = -0.0307x + 8.687
y = -0.0141x + 7.9182
Telomere length (kbp)
Telomere length (kbp)
9
8
7
6
5
30
40
50
60
70
80
Age (yrs)
Age (yrs)

Table 1. Rates of blood telomere loss. These published data, in which a total of 1,094 individuals were analyzed, were plotted on the graph in Figure 9B. Each study was done independently, has different statistical power and used varied experimental methodology, but in all cases was statistically significant ($p<0.01$).

Study	Rate of Loss (bp/yr)	Age range (yrs)	Median age (~yrs)	n
Hastie et al. (1990)	33	20-85	52.5	47
Vaziri et al. (1993)	41	0-107	48.3	119
Slagboom et al. (1994)	31	2-95	29.6	123
Mondello et al. (1999)	42.6	26-72	44	26
	15.6	50-104	79.5	26
Rufer et al. (1999)	1,088	0-1.5	0.75	38
	52	1.5-90	37.7	246
von Zglinicki et al. (2000)	20	18-98	63.9	186
Bestilny et al. (2000)	38.3	0-82	45	15
Cawthon et al. (2003)	14	60-97	78.5	143
Unryn et al. (2005)	51.3	30-49	42	36
this study	19.8	50-80	63	89
	21.5	30-80	57	125

Figure 10. Offspring with older fathers have longer telomeres. Plot generated from the linear regression of mean TRF of non-cancer subjects versus the age of their father (prior to age-adjustment). Each open circle represents a subject sample, and the solid line represent the linear regression trendline. Following age-adjustment by multiple regression, an increase of 22 bp is seen in the length of children's telomeres per year of increasing paternal age ($p = 0.01$).

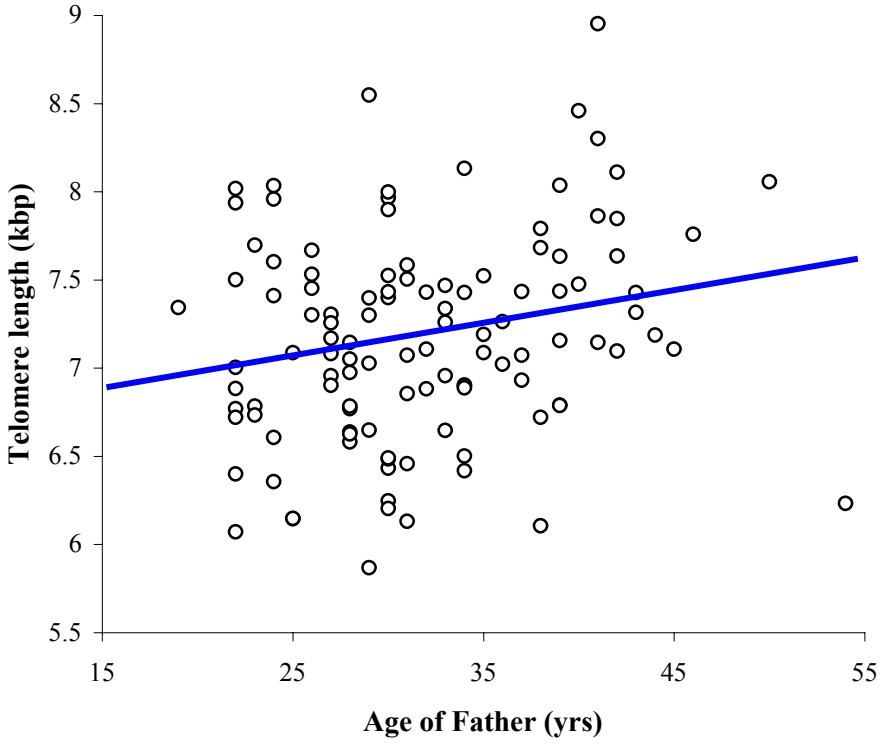
Telomere length (kbp)
9
8.5
8
7.5
7
6.5
6
5.5
15
25
35
45
55
Age of Father (yrs)

B) Telomeres in the blood cells of head and neck cancer patients compared to those in a control population

A total of twenty head and neck cancer patients were enrolled our study that began in the fall of 2003. Blood samples were collected from all the patients before they received any form of treatment. The mean terminal restriction fragment (mTRF) lengths from PBMCs of cancer patients prior to treatment were compared to the mTRF data from the 125 non-cancer control subjects. Linear regression analysis of each group reveals a loss of 27 base pairs per year in the cancer patients as compared to 22 base pairs in the non-cancer subjects (Figure 11). No significant difference was seen between the means of each group before or after adjusting for age (cancer – 7.06kb, non-cancer – 7.08kb). When the data is further divided into males and females and visualized with the help of Box-and-whisker plots, once again no difference between head and neck cancer patients prior to treatment and non-cancer control individuals was seen (Figure 11B). The Box-and-whisker plot is useful in showing key features present in the data set, such as the shape of distribution, median value (black line), upper and lower quartiles (limits of the box), extreme values (whiskers) and even potential outliers (small circles outside the boxes). Other than slight differences in the shape of the distribution, owing to small sample size in the cancer subset, the data are very similar between the two groups. These data demonstrate that in our small subset of head and neck cancer patients, telomere length prior to treatment is not significantly different from that found in the controls without cancer. Intra-subject variability for the studies was assessed by comparing samples from non-cancer control individuals collected at 2 different timepoints (approximately two months apart). An average change of 170 bp was seen between time

Figure 11. Mean telomere length comparison of normal individuals and chemoradiotherapy study patients. Panel A). The age dependency of telomere length in peripheral blood mononuclear cells (PBMCs) from control subjects (closed circles) and CRT patients (open boxes) is shown by linear regression analysis. Mean TRF data from 125 randomly recruited healthy individuals and twenty head and neck cancer patients was generated through multiple southern blot analyses. The Pilot study and Chemoradiotherapy study regression lines are represented by the formulas: $y = -0.0218x + 8.2821$ and $y = -0.0268x + 8.5594$, respectively. The slope represents the average base pair change per year of subject age. **Panel B).** Box-and-whisker plots that represent the median TRF (center line), upper and lower quartiles (top and bottom of box), and extreme values in the data set (whiskers) for the Pilot and CRT studies. Both studies were divided by gender (males – dark boxes, females –light boxes). Potential outliers (small circles) represent values that are over 1.5 times the inter-quarantile range.

A

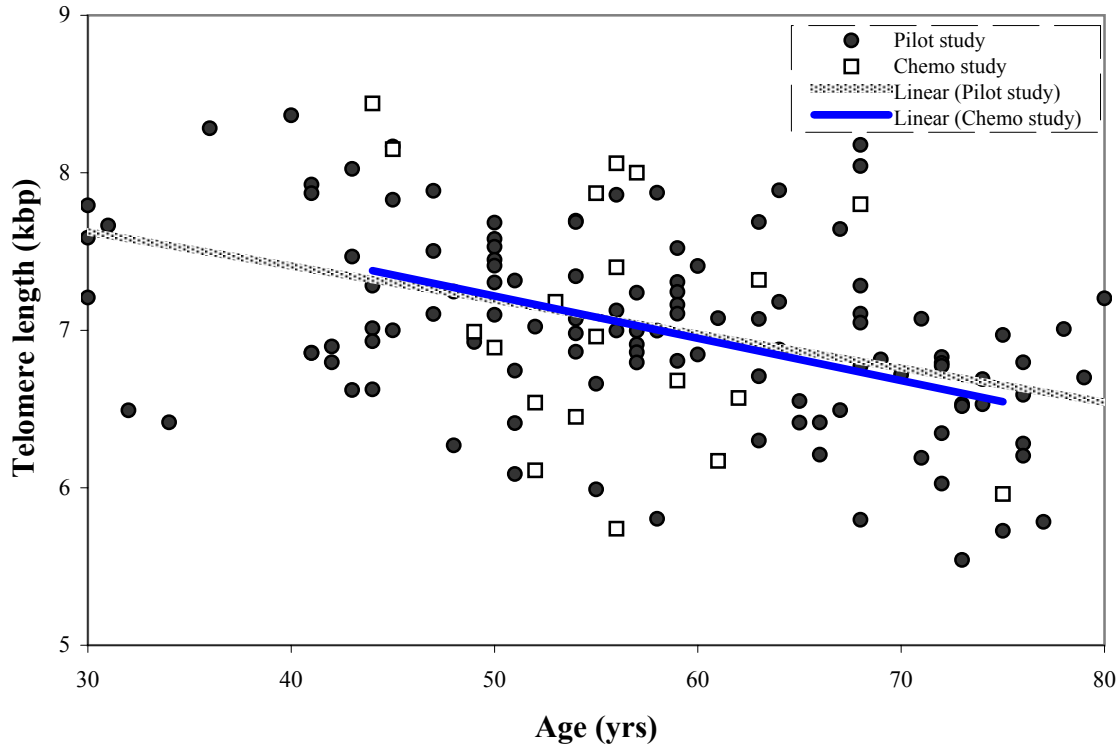
Pilot study
Chemo study
Linear (Pilot study)
Linear (Chemo study)
Telomere length (kbp)
9
8
7
6
5
30
40
50
60
70
80
Age (yrs)

B

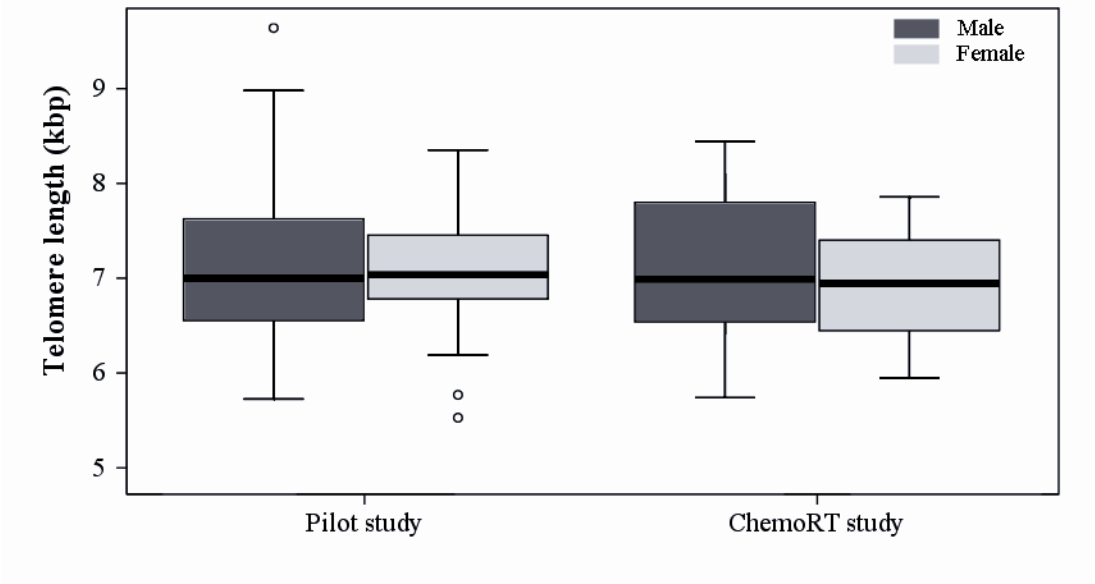
Male
Female
Telomere length (kbp)
9
8
7
6
5
Pilot study
ChemoRT study

points (both telomere length increases and decreases were seen) (Subject #1: 7.07kb vs 7.30kb, Subject #2: 7.37kb vs 7.35kb, Subject #3: 7.08 vs 7.38kb).

One of the pre-treatment factors did have an effect on the mean TRF of cancer patients. The number of pack years that an individual had smoked (calculated by multiplying the number of packs per day by the number of years the individual has smoked) had a negative influence on their starting mTRF length. This was determined by the linear regression of mTRF of cancer patients before treatment to pack years. Both before and after subject age adjustment, a change of 17 bp per pack year was seen ($p = 0.005$ and $p = 0.022$, respectively). In the control set, this factor did not seem to play a role in telomere length ($p = 0.509$).

C) The shortening of telomere length throughout chemoradiotherapy treatment in head and neck cancer

Until our study, the chemotherapy and telomere length studies that have been published by other groups (Engelhardt et al. 1998; Schroder et al. 2001; Franco et al. 2003; Lee et al. 2003; Ricca et al. 2005) have examined mTRF after patient treatment with multiple chemical agents (i.e. combination chemotherapy). While the importance of these studies is clear, the use of a combination of treatments will affect many different systems in the organism. This fact makes it quite difficult to interpret which agent might be primarily responsible for the effects being examined. In an attempt to better understand telomere loss due to chemotherapeutic agents, a study that involved head and neck cancer patients, which receive a single form of treatment, was initiated (following

ethics and project approval). Patients that were enrolled in the study did not have any form of cancer or cancer treatment previously.

Standard treatment for these patients was cisplatin plus radiation therapy (i.e. chemoradiotherapy, CRT) or radiation therapy alone (RT). Cisplatin ($20mg/m^2$) was administered four consecutive days on weeks 1 and 5, while local radiation therapy entailed 35 fractions of 2 Grays each over a 7-week period. The demographics and raw mean telomere length data from all twenty patients is shown in Table 2. Patients that agreed to participate in the study also agreed to donate three blood samples (one prior to treatment, one at week 5 – prior to their second cycle of cisplatin, and one following treatment). Two co-operating oncologists at the Tom Baker Cancer Center in Calgary, Alberta, Canada were involved in patient recruitment for the study (Dr. Desiree Hao – CRT patients and Dr. Harold Lau – RT patients). In Figure 12, an autoradiogram that represents telomere length distributions from a few of the cancer patients is shown. As in the control mTRF analysis and the *in vitro* analyses, all of the samples were analyzed using a fully blind protocol (with the exception that all 3 draws from each patient had to be loaded on the same gel – to eliminate additional inter-gel variability). After mTRF data was generated from all of the patients, a variety of repeated measures analyses were performed. A highly significant telomere length decrease was seen after chemoradiotherapy, while no decrease was seen after radiotherapy alone. Differences in the shape of the distributions, the median and the mean are shown in the Box-and-whisker plot in Figure 13A.

To assess possible external factors that contributed to the changes seen in mTRF throughout treatment, data was analyzed for random effects. In brief, repeated measures

Table 2. Demographics and telomere length measurements in head and neck cancer patients. Patient information of individuals enrolled in our "Telomere Length in Peripheral Immune System & Chemotherapy" study since the Fall of 2003. Patients that received cisplatin treatment in addition to radiation therapy are denoted by CRT, while patients that only received radiotherapy are represented by RT. The staging system used to determine the disease stage at the time of diagnosis summarizes information from the TNM classification system (Sobin et al. 1997), which describes the anatomic extent of the cancer. Stage II is representative of cancers with a primary tumor size (T) of 2 (out of 4), regional lymph node involvement (N) of 0 (out of 3) and distant metastases (M) of 0 (out of 1). Stage III is representative of cancers with a TNM of $T_{1\text{-}3}$, $N_{0\text{-}1}$ and M_0, while Stage IVa is representative of cancers with a TNM of $T_{1\text{-}4}$,$N_{1\text{-}2c}$,M_0. Smoking status is divided between non-smokers, former-smokers (quit over 3 months ago) and current smokers. Pack years was calculated by multiplying the number of packs per day by the number of years the individual has smoked. Best response to treatment was classified as a complete response (CR), partial response (PR), minor response, stable or progressive disease. Total dose of cisplatin received (in mg) is also listed for CRT patients. Mean telomere length (mTRF) and telomere length changes between the various collection timepoints (pre-treatment, during-treatment, after-treatment) are also shown for each patient that was enrolled.

Patient #	Treatment	Age	Gender	Stage @ Dx	Smoking	Pack years	Response
1	CRT	44	Male	IVA	non	0	CR
2	CRT	52	Male	IVA	current	30	PR
3	CRT	49	Male	IVA	non	0	CR
4	CRT	49	Male	IVA	non	0	CR
5	CRT	55	Male	IVA	current	25	PR
6	CRT	56	Male	IVA	current	20	CR
7	CRT	55	Female	IVA	current	38	CR
8	CRT	44	Male	IIB	non	5	PR
9	CRT	62	Male	n/a	former	47	PR
10	CRT	75	Female	IVA	former	100	CR
11	CRT	55	Female	IVA	non	0	PR
12	CRT	52	Male	IVA	current	50	CR
13	CRT	61	Male	IVA	current	45	PR
14	CRT	59	Male	IVA	current	50	PR
15	CRT	54	Male	III	current	98	CR
16	CRT	63	Male	IVA	current	50	CR
17	CRT	56	Male	III	former	10	CR
18	CRT	52	Male	IVA	current	35	n/a
19	RT	56	Male	III	current	48	PR
20	CRT	68	Male	IVA	current	35	n/a

Patient #	Cisplatin dose (mg)	mTRF pre-Tx	mTRF during-Tx	mTRF post-Tx	mTRFΔ (pre-during)	mTRFΔ (during-post)	mTRFΔ (pre-post)
1	144	8.15	7.83	7.42	0.32	0.41	0.73
2	328	7.18	6.79	6.82	0.39	-0.03	0.36
3	340	6.99	6.84	6.72	0.15	0.12	0.27
4	316	6.89	6.99	6.73	-0.1	0.26	0.16
5	256	7.4	6.39	6.37	1.01	0.02	1.03
6	376	8	6.89	6.25	1.11	0.64	1.75
7	260	7.87	6.99	7.26	0.88	-0.27	0.61
8	400	8.44	7.97	7.75	0.47	0.22	0.69
9	364	6.57	6.67	6.04	-0.1	0.63	0.53
10	300	5.96	5.48	5.04	0.48	0.44	0.92
11	232	6.96	6.87	6.81	0.09	0.06	0.15
12	252	6.11	5.92	5.73	0.19	0.19	0.38
13	292	6.17	6.13	5.88	0.04	0.25	0.29
14	256	6.68	6.52	6.01	0.16	0.51	0.67
15	340	6.45	6.11	5.92	0.34	0.19	0.53
16	248	7.32	6.67	n/a	0.65	n/a	n/a
17	280	8.06	7.25	6.77	0.81	0.48	1.29
18	332	6.54	6.3	n/a	0.24	n/a	n/a
19	0	5.74	5.94	6.17	-0.2	-0.23	-0.43
20	228	7.8	7.85	7.2	-0.05	0.65	0.6

Figure 12. Changes in mean telomere length in peripheral blood mononuclear cells (PBMCs) after chemoradiotherapy. Southern blot analysis showing terminal restriction fragment (TRF) distributions at all three collection points (pre-Tx, during-Tx, post-Tx) from 5 head and neck cancer patients receiving chemotherapy plus radiation therapy. Five micrograms of digested genomic DNA from each sample was separated by electrophoresis and hybridized to a radiolabelled telomere specific probe. All three time-points from each patient were loaded randomly to ensure that the analyis was performed blind. The numbers shown at the top of the gel represent patient numbers (seen in Table 1). M represents radiolabelled Hind-III digested lambda DNA (molecular weight marker) and is used to determine the mean TRF of each sample.

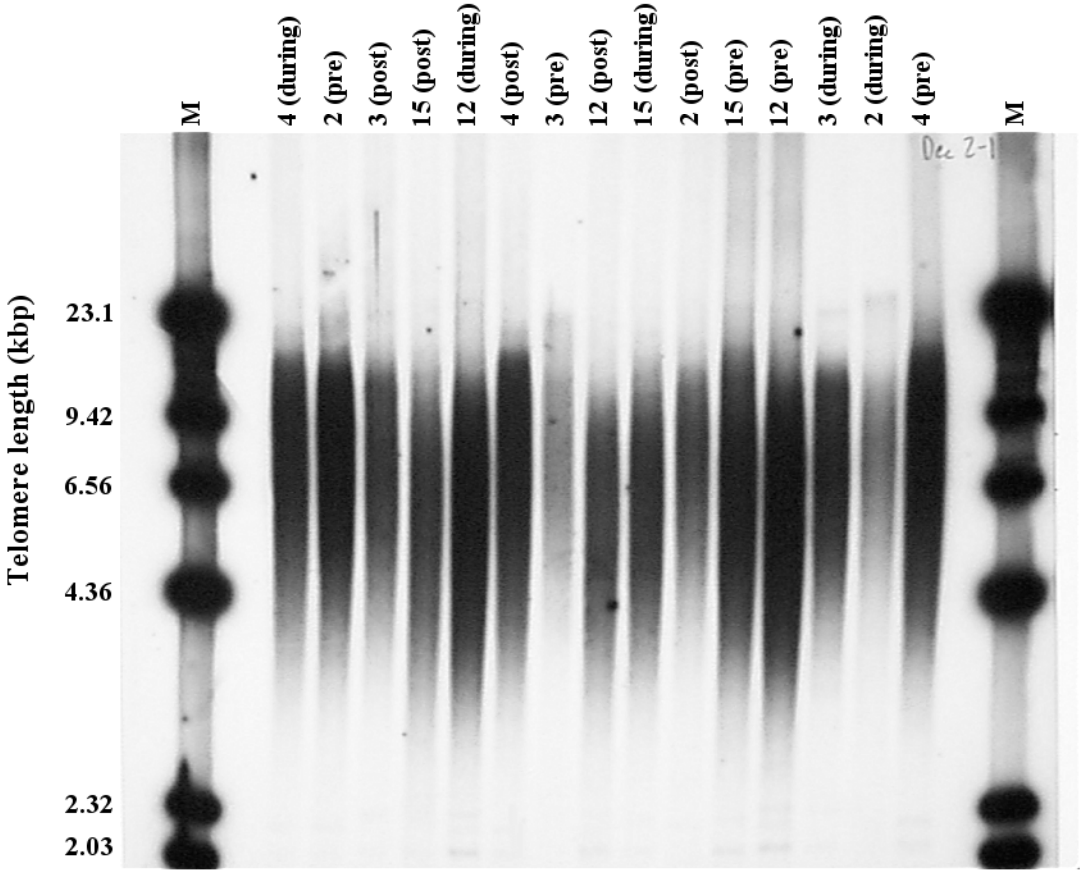
M
4 (during)
2 (pre)
3 (post)
15 (post)
12 (during)
4 (post)
3 (pre)
12 (post)
15 (during)
2 (post)
15 (pre)
12 (pre)
3 (during)
2 (during)
4 (pre)
M
Dec 2-1
Telomere length (kbp)
23.1
9.42
6.56
4.36
2.32
2.03

analysis of variance allows us to examine multiple dependent variables that were measured at different times (i.e. mTRF values from a pre-, during- and post-Tx blood draw). In addition it allows for the investigation of between-subject effects (such as differences between males and females) and within-subject effects (such as differences in mTRF between individuals or treatment time-points). The model assumes that factors involved have a linear relationship to the dependent variable (i.e. mTRF) and the significance level of 0.05 was used. Following the analysis of all of the data seen in Table 2, it was evident that certain factors contribute to the telomere length differences seen throughout cisplatin treatment. As was mentioned earlier, the time at which the draw was taken (i.e. pre-, during- or post-) significantly affected mTRF ($p < 0.0001$). An average rate of loss of 330 base pairs per time point was seen in all CRT patients (means: pre- 7.13kb, during- 6.76kb, post- 6.47kb).

The only other circumstance where the change in telomere length was influenced was when patients were divided into two age groups, those under 55 years of age and those 55 and up (Figure 13B). A significant difference in means and rate of loss was seen between the two subsets ($p = 0.025$). In patients under 55 years of age, a loss of 205 bpper time point was seen (means: pre- 7.07, during- 6.85, post- 6.67), while patients 55 years or older showed a loss of 440 bp per time point during treatment (means: pre- 7.18, during- 6.68, post- 6.30). Other factors such as disease stage ($p = 0.944$), smoking status (0.283), number of pack years (0.269), patient response (0.537) and total cisplatin dose received (0.598) did not have a significant impact with respect to mTRF loss, despite the fact that large factor differences (such as number of pack years) between patients did exist. In summary, these data show that chemoradiotherapy induces a large decrease in

Figure 13. Distribution change and telomere length decrease in chemo-radiotherapy patients throughout treatment. Panel A). Box-and-whisker plots summarizing the mTRF data from head and neck cancer patients receiving CRT. Triangles represent mean TRF data from each collection time point, while solid lines represent the median. Upper and lower quartiles provide the top and bottom of the box, respectively, while the extreme values in the data set are represented by the whiskers. The values that lie outside 1.5 times the inter-quarantile range represent potential outliers (small open circles). Head and neck cancer treatment caused a highly significant reduction in mean telomere length. Overall mean telomere lengths in CRT patients (both groups) were 7.13 kb (pre-Tx), 6.76 kb (during-Tx) and 6.47 kb (post-Tx). **Panel B).** Mean and rate changes are seen between different head and neck cancer age groups. When patients were divided into young (under 55 yrs, n=8) and old (55 yrs and up, n=12) subsets, a significant difference is seen in mTRF length throughout treatment, The average loss seen in young patients was 205 bp per time point (dark line), while a loss of 440 bp per time point was seen in old patients (light line).

A

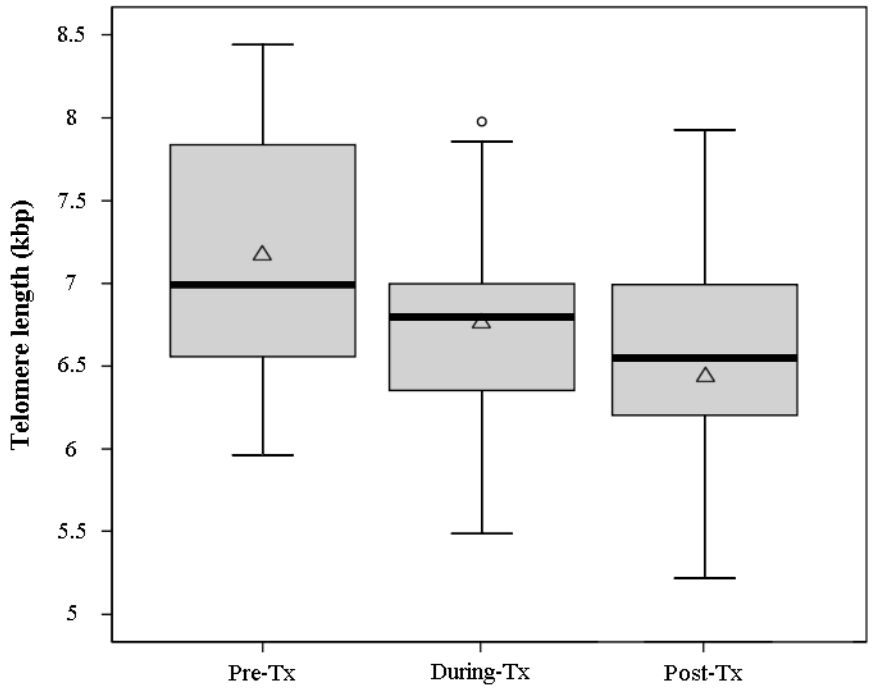
Telomere length (kbp)
8.5
8
7.5
7
6.5
6
5.5
5
Pre-Tx
During-Tx
Post-Tx

B

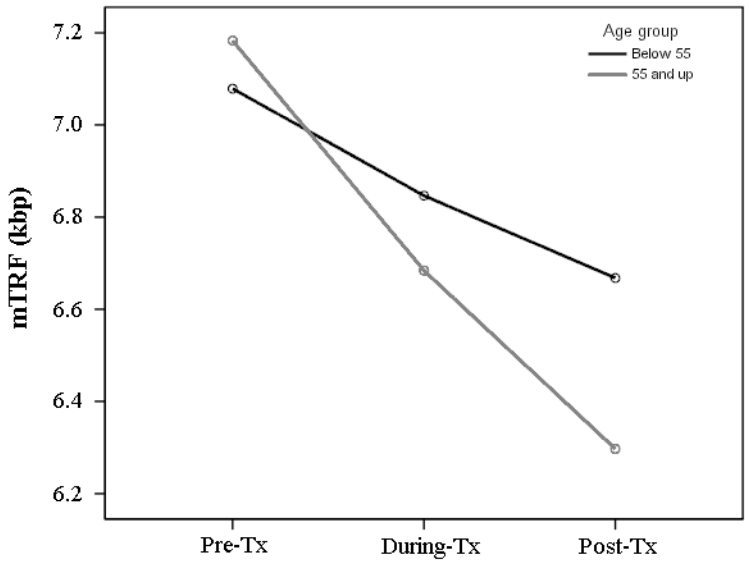
mTRF (kbp)
7.2
7.0
6.8
6.6
6.4
6.2
Age group
Below 55
55 and up
Pre-Tx
During-Tx
Post-Tx

the length of telomeres in PBMCs and that this effect is much greater in the more elderly patients.

VI. DISCUSSION

Part 1. Variation in telomere length after chemotherapeutic treatment *in vitro*.

The aim of this part of my project was to investigate the effects of alkylating agents on telomere length, cell morphology and biochemistry, gene expression and cell cycle distribution in normal and in NER-deficient fibroblast strains. This work was based on the knowledge that the loss of telomeric DNA from chromosome ends is seen in certain types cell types after oxidative damage (von Zglinicki et al. 1995) provides evidence that external factors other than the end-replication problem (Olovnikov 1971), contribute to telomere shortening and replicative aging *in vitro*. Additional cell culture work demonstrated that telomeres not only are affected by external damaging agents, but they might be preferential targets for damage initiated by intracellular metabolism, such as single-strand breaks (Petersen et al. 1998). Many forms of DNA damage exist that influence cellular replication and repair in different manners. Alkylating agents, such as cisplatin, cross-link DNA and are typically repaired by nucleotide excision repair (Zamble et al. 1996). These adducts evoke structural changes and distortion in the DNA helix, which lead to the unwinding and bending of DNA and contribute to inhibition of DNA replication or the accumulation of mutations (Bellon et al. 1991).

A) Sensitivity to treatment with anticancer agents varies between fibroblast strains

The cytotoxicity of three anti-cancer agents was tested in two different fibroblast strains, results of which revealed substantial differences in strain sensitivity to treatment type and treatment dose. In both cell types, a very high dose of transplatin was required to

produce an effect similar to a low dose of cisplatin. This is consistent with early reports demonstrating a lack of t-DDP toxicity by a factor of 20 in leukemia cells (Macquet et al. 1983), despite the fact that adduct formation kinetics for the two agents are similar (Lepre et al. 1990). This leads us to believe that recognition and subsequent processing of adducts differs between the two compounds.

Sensitivity to cisplatin was increased dramatically in fibroblasts deficient in both forms of nucleotide excision repair (TC-NER and GG-NER), while no significant difference was seen in transplatin or methotrexate sensitivity. A ten-fold lower dose of c-DDP was required to cause a similar level of cytotoxicity in XPA cells compared to normal wild-type human diploid fibroblasts. This finding reinforces the idea that the NER-pathway plays a key role in the repair and removal of c-DDP adducts (Zamble et al. 1996). The sensitivity seen in cells after cisplatin treatment implies that in the absence of the XPA protein, which is involved in damage recognition, cells are unable to properly detect and repair the intra-strand cross-links that are specifically formed by c-DDP (but not t-DDP). The absence of t-DDP sensitivity in XPA cells suggests that (a) proteins that recognize and repair damage caused by cisplatin and transplatin might be different (with t-DDP cross-link recognition unrelated to NER or the XPA protein), or (b) structural differences between cross-links formed by cisplatin and transplatin prevent the access of NER proteins to t-DDP damaged DNA. The latter situation would indicate that even in the absence of NER, no change in cytotoxicity would be seen between the two fibroblast strains.

B) G2/M accumulation in platinum treated fibroblasts

Cell cycle progression between G1, S, G2 and M is, in part, regulated by cyclins, cyclin-dependent kinases and cyclin-dependent kinase inhibitors (reviewed in (Nasmyth 1996). Under circumstances where genotoxic stresses are present, proteins involved in DNA damage checkpoints arrest the cell cycle, and cellular repair occurs. In conditions where damage exceeds a particular threshold, apoptosis occurs (Schulte-Hermann et al. 2000). The G1/S checkpoint is thought to prevent the replication of damaged DNA, while the G2/M checkpoint prevents DNA damaged in the S or G2 phase from being transmitted to daughter cells by mitosis (Zhou et al. 2000). Any breakdowns in this process can lead to excessive proliferation, accelerated aging, instability and cancer development (Hartwell 1992). In budding yeast *S. cerevisiae*, cisplatin treatment causes a G2/M arrest, without a delay in the replication phase of the cell cycle (Grossmann et al. 1999). In contrast, in a human cancer cell line, no G2/M arrest was seen at any c-DDP concentration or time point (Ishibashi et al. 1998) while a recent study reported G1 blockage after c-DDP in human lung fibroblasts (Zhao et al. 2004). It is clear from Figure 2B and 3B that the treatment of Hs68 and XPA human fibroblasts with cisplatin causes a time-dependant G2/M accumulation, as seen in yeast. This effect also varied depending on the dose that was administered, with higher doses leading to more pronounced cellular arrest and apoptosis. The kinetics of arrest differed between the two strains. Normal fibroblasts appeared to be more capable of enduring the stresses associated with platinum treatment, while XPA cells showed a faster build-up in G2/M and in the sub-G1 population at a similar IC_{50}. This hypersensitivity, and eventual cell death, could be attributed to the presence of other functional components, such as the

damage binding complex XPC-HR23B, which is able to recognize c-DDP damage, and recruit checkpoint complexes that halt cell cycle progression. Adduct repair attempts likely fail, and eventually cell death is seen. No strain differences were seen in the cell cycle following transplatin treatment (both had a G2/M build up similar to c-DDP). The G1 and S-phase arrest due to methotrexate that is seen in both cell types at all concentrations confirms previous reports in the literature (Tsurusawa et al. 1988; Bruce-Gregorios et al. 1991; Hattangadi et al. 2004).

C) Platinum-induced senescence-like phenotype in fibroblasts

Replicative senescence and stress-induced premature senescence (SIPS) show similar morphological traits and share many markers of replicative aging (Toussaint et al. 2000). Increased cells size, microfilament and stress fiber content, and population heterogeneity are a few of the visible hallmarks of cellular aging (Cristofalo et al. 1969; Kill et al. 1994). Senescence due to DNA damage from cisplatin was only recently reported as this study was concluding (Zhao et al. 2004). In my study, minor morphological differences, such as increased cell size, were noted 24 and 48 hours after treatment. The morphological and senescence-associated β-Galactosidase data gathered in Hs68 and XPA cells clearly show that the long-term treatment with platinum agents (even at low concentrations) causes stress-induced premature senescence (Figure 4 and 5). In normal fibroblasts morphological and SA-β-Gal changes appeared within a week of high-dose cisplatin treatment (5 μM), while SIPS was only visible in some of the cells at a low-dose treatment (1 μM) after two weeks. Fibroblasts deficient in NER showed similar results, but also displayed increased heterogeneity at platinum doses that were

unable to cause a significant increase in SA-β-Gal activity. This result signifies that SIPS that is due to platinum agents might be tightly tied to β-Gal activity. In the absence of c-DDP or t-DDP, cells that have an increased sensitivity to many forms of DNA damage (such as XPA fibroblasts) can still undergo premature senescence in a small population of cells (as seen through increased culture heterogeneity). The 8 week culture of Hs68 and XPA cells at a low-dose (cells which were for telomere length measurements) revealed further increased size and altered cell characteristics, which were comparable to, or exceeded those of 2 week high-dose treatment (data not shown). These data, together with FACS data, suggest that sub-cytotoxic platinum levels caused a cell cycle arrest that led to the induction of SIPS. In conditions where arrest due to platinum agents is profound, cells reach SIPS faster (or the number of cells in a population entering into a SIPS state increase more rapidly). In methotrexate-treated cells (Hs68 and XPA) with no pronounced G2/M arrest, no SIPS or increased SA-β-Gal activity were seen. Changes in the cytoskeletal system and actin accumulation are, in part, regulated by Rho family proteins that are involved in a number of cell functions including cell adhesion and stress fiber formation (Zohn et al. 1998). Alteration of the Rho signaling pathway by cisplatin (Villalonga et al. 2004), could cause a loss in cytoskeletal adhesion and promote a SIPS phenotype.

D) Altered levels of specific proteins in fibroblasts due to platinum

The pathways that are tied to damage-induced cell killing and senescence involve the regulation of a variety of cell cycle checkpoint proteins (Ben-Porath et al. 2005). Important players in this process include $p21^{CIP1/WAF1/SDI1}$, involved in the inhibition of

cyclin-cdk2 complexes (Harper et al. 1993), $p16^{INK4A}$, involved in the inhibition of cyclinD-cdk4,6 complexes (Serrano et al. 1993), and p53, a central regulator of cell cycle progression (Kastan et al. 1991). Changes in the levels of p16 and p21 and the activity of p53 are observed in replicatively senescent cells (Noda et al. 1994; Atadja et al. 1995; Wong et al. 1996). In p21 or p53 null colon carcinoma cell lines, treatment with doxorubicin, an anti-tumor antibiotic resulted in a decrease in the severity of the senescence-like phenotype (Chang et al. 1999), suggesting a potential role for both proteins in the induction of SIPS. It is evident from Figure 6 that platinum treatment results in an increase in p16, p21 and p53 in normal fibroblasts. The highest detected levels of each protein correspond to cells treated with a high dose of c-DDP or t-DDP and also represent cells that showed the most dramatic changes in morphology and the induction of SIPS. A recent report found time-dependent changes in the level of p53 after hydrogen peroxide induced DNA damage (initial increase followed by a return to basal levels within a few days) (Chen et al. 2004). In Hs68 fibroblasts no such long-term decrease in p53 was seen following platinum damage. The robust increase in p21 agrees with reports linking it to senescence initiation (Noda et al. 1994; Wong et al. 1996), while the higher levels of p16 in t-DDP compared to c-DDP implies that a higher number of cells might be in a senescence-like state (likely as a result of less apoptosis). In XPA fibroblasts, detectable p16 and p21 levels were seen in the untreated sample. The substantial increase in p16 and p21 after treatment was more pronounced after high-dose c-DDP, similar to Hs68s. High levels of p16 seen after low concentrations of cisplatin indicate that a large proportion of cells are in a state of SIPS. The absence of substantial SA-β-Gal activity in that sample suggests that the increases in p16 and SIPS in XPA cells

at a low dose could be due to hypersensitivity to other forms of DNA damage, rather than direct adduct-related damage. In the absence of the XPA protein, detection of DNA damage, up-regulation of senescence-related proteins and the induction of stress induced premature senescence, all still occur. Since initial adduct recognition involves proteins other than XPA, it is safe to assume that recognition is still functional in these cells, while NER-related repair likely is not. Many of the molecular changes seen in SIPS due to platinum agents are similar to those seen in replicative senescence. Future experiments could explore the levels of other checkpoint or senescence-related proteins at varying c-DDP concentrations (through micro-array or Western blot analysis). This would be important to mechanistically differentiate proteins involved in the cell cycle progression, induction and maintenance of SIPS from those involved in replicative senescence per se.

E) Telomere length reduction following long-term platinum treatment

Telomeres that are "critically" short are involved in the activation of replicative senescence, and therefore, the regulation of cellular lifespan *in vitro* (Chiu et al. 1997). The same circumstances might not hold true in cells treated with DNA damaging agents *in vitro*. If SIPS were to occur as a result of telomere shortening, then the agent would be required to cause a profound effect (> few kilobases) within a few rounds of cellular replication. The results seen in Figure 7 reveal the presence of accelerated shortening after cisplatin treatment in primary fibroblasts. Untreated Hs68 cells showed a total loss of 210 bp (average of 30bp per MPD), while a single one-time high-dose treatment caused a 550bp (average of 110bp per MPD) reduction in the mean TRF length of the cell population. The absence of collection time-points during the course of the 8 week period

prevented proper analyses (per MPD). A second treatment did not increase the total telomere loss seen in normal fibroblasts.

The pattern of loss in the two regimens might be based on c-DDP levels in the cell. After one treatment X number of adducts are formed on DNA. At a single low dose, the number of adducts present in the genome would be much lower than after a single high dose. If there was preferential targeting of c-DDP to telomeric DNA, due to a higher frequency of guanine-guanine and adenine-guanine repeats (Redon et al. 2003), then more adducts would be present on the telomeres in cells treated with high levels of c-DDP. It would take multiple low-dose treatments to achieve the same X value of adducts in cells (which is in agreement with a dose-dependent mTRF loss in low-dose treatment). If the adduct levels at telomeric DNA were near maximal after one high-dose treatment, then additional treatment would not have a significant effect. This mechanism would apply to cells that were allowed to continue to proliferate (albeit at a slower rate) and avoid severe cell cycle arrest and apoptosis. If a permanent cell cycle arrest occurred in cells, cell death would likely occur prior to cisplatin-based telomere reduction. The continuous low-dose treatment of normal fibroblasts would result in maximal adduct concentration without the dramatic cell cycle and apoptotic effects seen at high-doses. In these cells, the largest mTRF loss was seen (675bp over 8 weeks).

Fibroblasts deficient in NER saw a reduction in telomere length as a result of c-DDP treatment. The greatest loss, corresponding to 460bp over 8 weeks, was seen after a single high-dose regimen. The lack of telomere loss seen after a second high-dose of cisplatin in XPA cells could be attributed to cell death. At the end of week 5, over 75% of

cells had undergone apoptosis. The cells remaining were in a state of permanent cell cycle arrest and did not proliferate enough to be sub-cultured again.

Due to the fact that both strains underwent a similar number of MPDs, it can be safely assumed that a greater mTRF loss is seen in Hs68 cells at a similar relative cytotoxicity. If the XPA low dosage of c-DDP were given to Hs68s, the mTRF losses in XPA cells would exceed those seen in normal fibroblasts. Assuming the proposed adduct-dependent loss also applies to XPA cells, a much lower number of adducts could be formed on XPA DNA than on Hs68 DNA (based solely on a 10-fold concentration difference in the culture media), leading to less telomere length reduction in XPA cells. Nucleotide excision repair increases the platinum sensitivity in XPA cells, but no obvious role in the repair of c-DDP-related telomeric damage could be seen.

Transplatin did not affect telomere loss to a great extent at any dose in either of the strains. Cells exposed to a continuous dose of t-DDP, proliferated at a rate equal to that seen in c-DDP treatment (low dose – 8 MPD, high dose – 5 MPD). The greatest effect seen was in high-dose continuous treatment, which resulted in an average rate of loss equal to 64bp per MPD (320bp loss in 5 MPDs). Differences in the cross-link stability and structure formed by each agent likely play a role in how they are detected and removed.

The interstrand cross-links and monofunctional adducts formed by t-DDP not only differ in structure from intrastrand cross-links formed by c-DDP, but they are also much less stable (Marchan et al. 2004). In addition t-DDP adducts have been shown to stimulate repair synthesis more efficiently in an *in vitro* replication system (Heiger-Bernays et al. 1990). If telomere loss were based on replication, the presence of any

additional proteins that are selectively bound to platinum-modified DNA (such as the cellular protein HMG1 (chromosomal high mobility group) that only binds to c-DDP modified DNA) (Perez et al. 2000), could possibly cause a block to the replication mechanism at the DNA ends, and induce an increase in telomere loss compared to t-DDP treated cells with no bound HMG1 proteins.

From the results of this study, there are at least two explanations for the role of NER in telomeric DNA damage; (a) nucleotide excision repair does not increase the repair efficiency of platinum-damaged telomeric DNA, or (b) even in the presence of a functional NER, too much adduct damage is present to be adequately repaired, resulting in no difference in mTRF loss between the two strains. In addition, no link could be made between SIPS and the loss of telomeric DNA due to platinum treatment, reinforcing the mechanistically important idea that stress-induced premature senescence is a telomere-independent event (Dumont et al. 2001). Future experiments could help clarify the effects seen in primary fibroblasts. Samples could be collected after each round of treatment. This would help determine whether the large telomere loss seen *in vitro* after a single-treatment is due to a one-time loss during one cycle of replication, or whether a gradual continuous loss over the 8 week period is seen. It would also be beneficial to determine the rate of telomere loss for untreated fibroblast cells over dozens of MPDs. Assuming that the loss is consistent, it would be valuable to determine whether or not cells at different MPDs (young versus old), and therefore cells with different remaining replicative potentials, show different responses to platinum-treatment.

Part 2: Variation in telomere length in the population and during chemotherapy

The use of telomeres as a marker in the study of human aging was based on observations that progressive telomere shortening occurs as cells age *in vitro* (Harley et al. 1990). This replication-dependent attrition occurs in peripheral blood mononuclear cells (Hastie et al. 1990; Vaziri et al. 1993), hematopoietic stem cells (Vaziri et al. 1994) and a variety of other tissues (Takubo et al. 2002). Many studies have also linked increased rates of shortening to various diseases (reviewed in (Djojosubroto et al. 2003) and treatment with DNA damaging agents (de Magalhaes 2004). To investigate population based telomere variability and examine telomere length during chemotherapy, telomere lengths in two populations were studied; one control group without cancer and one head and neck cancer group.

A) Population variation in the rate of telomere shortening

The variability in telomere length between individuals is not only present in adults. In fetuses and newborns, differences are as large as that observed later in life (Youngren et al. 1998; Bestilny et al. 2000; Okuda et al. 2002). To assess possible factors contributing to this variation, mTRF from the control group, comprising 125 individuals, was compared to various factors such as tobacco use, gender, hormone use and parental age. Regression analysis revealed age-group differences in telomere length that might be related to the age-associated decrease in immune cell turnover with age (Segerstrom et al. 2004). Analysis also revealed a significant difference in the rate of telomere loss with gender (which was at the time a novel discovery). Older males had telomeres that were shorter compared to their female counterparts, while younger males had telomeres that

were longer compared to their female counterparts. This difference in average telomere length between sexes might contribute to the sex-related differences in lifespan seen in most societies (Samaras et al. 2003).

Additional analysis also revealed a novel and significant finding that could contribute to the variability of telomere length seen in the human population; paternal age. It was shown that as paternal age increases, the telomere length of the resultant offspring also increase (Unryn et al. 2005). This difference is attributed to the increase in sperm telomere length with age (Allsopp et al. 1992) and through successive generations the difference in telomere length in offspring of young and old fathers could be on the order of a few kilobases. Together these findings provide additional insight into telomere length variation at birth and throughout aging and development, and this mechanism may be fully responsible for the variation seen in the human population since there is no evidence for any other form of heritable variability in telomere loss from early development to death (Slagboom et al. 1994; Graakjaer et al. 2004).

B) Similar telomere lengths in head and neck cancer patients and controls

Mean terminal restriction fragment (mTRF) length has been shown to be shorter in solid tumors than surrounding normal tissues by up to 2.8kb (Engelhardt et al. 1997). In numerous hematological disorders, a significant mTRF reduction is seen in patients versus age-matched controls (Ball et al. 1998; Leteurtre et al. 1999; Bestilny et al. 2000). Evidence in Figure 11 suggests that no mTRF difference is seen in head and neck cancer at diagnosis compared to individuals without cancer. Both groups displayed similar rates of telomere loss (as seen through regression analysis) and similar distribution (even after

age-adjustments). These data challenge a large recent report (n = 626) of four cancer populations that found shorter telomeres in head and neck, bladder, lung and renal cell cancer patients as compared to controls (Wu et al. 2003).

Of the pre-treatment factors that were analyzed, the number of cigarette packs years did seem to significantly affect the mTRF of patients at diagnosis (this was not seen in the control group). The difference between the two groups of patients (or the lack of effect seen in the control group) could be attributed to the low number of smokers with a high number of pack years in the control set (mean pack years: 12 – control, 35 – patients) or to the failure of individuals in the control group to reach some threshold of exposure, compared to head and neck cancer patients. This finding is not unexpected due to the fact that cigarette smoke increases the risk of heart disease, lung cancer and microbial infections (McAllister-Sistilli et al. 1998), and so may be expected to increase turnover of cellular components of the immune system. In support of this idea, tobacco smoke has been linked with a reduction in the proliferative capacity of lymphocytes (Barbour et al. 1997).

These results suggest that in the subset of patients analyzed, increased turnover of the immune system as detected by a decrease in telomere length did not occur in response to the presence of a tumor. In contrast, increased tobacco use, as measured through the number of pack years, was correlated with a reduction in mean telomere length in peripheral blood mononuclear cells.

C) Telomere shortening throughout chemoradiotherapy treatment

The "Telomere Length in Peripheral Immune System & Chemotherapy" study that includes twenty head and neck cancer patients is the only longitudinal study performed thus far investigating telomere length changes due to a single form of treatment. Recent studies have involved the grouped analysis of subsets of patients undergoing a variety of combination chemotherapy treatments for a variety of different cancers (Engelhardt et al. 1998; Schroder et al. 2001; Franco et al. 2003; Lee et al. 2003; Ricca et al. 2005). Patients enrolled in this study showed limited diversity, in terms of age, gender, and tumor status (Table 2). A dramatic loss of telomere length was seen during the chemoradiotherapy treatment (mean loss of 660bp over an 8 week span). Assuming an average annual loss of 30bp per year in the absence of treatment (in subjects of a similar age), the telomere loss seen in 8 weeks equates to 22 years "worth" of attrition in control subjects, or an ~145 fold acceleration of telomere loss. When the patients were divided into two halves, the individuals over the age of 54 had a treatment-related loss twice that of individuals between the ages of 44 and 54. This implies that over an 8 week span, older head and neck cancer patients lose roughly 30 years "worth" of telomeres (assuming a similar annual loss). A change in the distribution or composition of various populations of immune cells might play a role in the larger average telomere length losses seen in the elderly. By analogy with these losses seen during chronic infection by various agents, this could clearly impact the efficiency of the immune system to respond to subsequent challenges and suggest that the use of chemotherapeutic drugs and radiotherapy in the elderly should be further examined for possible secondary effects. In the single patient that received radiotherapy alone, no

dramatic loss of telomere length was seen (Table 2). Changes in telomere length between the three blood draws were similar in magnitude to intra-subject changes in non-cancer controls. No other factors examined, such as stage of disease or total milligrams of cisplatin received, were seen to affect the rate of mTRF loss in patients.

Regardless of patient age, chemoradiotherapy caused a staggering reduction in mean telomere length that merits future investigation in both telomere length research and patient care. An increased number of radiotherapy alone patients is required before it can be determined if cisplatin is the primary agent responsible for the drastic telomere loss. In a previously examined head and neck cancer subset, similar in patient demographics, a significant improvement in overall survival and disease-free survival was seen after treatment with concomitant chemotherapy and radiotherapy versus radiotherapy alone (Jeremic et al. 1997). This study found a 14-16% increase in 5 year survival depending on which chemotherapeutic agent was used (c-DDP 6mg/m^2 or carboplatin 25mg/m^2 everyday throughout the 8 week treatment). While these findings do show a clinical benefit to the use of concurrent therapies, the presence of sustained telomere shortening after therapy in a follow-up study (Franco et al. 2003) raises concerns for patients treated with chemotherapy. For our study, we will be following short- and long-term patient outcome (through both overall survival and disease-free survival). In addition we will likely be collecting patient blood at 1 and 2 year follow-ups in order to determine what effect CRT treatment has on mTRF length, years after treatment, and also what effect telomere length has on patient outcome. This will allow us to better gauge the long-term effects of chemoradiotherapy and cisplatin *in vivo*.

Understanding the mechanisms behind the process of cellular aging will ultimately lead to better knowledge of the prevention of age-related disease. Aging is both a biological and social issue. The loss of telomeric DNA is a very important effect of chemoradiotherapy in cancer patients. Further research in the area of telomere biology is needed to design a better course of treatment for patients. If the loss is sustained, physicians need to consider balancing the benefits of treating the primary tumor with limiting telomere loss to minimize the acceleration of replicative aging as measured by telomere attrition.

VII. CONCLUSIONS

The aim of this masters project was to gain an understanding of the relationship between telomere length and chemotherapeutic treatment. I used both *in vitro* and *in vivo* approaches to achieve this. The first was to examine the effects of alkylating agents on telomere length in normal primary cells and in primary cells deficient in the nucleotide excision repair pathway. The second was to examine the effect of cisplatin and radiation therapy on the telomere lengths of head and neck cancer patients and also to explore differences in telomere length variation in cancer and non-cancer subjects.

Data generated from the *in vitro* experiments suggest that the platinum agents, cisplatin and transplatin, do cause significant telomere erosion in primary fibroblast cells, and differences do exist in cells deficient in the nucleotide excision repair pathway. The XPA fibroblast cells show increased drug sensitivity compared to Hs68s, seen through increased cytotoxicity and more pronounced cisplatin-dependent cell cycle effects at similar drug concentrations. Both cells behave in a similar manner in response to treatment with the same dose of transplatin or methotrexate, suggesting the effects seen are not related to the XPA pathway. In both fibroblast strains, an increase in senescence-associated β-Galactosidase activity accompanies a significant increase in proteins that are involved in senescence and the inhibition of cell cycle progression (p16, p21, and p53).

The data from the *in vivo* experiments demonstrate extreme telomere loss in PBMCs of head and neck cancer patients following chemoradiotherapy treatment, a loss which is further embellished in older patients where roughly 30 years “worth” of telomeres occurs in a span of eight weeks. The pre-treatment telomere length in cancer

patients was found to be similar to individuals without cancer, before and after age-adjustments were made. Other novel findings were also evident within the patient and control groups. Non-cancer patients showed a decrease in telomere length with age, the rate of telomere shortening in men was higher than in women, and paternal age was highly correlated with the telomeric DNA of offspring. In cancer patients, a reduction in telomere length was correlated with an increase in the number of pack years.

VIII. BIBLIOGRAPHY

Aboussekhra, A., M. Biggerstaff, M. K. Shivji, J. A. Vilpo, V. Moncollin, V. N. Podust, M. Protic, U. Hubscher, J. M. Egly and R. D. Wood (1995). "Mammalian DNA nucleotide excision repair reconstituted with purified protein components." Cell **80**(6): 859-68.

Achi, M. V., N. Ravindranath and M. Dym (2000). "Telomere length in male germ cells is inversely correlated with telomerase activity." Biol Reprod **63**(2): 591-8.

Allsopp, R. C., E. Chang, M. Kashefi-Aazam, E. I. Rogaev, M. A. Piatyszek, J. W. Shay and C. B. Harley (1995). "Telomere shortening is associated with cell division in vitro and in vivo." Exp Cell Res **220**(1): 194-200.

Allsopp, R. C., H. Vaziri, C. Patterson, S. Goldstein, E. V. Younglai, A. B. Futcher, C. W. Greider and C. B. Harley (1992). "Telomere length predicts replicative capacity of human fibroblasts." Proc Natl Acad Sci U S A **89**(21): 10114-8.

Asai, A., Y. Kiyozuka, R. Yoshida, T. Fujii, K. Hioki and A. Tsubura (1998). "Telomere length, telomerase activity and telomerase RNA expression in human esophageal cancer cells: correlation with cell proliferation, differentiation and chemosensitivity to anticancer drugs." Anticancer Res **18**(3A): 1465-72.

Atadja, P., H. Wong, I. Garkavtsev, C. Veillette and K. Riabowol (1995). "Increased activity of p53 in senescing fibroblasts." Proc Natl Acad Sci U S A **92**(18): 8348-52.

Ball, S. E., F. M. Gibson, S. Rizzo, J. A. Tooze, J. C. Marsh and E. C. Gordon-Smith (1998). "Progressive telomere shortening in aplastic anemia." Blood **91**(10): 3582-92.

Barbour, S. E., K. Nakashima, J. B. Zhang, S. Tangada, C. L. Hahn, H. A. Schenkein and J. G. Tew (1997). "Tobacco and smoking: environmental factors that modify the host response (immune system) and have an impact on periodontal health." Crit Rev Oral Biol Med **8**(4): 437-60.

Bartelink, H., R. F. Kallman, D. Rapacchietta and G. A. Hart (1986). "Therapeutic enhancement in mice by clinically relevant dose and fractionation schedules of cis-diamminedichloroplatinum (II) and irradiation." Radiother Oncol **6**(1): 61-74.

Bartelink, H., J. H. Schellens and M. Verheij (2002). "The combined use of radiotherapy and chemotherapy in the treatment of solid tumours." Eur J Cancer **38**(2): 216-22.

Beattie, T. L., W. Zhou, M. O. Robinson and L. Harrington (1998). "Reconstitution of human telomerase activity in vitro." Curr Biol **8**(3): 177-80.

Bellon, S. F., J. H. Coleman and S. J. Lippard (1991). "DNA unwinding produced by site-specific intrastrand cross-links of the antitumor drug cis-diamminedichloroplatinum(II)." Biochemistry **30**(32): 8026-35.

Ben-Porath, I. and R. A. Weinberg (2005). "The signals and pathways activating cellular senescence." Int J Biochem Cell Biol **37**(5): 961-76.

Benetos, A., K. Okuda, M. Lajemi, M. Kimura, F. Thomas, J. Skurnick, C. Labat, K. Bean and A. Aviv (2001). "Telomere length as an indicator of biological aging: The

gender effect and relation with pulse pressure and pulse wave velocity." Hypertension **37**(2): 381-5.

Bestilny, L. J., M. J. Gill, C. H. Mody and K. T. Riabowol (2000). "Accelerated replicative senescence of the peripheral immune system induced by HIV infection." Aids **14**(7): 771-80.

Bilaud, T., C. Brun, K. Ancelin, C. E. Koering, T. Laroche and E. Gilson (1997). "Telomeric localization of TRF2, a novel human telobox protein." Nat Genet **17**(2): 236-9.

Blackburn, E. H. (1990). "Telomeres: structure and synthesis." J Biol Chem **265**(11): 5919-21.

Blackburn, E. H. (1994). "Telomeres: no end in sight." Cell **77**(5): 621-3.

Blackburn, E. H. (2005). "Telomeres and telomerase: their mechanisms of action and the effects of altering their functions." FEBS Lett **579**(4): 859-62.

Bodnar, A. G., N. W. Kim, R. B. Effros and C. P. Chiu (1996). "Mechanism of telomerase induction during T cell activation." Exp Cell Res **228**(1): 58-64.

Bodnar, A. G., M. Ouellette, M. Frolkis, S. E. Holt, C. P. Chiu, G. B. Morin, C. B. Harley, J. W. Shay, S. Lichtsteiner and W. E. Wright (1998). "Extension of life-span by introduction of telomerase into normal human cells." Science **279**(5349): 349-52.

Boulikas, T. (1996). "Xeroderma pigmentosum and molecular cloning of DNA repair genes." Anticancer Res **16**(2): 693-708.

Broccoli, D., A. Smogorzewska, L. Chong and T. de Lange (1997). "Human telomeres contain two distinct Myb-related proteins, TRF1 and TRF2." Nat Genet **17**(2): 231-5.

Broccoli, D., J. W. Young and T. de Lange (1995). "Telomerase activity in normal and malignant hematopoietic cells." Proc Natl Acad Sci U S A **92**(20): 9082-6.

Bruce-Gregorios, J. H., D. Soucy, M. G. Chen and N. Benson (1991). "Effect of methotrexate on cell cycle and DNA synthesis of astrocytes in primary culture: flow cytometric studies." J Neuropathol Exp Neurol **50**(1): 63-72.

Burstyn, J. N., W. J. Heiger-Bernays, S. M. Cohen and S. J. Lippard (2000). "Formation of cis-diamminedichloroplatinum(II) 1,2-intrastrand cross-links on DNA is flanking-sequence independent." Nucleic Acids Res **28**(21): 4237-43.

Campisi, J., S. H. Kim, C. S. Lim and M. Rubio (2001). "Cellular senescence, cancer and aging: the telomere connection." Exp Gerontol **36**(10): 1619-37.

Cawthon, R. M., K. R. Smith, E. O'Brien, A. Sivatchenko and R. A. Kerber (2003). "Association between telomere length in blood and mortality in people aged 60 years or older." Lancet **361**(9355): 393-5.

Chang, B. D., Y. Xuan, E. V. Broude, H. Zhu, B. Schott, J. Fang and I. B. Roninson (1999). "Role of p53 and p21waf1/cip1 in senescence-like terminal proliferation arrest induced in human tumor cells by chemotherapeutic drugs." Oncogene **18**(34): 4808-18.

Chellappan, S. P., S. Hiebert, M. Mudryj, J. M. Horowitz and J. R. Nevins (1991). "The E2F transcription factor is a cellular target for the RB protein." Cell **65**(6): 1053-61.

Chen, H. J., C. L. Liang, K. Lu, J. W. Lin and C. L. Cho (2000). "Implication of telomerase activity and alternations of telomere length in the histologic characteristics of intracranial meningiomas." Cancer **89**(10): 2092-8.

Chen, J. H., K. Stoeber, S. Kingsbury, S. E. Ozanne, G. H. Williams and C. N. Hales (2004). "Loss of proliferative capacity and induction of senescence in oxidatively stressed human fibroblasts." J Biol Chem **279**(47): 49439-46.

Chen, J. L., M. A. Blasco and C. W. Greider (2000). "Secondary structure of vertebrate telomerase RNA." Cell **100**(5): 503-14.

Chen, Q. and B. N. Ames (1994). "Senescence-like growth arrest induced by hydrogen peroxide in human diploid fibroblast F65 cells." Proc Natl Acad Sci U S A **91**(10): 4130-4.

Chen, Q., A. Fischer, J. D. Reagan, L. J. Yan and B. N. Ames (1995). "Oxidative DNA damage and senescence of human diploid fibroblast cells." Proc Natl Acad Sci U S A **92**(10): 4337-41.

Chen, Q. M., J. C. Bartholomew, J. Campisi, M. Acosta, J. D. Reagan and B. N. Ames (1998). "Molecular analysis of H2O2-induced senescent-like growth arrest in normal human fibroblasts: p53 and Rb control G1 arrest but not cell replication." Biochem J **332 (Pt 1)**: 43-50.

Chiu, C. P. and C. B. Harley (1997). "Replicative senescence and cell immortality: the role of telomeres and telomerase." Proc Soc Exp Biol Med **214**(2): 99-106.

Chong, L., B. van Steensel, D. Broccoli, H. Erdjument-Bromage, J. Hanish, P. Tempst and T. de Lange (1995). "A human telomeric protein." Science **270**(5242): 1663-7.

Cleaver, J. E., B. Zelle, N. Hashem, M. H. El-Hefnawi and J. German (1981). "Xeroderma pigmentosum patients from Egypt: II. Preliminary correlations of epidemiology, clinical symptoms and molecular biology." J Invest Dermatol **77**(1): 96-101.

Coviello-McLaughlin, G. M. and K. R. Prowse (1997). "Telomere length regulation during postnatal development and ageing in Mus spretus." Nucleic Acids Res **25**(15): 3051-8.

Cristofalo, V. J. and D. Kritchevsky (1969). "Cell size and nucleic acid content in the diploid human cell line WI-38 during aging." Med Exp Int J Exp Med **19**(6): 313-20.

Cristofalo, V. J. and R. J. Pignolo (1993). "Replicative senescence of human fibroblast-like cells in culture." Physiol Rev **73**(3): 617-38.

Cross, S. H., R. C. Allshire, S. J. McKay, N. I. McGill and H. J. Cooke (1989). "Cloning of human telomeres by complementation in yeast." Nature **338**(6218): 771-4.

de Lange, T. (2002). "Protection of mammalian telomeres." Oncogene **21**(4): 532-40.

de Magalhaes, J. P. (2004). "From cells to ageing: a review of models and mechanisms of cellular senescence and their impact on human ageing." Exp Cell Res **300**(1): 1-10.

de Waard, H., J. de Wit, T. G. Gorgels, G. van den Aardweg, J. O. Andressoo, M. Vermeij, H. van Steeg, J. H. Hoeijmakers and G. T. van der Horst (2003). "Cell type-specific hypersensitivity to oxidative damage in CSB and XPA mice." DNA Repair (Amst) **2**(1): 13-25.

Di Leonardo, A., S. P. Linke, K. Clarkin and G. M. Wahl (1994). "DNA damage triggers a prolonged p53-dependent G1 arrest and long-term induction of Cip1 in normal human fibroblasts." Genes Dev **8**(21): 2540-51.

Dimri, G. P., X. Lee, G. Basile, M. Acosta, G. Scott, C. Roskelley, E. E. Medrano, M. Linskens, I. Rubelj, O. Pereira-Smith and et al. (1995). "A biomarker that identifies senescent human cells in culture and in aging skin in vivo." Proc Natl Acad Sci U S A **92**(20): 9363-7.

Djojosubroto, M. W., Y. S. Choi, H. W. Lee and K. L. Rudolph (2003). "Telomeres and telomerase in aging, regeneration and cancer." Mol Cells **15**(2): 164-75.

Drayton, S. and G. Peters (2002). "Immortalisation and transformation revisited." Curr Opin Genet Dev **12**(1): 98-104.

Dumont, P., V. Royer, T. Pascal, J. F. Dierick, F. Chainiaux, C. Frippiat, J. P. de Magalhaes, F. Eliaers, J. Remacle and O. Toussaint (2001). "Growth kinetics rather than stress accelerate telomere shortening in cultures of human diploid fibroblasts in oxidative stress-induced premature senescence." FEBS Lett **502**(3): 109-12.

Engelhardt, M., J. Albanell, P. Drullinsky, W. Han, J. Guillem, H. I. Scher, V. Reuter and M. A. Moore (1997). "Relative contribution of normal and neoplastic cells determines telomerase activity and telomere length in primary cancers of the prostate, colon, and sarcoma." Clin Cancer Res **3**(10): 1849-57.

Engelhardt, M., M. F. Ozkaynak, P. Drullinsky, C. Sandoval, O. Tugal, S. Jayabose and M. A. Moore (1998). "Telomerase activity and telomere length in pediatric patients with malignancies undergoing chemotherapy." Leukemia **12**(1): 13-24.

Epel, E. S., E. H. Blackburn, J. Lin, F. S. Dhabhar, N. E. Adler, J. D. Morrow and R. M. Cawthon (2004). "Accelerated telomere shortening in response to life stress." Proc Natl Acad Sci U S A **101**(49): 17312-5.

Feng, J., W. D. Funk, S. S. Wang, S. L. Weinrich, A. A. Avilion, C. P. Chiu, R. R. Adams, E. Chang, R. C. Allsopp, J. Yu and et al. (1995). "The RNA component of human telomerase." Science **269**(5228): 1236-41.

Ferro, S. and I. E. Salit (1992). "HIV infection in patients over 55 years of age." J Acquir Immune Defic Syndr **5**(4): 348-53.

Fortini, P., B. Pascucci, E. Parlanti, M. D'Errico, V. Simonelli and E. Dogliotti (2003). "The base excision repair: mechanisms and its relevance for cancer susceptibility." Biochimie **85**(11): 1053-71.

Franco, S., M. F. Ozkaynak, C. Sandoval, O. Tugal, S. Jayabose, M. Engelhardt and M. A. Moore (2003). "Telomere dynamics in childhood leukemia and solid tumors: a follow-up study." Leukemia **17**(2): 401-10.

Frenck, R. W., Jr., E. H. Blackburn and K. M. Shannon (1998). "The rate of telomere sequence loss in human leukocytes varies with age." Proc Natl Acad Sci U S A **95**(10): 5607-10.

Friedrich, U., E. Griese, M. Schwab, P. Fritz, K. Thon and U. Klotz (2000). "Telomere length in different tissues of elderly patients." Mech Ageing Dev **119**(3): 89-99.

Gershon, H. and D. Gershon (2001). "Critical assessment of paradigms in aging research." Exp Gerontol **36**(7): 1035-47.

Graakjaer, J., L. Pascoe, H. Der-Sarkissian, G. Thomas, S. Kolvraa, K. Christensen and J. A. Londono-Vallejo (2004). "The relative lengths of individual telomeres are defined in the zygote and strictly maintained during life." Aging Cell **3**(3): 97-102.

Griffith, J. D., L. Comeau, S. Rosenfield, R. M. Stansel, A. Bianchi, H. Moss and T. de Lange (1999). "Mammalian telomeres end in a large duplex loop." Cell **97**(4): 503-14.

Grossmann, K. F., J. C. Brown and R. E. Moses (1999). "Cisplatin DNA cross-links do not inhibit S-phase and cause only a G2/M arrest in Saccharomyces cerevisiae." Mutat Res **434**(1): 29-39.

Hanawalt, P. C. (1996). "Role of transcription-coupled DNA repair in susceptibility to environmental carcinogenesis." Environ Health Perspect **104 Suppl 3**: 547-51.

Hansson, J. and R. D. Wood (1989). "Repair synthesis by human cell extracts in DNA damaged by cis- and trans-diamminedichloroplatinum(II)." Nucleic Acids Res **17**(20): 8073-91.

Hara, E., R. Smith, D. Parry, H. Tahara, S. Stone and G. Peters (1996). "Regulation of p16CDKN2 expression and its implications for cell immortalization and senescence." Mol Cell Biol **16**(3): 859-67.

Harle-Bachor, C. and P. Boukamp (1996). "Telomerase activity in the regenerative basal layer of the epidermis inhuman skin and in immortal and carcinoma-derived skin keratinocytes." Proc Natl Acad Sci U S A **93**(13): 6476-81.

Harley, C. B. (1991). "Telomere loss: mitotic clock or genetic time bomb?" Mutat Res **256**(2-6): 271-82.

Harley, C. B., A. B. Futcher and C. W. Greider (1990). "Telomeres shorten during ageing of human fibroblasts." Nature **345**(6274): 458-60.

Harper, J. W., G. R. Adami, N. Wei, K. Keyomarsi and S. J. Elledge (1993). "The p21 Cdk-interacting protein Cip1 is a potent inhibitor of G1 cyclin-dependent kinases." Cell **75**(4): 805-16.

Hartwell, L. (1992). "Defects in a cell cycle checkpoint may be responsible for the genomic instability of cancer cells." Cell **71**(4): 543-6.

Hastie, N. D., M. Dempster, M. G. Dunlop, A. M. Thompson, D. K. Green and R. C. Allshire (1990). "Telomere reduction in human colorectal carcinoma and with ageing." Nature **346**(6287): 866-8.

Hattangadi, D. K., G. A. DeMasters, T. D. Walker, K. R. Jones, X. Di, I. F. Newsham and D. A. Gewirtz (2004). "Influence of p53 and caspase 3 activity on cell death and senescence in response to methotrexate in the breast tumor cell." Biochem Pharmacol **68**(9): 1699-708.

Hayflick, L. (1965). "The Limited In Vitro Lifetime Of Human Diploid Cell Strains." Exp Cell Res **37**: 614-36.

Heiger-Bernays, W. J., J. M. Essigmann and S. J. Lippard (1990). "Effect of the antitumor drug cis-diamminedichloroplatinum(II) and related platinum complexes on eukaryotic DNA replication." Biochemistry **29**(36): 8461-6.

Hiraga, S., T. Ohnishi, S. Izumoto, E. Miyahara, Y. Kanemura, H. Matsumura and N. Arita (1998). "Telomerase activity and alterations in telomere length in human brain tumors." Cancer Res **58**(10): 2117-25.

Ho, D. D., A. U. Neumann, A. S. Perelson, W. Chen, J. M. Leonard and M. Markowitz (1995). "Rapid turnover of plasma virions and CD4 lymphocytes in HIV-1 infection." Nature **373**(6510): 123-6.

Ishibashi, T. and S. J. Lippard (1998). "Telomere loss in cells treated with cisplatin." Proc Natl Acad Sci U S A **95**(8): 4219-23.

Jeremic, B., Y. Shibamoto, B. Stanisavljevic, L. Milojevic, B. Milicic and N. Nikolic (1997). "Radiation therapy alone or with concurrent low-dose daily either cisplatin or carboplatin in locally advanced unresectable squamous cell carcinoma of the head and neck: a prospective randomized trial." Radiother Oncol **43**(1): 29-37.

Kammori, M., K. Takubo, K. Nakamura, E. Furugouri, H. Endo, H. Kanauchi, Y. Mimura and M. Kaminishi (2000). "Telomerase activity and telomere length in benign and malignant human thyroid tissues." Cancer Lett **159**(2): 175-81.

Kartalou, M. and J. M. Essigmann (2001). "Mechanisms of resistance to cisplatin." Mutat Res **478**(1-2): 23-43.

Kastan, M. B., O. Onyekwere, D. Sidransky, B. Vogelstein and R. W. Craig (1991). "Participation of p53 protein in the cellular response to DNA damage." Cancer Res **51**(23 Pt 1): 6304-11.

Kill, I. R., R. G. Faragher, K. Lawrence and S. Shall (1994). "The expression of proliferation-dependent antigens during the lifespan of normal and progeroid human fibroblasts in culture." J Cell Sci **107 (Pt 2)**: 571-9.

Kim, N. W., M. A. Piatyszek, K. R. Prowse, C. B. Harley, M. D. West, P. L. Ho, G. M. Coviello, W. E. Wright, S. L. Weinrich and J. W. Shay (1994). "Specific association of human telomerase activity with immortal cells and cancer." Science **266**(5193): 2011-5.

Kim, S. H., P. Kaminker and J. Campisi (1999). "TIN2, a new regulator of telomere length in human cells." Nat Genet **23**(4): 405-12.

Kim Sh, S. H., P. Kaminker and J. Campisi (2002). "Telomeres, aging and cancer: in search of a happy ending." Oncogene **21**(4): 503-11.

Kiyozuka, Y., D. Yamamoto, J. Yang, Y. Uemura, H. Senzaki, S. Adachi and A. Tsubura (2000). "Correlation of chemosensitivity to anticancer drugs and telomere length, telomerase activity and telomerase RNA expression in human ovarian cancer cells." Anticancer Res **20**(1A): 203-12.

Kruk, P. A., N. J. Rampino and V. A. Bohr (1995). "DNA damage and repair in telomeres: relation to aging." Proc Natl Acad Sci U S A **92**(1): 258-62.

Kuranaga, N., N. Shinomiya and H. Mochizuki (2001). "Long-term cultivation of colorectal carcinoma cells with anti-cancer drugs induces drug resistance and telomere elongation: an in vitro study." BMC Cancer **1**(1): 10.

Lee, J. J., C. E. Nam, S. H. Cho, K. S. Park, I. J. Chung and H. J. Kim (2003). "Telomere length shortening in non-Hodgkin's lymphoma patients undergoing chemotherapy." Ann Hematol **82**(8): 492-5.

Lepre, C. A., L. Chassot, C. E. Costello and S. J. Lippard (1990). "Synthesis and characterization of trans-[Pt(NH3)2Cl2] adducts of d(CCTCGAGTCTCC).d(GGAGACTCGAGG)." Biochemistry **29**(3): 811-23.

Leteurtre, F., X. Li, P. Guardiola, G. Le Roux, J. C. Sergere, P. Richard, E. D. Carosella and E. Gluckman (1999). "Accelerated telomere shortening and telomerase activation in Fanconi's anaemia." Br J Haematol **105**(4): 883-93.

Lewis, S. M., I. C. Collier and M. M. Heitkemper (1996). Medical-surgical nursing: Assessment and management of clinical problems., Mosby-Year Book, Inc.

Li, S., J. E. Rosenberg, A. A. Donjacour, I. L. Botchkina, Y. K. Hom, G. R. Cunha and E. H. Blackburn (2004). "Rapid inhibition of cancer cell growth induced by lentiviral delivery and expression of mutant-template telomerase RNA and anti-telomerase short-interfering RNA." Cancer Res **64**(14): 4833-40.

Lieber, M. R., Y. Ma, U. Pannicke and K. Schwarz (2003). "Mechanism and regulation of human non-homologous DNA end-joining." Nat Rev Mol Cell Biol **4**(9): 712-20.

Lisker, R. and A. Cobo (1970). "Chromosome breakage in ataxia-telangiectasia." Lancet **1**(7647): 618.

Liu, D., M. S. O'Connor, J. Qin and Z. Songyang (2004). "Telosome, a mammalian telomere-associated complex formed by multiple telomeric proteins." J Biol Chem **279**(49): 51338-42.

Macquet, J. P. and J. L. Butour (1983). "Platinum-amine compounds: importance of the labile and inert ligands for their pharmacological activities toward L1210 leukemia cells." J Natl Cancer Inst **70**(5): 899-905.

Maniatis, T., E. F. Fritsch and J. Sambrook (1982). Molecular cloning: a laboratory manual. Cold Spring Harbor, N.Y., Cold Spring Harbor Laboratory.

Marchan, V., E. Pedroso and A. Grandas (2004). "Insights into the reaction of transplatin with DNA and proteins: methionine-mediated formation of histidine-guanine trans-Pt(NH3)2 cross-links." Chemistry **10**(21): 5369-75.

Marti, T. M., C. Kunz and O. Fleck (2002). "DNA mismatch repair and mutation avoidance pathways." J Cell Physiol **191**(1): 28-41.

McAllister-Sistilli, C. G., A. R. Caggiula, S. Knopf, C. A. Rose, A. L. Miller and E. C. Donny (1998). "The effects of nicotine on the immune system." Psychoneuroendocrinology **23**(2): 175-87.

Meyerson, M., C. M. Counter, E. N. Eaton, L. W. Ellisen, P. Steiner, S. D. Caddle, L. Ziaugra, R. L. Beijersbergen, M. J. Davidoff, Q. Liu, S. Bacchetti, D. A. Haber and R. A. Weinberg (1997). "hEST2, the putative human telomerase catalytic subunit gene, is up-regulated in tumor cells and during immortalization." Cell **90**(4): 785-95.

Milas, L., K. A. Mason, Z. Liao and K. K. Ang (2003). "Chemoradiotherapy: emerging treatment improvement strategies." Head Neck **25**(2): 152-67.

Mitchell, J. R., J. H. Hoeijmakers and L. J. Niedernhofer (2003). "Divide and conquer: nucleotide excision repair battles cancer and ageing." Curr Opin Cell Biol **15**(2): 232-40.

Modrich, P. (1989). "Methyl-directed DNA mismatch correction." J Biol Chem **264**(12): 6597-600.

Mondello, C., C. Petropoulou, D. Monti, E. S. Gonos, C. Franceschi and F. Nuzzo (1999). "Telomere length in fibroblasts and blood cells from healthy centenarians." Exp Cell Res **248**(1): 234-42.

Nasmyth, K. (1996). "Viewpoint: putting the cell cycle in order." Science **274**(5293): 1643-5.

Nawrot, T. S., J. A. Staessen, J. P. Gardner and A. Aviv (2004). "Telomere length and possible link to X chromosome." Lancet **363**(9408): 507-10.

Neglia, J. P., D. L. Friedman, Y. Yasui, A. C. Mertens, S. Hammond, M. Stovall, S. S. Donaldson, A. T. Meadows and L. L. Robison (2001). "Second malignant neoplasms in five-year survivors of childhood cancer: childhood cancer survivor study." J Natl Cancer Inst **93**(8): 618-29.

Nehme, A., R. Baskaran, S. Aebi, D. Fink, S. Nebel, B. Cenni, J. Y. Wang, S. B. Howell and R. D. Christen (1997). "Differential induction of c-Jun NH2-terminal kinase and c-Abl kinase in DNA mismatch repair-proficient and -deficient cells exposed to cisplatin." Cancer Res **57**(15): 3253-7.

Nicoletti, I., G. Migliorati, M. C. Pagliacci, F. Grignani and C. Riccardi (1991). "A rapid and simple method for measuring thymocyte apoptosis by propidium iodide staining and flow cytometry." J Immunol Methods **139**(2): 271-9.

Noda, A., Y. Ning, S. F. Venable, O. M. Pereira-Smith and J. R. Smith (1994). "Cloning of senescent cell-derived inhibitors of DNA synthesis using an expression screen." Exp Cell Res **211**(1): 90-8.

Ohashi, K., M. Tsutsumi, Y. Nakajima, K. Kobitsu, H. Nakano and Y. Konishi (1996). "Telomere changes in human hepatocellular carcinomas and hepatitis virus infected noncancerous livers." Cancer **77**(8 Suppl): 1747-51.

Ohtani, N., K. Yamakoshi, A. Takahashi and E. Hara (2004). "The p16INK4a-RB pathway: molecular link between cellular senescence and tumor suppression." J Med Invest **51**(3-4): 146-53.

Okuda, K., A. Bardeguez, J. P. Gardner, P. Rodriguez, V. Ganesh, M. Kimura, J. Skurnick, G. Awad and A. Aviv (2002). "Telomere length in the newborn." Pediatr Res **52**(3): 377-81.

Olovnikov, A. M. (1971). "[Principle of marginotomy in template synthesis of polynucleotides]." Dokl Akad Nauk SSSR **201**(6): 1496-9.

Olovnikov, A. M. (1973). "A theory of marginotomy. The incomplete copying of template margin in enzymic synthesis of polynucleotides and biological significance of the phenomenon." J Theor Biol **41**(1): 181-90.

Operskalski, E. A., D. O. Stram, H. Lee, Y. Zhou, E. Donegan, M. P. Busch, C. E. Stevens, E. R. Schiff, S. L. Dietrich and J. W. Mosley (1995). "Human

immunodeficiency virus type 1 infection: relationship of risk group and age to rate of progression to AIDS. Transfusion Safety Study Group." J Infect Dis **172**(3): 648-55.

Opresko, P. L., J. Fan, S. Danzy, D. M. Wilson, 3rd and V. A. Bohr (2005). "Oxidative damage in telomeric DNA disrupts recognition by TRF1 and TRF2." Nucleic Acids Res **33**(4): 1230-9.

Patel, M. M., L. J. Parekh, F. P. Jha, R. N. Sainger, J. B. Patel, D. D. Patel, P. M. Shah and P. S. Patel (2002). "Clinical usefulness of telomerase activation and telomere length in head and neck cancer." Head Neck **24**(12): 1060-7.

Perez, J. M., M. A. Fuertes, C. Alonso and C. Navarro-Ranninger (2000). "Current status of the development of trans-platinum antitumor drugs." Crit Rev Oncol Hematol **35**(2): 109-20.

Petersen, S., G. Saretzki and T. von Zglinicki (1998). "Preferential accumulation of single-stranded regions in telomeres of human fibroblasts." Exp Cell Res **239**(1): 152-60.

Popoff, S. C., D. J. Beck and W. D. Rupp (1987). "Repair of plasmid DNA damaged in vitro with cis- or trans-diamminedichloroplatinum(II) in Escherichia coli." Mutat Res **183**(2): 129-37.

Reardon, J. T. and A. Sancar (2002). "Molecular anatomy of the human excision nuclease assembled at sites of DNA damage." Mol Cell Biol **22**(16): 5938-45.

Reardon, J. T., L. H. Thompson and A. Sancar (1993). "Excision repair in man and the molecular basis of xeroderma pigmentosum syndrome." Cold Spring Harb Symp Quant Biol **58**: 605-17.

Redon, S., S. Bombard, M. A. Elizondo-Riojas and J. C. Chottard (2003). "Platinum cross-linking of adenines and guanines on the quadruplex structures of the AG3(T2AG3)3 and (T2AG3)4 human telomere sequences in Na+ and K+ solutions." Nucleic Acids Res **31**(6): 1605-13.

Reed, E., R. F. Ozols, R. Tarone, S. H. Yuspa and M. C. Poirier (1987). "Platinum-DNA adducts in leukocyte DNA correlate with disease response in ovarian cancer patients receiving platinum-based chemotherapy." Proc Natl Acad Sci U S A **84**(14): 5024-8.

Reed, E., S. H. Yuspa, L. A. Zwelling, R. F. Ozols and M. C. Poirier (1986). "Quantitation of cis-diamminedichloroplatinum II (cisplatin)-DNA-intrastrand adducts in testicular and ovarian cancer patients receiving cisplatin chemotherapy." J Clin Invest **77**(2): 545-50.

Ricca, I., M. Compagno, M. Ladetto, A. Rocci, M. Dell'aquila, P. Omede, F. De Marco, S. D'Antico, D. Caracciolo, D. Ferrero, C. Carlo-Stella and C. Tarella (2005). "Marked telomere shortening in mobilized peripheral blood progenitor cells (PBPC) following two tightly spaced high-dose chemotherapy courses with G-CSF." Leukemia.

Romero, D. P. and E. H. Blackburn (1991). "A conserved secondary structure for telomerase RNA." Cell **67**(2): 343-53.

Rufer, N., T. H. Brummendorf, S. Kolvraa, C. Bischoff, K. Christensen, L. Wadsworth, M. Schulzer and P. M. Lansdorp (1999). "Telomere fluorescence measurements in granulocytes and T lymphocyte subsets point to a high turnover of hematopoietic stem cells and memory T cells in early childhood." J Exp Med **190**(2): 157-67.

Samaras, T. T., H. Elrick and L. H. Storms (2003). "Is height related to longevity?" Life Sci **72**(16): 1781-802.

Sancar, A., L. A. Lindsey-Boltz, K. Unsal-Kacmaz and S. Linn (2004). "Molecular mechanisms of mammalian DNA repair and the DNA damage checkpoints." Annu Rev Biochem **73**: 39-85.

Schroder, C. P., G. B. Wisman, S. de Jong, W. T. van der Graaf, M. H. Ruiters, N. H. Mulder, L. F. de Leij, A. G. van der Zee and E. G. de Vries (2001). "Telomere length in breast cancer patients before and after chemotherapy with or without stem cell transplantation." Br J Cancer **84**(10): 1348-53.

Schulte-Hermann, R., B. Grasl-Kraupp and W. Bursch (2000). "Dose-response and threshold effects in cytotoxicity and apoptosis." Mutat Res **464**(1): 13-8.

Schulz, V. P., V. A. Zakian, C. E. Ogburn, J. McKay, A. A. Jarzebowicz, S. D. Edland and G. M. Martin (1996). "Accelerated loss of telomeric repeats may not explain accelerated replicative decline of Werner syndrome cells." Hum Genet **97**(6): 750-4.

Segerstrom, S. C. and G. E. Miller (2004). "Psychological stress and the human immune system: a meta-analytic study of 30 years of inquiry." Psychol Bull **130**(4): 601-30.

Serrano, M., G. J. Hannon and D. Beach (1993). "A new regulatory motif in cell-cycle control causing specific inhibition of cyclin D/CDK4." Nature **366**(6456): 704-7.

Severino, J., R. G. Allen, S. Balin, A. Balin and V. J. Cristofalo (2000). "Is beta-galactosidase staining a marker of senescence in vitro and in vivo?" Exp Cell Res **257**(1): 162-71.

Shay, J. W., O. M. Pereira-Smith and W. E. Wright (1991). "A role for both RB and p53 in the regulation of human cellular senescence." Exp Cell Res **196**(1): 33-9.

Shay, J. W. and W. E. Wright (2005). "Senescence and immortalization: role of telomeres and telomerase." Carcinogenesis **26**(5): 867-74.

Slagboom, P. E., S. Droog and D. I. Boomsma (1994). "Genetic determination of telomere size in humans: a twin study of three age groups." Am J Hum Genet **55**(5): 876-82.

Smogorzewska, A., B. van Steensel, A. Bianchi, S. Oelmann, M. R. Schaefer, G. Schnapp and T. de Lange (2000). "Control of human telomere length by TRF1 and TRF2." Mol Cell Biol **20**(5): 1659-68.

Sobin, L. H. and C. Wittekind (1997). TNM classification of malignant tumors, 5th ed. New York, Wiley-Liss, Inc.

Swift, M., D. Morrell, R. B. Massey and C. L. Chase (1991). "Incidence of cancer in 161 families affected by ataxia-telangiectasia." N Engl J Med **325**(26): 1831-6.

Takubo, K., N. Izumiyama-Shimomura, N. Honma, M. Sawabe, T. Arai, M. Kato, M. Oshimura and K. Nakamura (2002). "Telomere lengths are characteristic in each human individual." Exp Gerontol **37**(4): 523-31.

Tanaka, K. and R. D. Wood (1994). "Xeroderma pigmentosum and nucleotide excision repair of DNA." Trends Biochem Sci **19**(2): 83-6.

Tannock, I. F. (1996). "Treatment of cancer with radiation and drugs." J Clin Oncol **14**(12): 3156-74.

Tchirkov, A. and P. M. Lansdorp (2003). "Role of oxidative stress in telomere shortening in cultured fibroblasts from normal individuals and patients with ataxia-telangiectasia." Hum Mol Genet **12**(3): 227-32.

Thomas, G. M. (1999). "Improved treatment for cervical cancer--concurrent chemotherapy and radiotherapy." N Engl J Med **340**(15): 1198-200.

Thompson, L. H. and D. Schild (2001). "Homologous recombinational repair of DNA ensures mammalian chromosome stability." Mutat Res **477**(1-2): 131-53.

Toussaint, O., P. Dumont, J. F. Dierick, T. Pascal, C. Frippiat, F. Chainiaux, J. P. Magalhaes, F. Eliaers and J. Remacle (2000). "Stress-induced premature senescence as alternative toxicological method for testing the long-term effects of molecules under development in the industry." Biogerontology **1**(2): 179-83.

Tsurusawa, M., M. Niwa, N. Katano and T. Fujimoto (1988). "Flow cytometric analysis by bromodeoxyuridine/DNA assay of cell cycle perturbation of methotrexate-treated mouse L1210 leukemia cells." Cancer Res **48**(15): 4288-93.

Umar, A., A. B. Buermeyer, J. A. Simon, D. C. Thomas, A. B. Clark, R. M. Liskay and T. A. Kunkel (1996). "Requirement for PCNA in DNA mismatch repair at a step preceding DNA resynthesis." Cell **87**(1): 65-73.

Unryn, B. M., L. S. Cook and K. T. Riabowol (2005). "Paternal age is positively linked to telomere length of children." Aging Cell **4**(2): 97-101.

van Steensel, B., A. Smogorzewska and T. de Lange (1998). "TRF2 protects human telomeres from end-to-end fusions." Cell **92**(3): 401-13.

Vaziri, H. and S. Benchimol (1998). "Reconstitution of telomerase activity in normal human cells leads to elongation of telomeres and extended replicative life span." Curr Biol **8**(5): 279-82.

Vaziri, H., W. Dragowska, R. C. Allsopp, T. E. Thomas, C. B. Harley and P. M. Lansdorp (1994). "Evidence for a mitotic clock in human hematopoietic stem cells: loss of telomeric DNA with age." Proc Natl Acad Sci U S A **91**(21): 9857-60.

Vaziri, H., F. Schachter, I. Uchida, L. Wei, X. Zhu, R. Effros, D. Cohen and C. B. Harley (1993). "Loss of telomeric DNA during aging of normal and trisomy 21 human lymphocytes." Am J Hum Genet **52**(4): 661-7.

Villalonga, P., R. M. Guasch, K. Riento and A. J. Ridley (2004). "RhoE inhibits cell cycle progression and Ras-induced transformation." Mol Cell Biol **24**(18): 7829-40.

von Zglinicki, T., R. Pilger and N. Sitte (2000). "Accumulation of single-strand breaks is the major cause of telomere shortening in human fibroblasts." Free Radic Biol Med **28**(1): 64-74.

von Zglinicki, T., G. Saretzki, W. Docke and C. Lotze (1995). "Mild hyperoxia shortens telomeres and inhibits proliferation of fibroblasts: a model for senescence?" Exp Cell Res **220**(1): 186-93.

Wei, X., S. K. Ghosh, M. E. Taylor, V. A. Johnson, E. A. Emini, P. Deutsch, J. D. Lifson, S. Bonhoeffer, M. A. Nowak, B. H. Hahn and et al. (1995). "Viral dynamics in human immunodeficiency virus type 1 infection." Nature **373**(6510): 117-22.

Weinrich, S. L., R. Pruzan, L. Ma, M. Ouellette, V. M. Tesmer, S. E. Holt, A. G. Bodnar, S. Lichtsteiner, N. W. Kim, J. B. Trager, R. D. Taylor, R. Carlos, W. H. Andrews, W. E. Wright, J. W. Shay, C. B. Harley and G. B. Morin (1997). "Reconstitution of human telomerase with the template RNA component hTR and the catalytic protein subunit hTRT." Nat Genet **17**(4): 498-502.

Weng, N. P., L. Granger and R. J. Hodes (1997). "Telomere lengthening and telomerase activation during human B cell differentiation." Proc Natl Acad Sci U S A **94**(20): 10827-32.

Weng, N. P., B. L. Levine, C. H. June and R. J. Hodes (1995). "Human naive and memory T lymphocytes differ in telomeric length and replicative potential." Proc Natl Acad Sci U S A **92**(24): 11091-4.

Winkler, G. S., K. Sugasawa, A. P. Eker, W. L. de Laat and J. H. Hoeijmakers (2001). "Novel functional interactions between nucleotide excision DNA repair proteins influencing the enzymatic activities of TFIIH, XPG, and ERCC1-XPF." Biochemistry **40**(1): 160-5.

Wong, H. and K. Riabowol (1996). "Differential CDK-inhibitor gene expression in aging human diploid fibroblasts." Exp Gerontol **31**(1-2): 311-25.

Wright, W. E., M. A. Piatyszek, W. E. Rainey, W. Byrd and J. W. Shay (1996). "Telomerase activity in human germline and embryonic tissues and cells." Dev Genet **18**(2): 173-9.

Wright, W. E. and J. W. Shay (2001). "Cellular senescence as a tumor-protection mechanism: the essential role of counting." Curr Opin Genet Dev **11**(1): 98-103.

Wright, W. E., V. M. Tesmer, K. E. Huffman, S. D. Levene and J. W. Shay (1997). "Normal human chromosomes have long G-rich telomeric overhangs at one end." Genes Dev **11**(21): 2801-9.

Wu, X., C. I. Amos, Y. Zhu, H. Zhao, B. H. Grossman, J. W. Shay, S. Luo, W. K. Hong and M. R. Spitz (2003). "Telomere dysfunction: a potential cancer predisposition factor." J Natl Cancer Inst **95**(16): 1211-8.

Youngren, K., E. Jeanclos, H. Aviv, M. Kimura, J. Stock, M. Hanna, J. Skurnick, A. Bardeguez and A. Aviv (1998). "Synchrony in telomere length of the human fetus." Hum Genet **102**(6): 640-3.

Zakian, V. A. (1995). "Telomeres: beginning to understand the end." Science **270**(5242): 1601-7.

Zamble, D. B., D. Mu, J. T. Reardon, A. Sancar and S. J. Lippard (1996). "Repair of cisplatin--DNA adducts by the mammalian excision nuclease." Biochemistry **35**(31): 10004-13.

Zeichner, S. L., P. Palumbo, Y. Feng, X. Xiao, D. Gee, J. Sleasman, M. Goodenow, R. Biggar and D. Dimitrov (1999). "Rapid telomere shortening in children." Blood **93**(9): 2824-30.

Zhang, R. G., R. P. Zhang, X. W. Wang and H. Xie (2002). "Effects of cisplatin on telomerase activity and telomere length in BEL-7404 human hepatoma cells." Cell Res **12**(1): 55-62.

Zhao, W., Z. X. Lin and Z. Q. Zhang (2004). "Cisplatin-induced premature senescence with concomitant reduction of gap junctions in human fibroblasts." Cell Res **14**(1): 60-6.

Zhou, B. B. and S. J. Elledge (2000). "The DNA damage response: putting checkpoints in perspective." Nature **408**(6811): 433-9.

Zohn, I. M., S. L. Campbell, R. Khosravi-Far, K. L. Rossman and C. J. Der (1998). "Rho family proteins and Ras transformation: the RHOad less traveled gets congested." Oncogene **17**(11 Reviews): 1415-38.

Zou, Y., A. Sfeir, S. M. Gryaznov, J. W. Shay and W. E. Wright (2004). "Does a sentinel or a subset of short telomeres determine replicative senescence?" Mol Biol Cell **15**(8): 3709-18.

Zwelling, L. A., J. Filipski and K. W. Kohn (1979). "Effect of thiourea on survival and DNA cross-link formation in cells treated with platinum(II) complexes, L-phenylalanine mustard, and bis(2-chloroethyl)methylamine." Cancer Res **39**(12): 4989-95.